Queen Mary
University of London

Organic-Magnetoresistance in Aluminium tris(8-hydroxyquinolinate) Light Emitting Diodes

Pratik Desai

Department of Physics
Queen Mary, University of London

Supervisor – Dr. William Gillin

July 2008

Submitted for the degree of Doctor of Philosophy

Declaration

Excluding the exception detailed below, all the work contained within this thesis is my own.

Exception:
Figure 3.2-7 – The three plots that are stated as containing BCP have been obtained, with consent, from the Ph. D. thesis of P. Shakya.

Abstract

The recent discovery of Organic Magnetoresistance (OMR) in Organic Light Emitting Diode (OLED) and other sandwich structures has led to a flurry of research activity. With all the recent research activity it is clear that neither the nature of OMR nor the mechanisms responsible are fully understood.

This work seeks to probe these phenomena in order to better characterise the nature of OMR, related effects and to highlight possible mechanisms behind OMR.

Devices were fabricated with differing electrodes in order to probe OMR for devices with differing injection efficiencies. It was found that the magnetic field acted to modulate the device devices efficiency as well as the current, hence modulation of luminescence cannot be a simple consequence of the change in current. The results from varying the cathode material are consistent with excitonic effects and indicate that triplet interactions are responsible for the observed magnetic field effects.

In varying the drive voltage, applied field and thickness of the Aluminium tris(8-hydroxyquinolinate) (Alq_3) layer it was found that both positive and negative OMR can be observed, while the effect on luminescence and efficiency remains positive. These findings are shown to be consistent with the presence of excitons and the modulation of the intersystem crossing between singlets and triplets. The observation of negative OMR can be explained by the significance of triplet dissociation at the cathode. The balance between dissociation effects and triplet interactions determines the overall characteristics of the observed OMR.

The effect of exciton generation through illumination has also been studied. Results show both a positive and negative OMR that is consistent with the results from thin devices and is observable below the device turn-on voltage. This confirms the identification of dissociation as an important factor in OMR and the significance of triplet interactions.

Acknowledgements

Time, that has allowed me to meet all those listed below. For their support I owe thanks, appreciation, a litany of favours, gratitude, several pints…

My second acknowledgement is to my parents, Navin and Kamal Desai, they have been patient, supportive, generally good sports (if a little irritating on occasion).

To Bill Gillin, thanks, for his patience, candidness, his open door, having a mild penchant for sarcasm (especially as an educational tool) and for making my time in the group interesting and amusing. Yo! to Theo Kreouzis, for his periodic procrastination in the PhD office, occasionally recalling that a bureaucrat decreed that I needed a co-supervisor and performing outstandingly in that role. Katie Whitehead deserves great thanks and G&T, for being a superb PhD mother and for her dedication beyond duty. Thanks to Lizzie for patiently watching Pingu while her mother read the ramblings of an idiot.

There are many (too many to name here) in the Physics department who have helped chisel away at the ignorance that comes with youth, so thanks go to all the academic staff in the department who either taught me, talked or drank with me. The delightful collection of personalities that make up the Physics admin and technical staff have been invaluable in helping to solve all those irksome little problems that experiments and bureaucracy are known to throw up, thank you all, especially Sneezy.

From the asylum of my office I thank Ken P'ng, Rendy Tan, Nicola Rolfe (who is a worthy replacement) and especially Pabitra Shakya who has been a supportive and amusing colleague. Thanks also go to the rest of the MMP PhD students (past and present) as well as the refugees from the materials department.

The MMP group is an amiable and amenable group who all have my gratitude, especially Dr. Kevin Donovan, Prof. David Dunstan and Geoff Gannaway.

Thanks go to old friends, David S. Thompson who has my constant admiration, Baris A. Tosun whose humanity is an example and Steve M. Hudziak for his good heart and partnership in endeavour. Dr. Rodney J. Baldwin for his constant dissatisfaction and desire to improve, thanks also go to Emma Iizuka and the rest of the Ropery street posse. Hannes Hübel and Isabelle M. Herbauts have gone from seniors to peers to friends and I am better for knowing them. Thank you Julie L. Haverkate, you were around when most others were not. Katie N. Mertens is a truly respect worthy individual who is always the perfect foil to my chauvinistic, misogynistic self. Allison R. McGuinn has a beautiful cheekiness that keeps me honest and I adore her for it. Isabelle G. M. Gressel.

The future, for destroying complacency, scaring me to the brink of incontinence, and simply, for being there…

Contents

List of figures

List of publications

Time-resolved photoluminescence excitation characterisation of lanthanide and group III tris-(8-hydroxyquinoline) molecules
P. Desai, M. Somerton, R. J. Curry and W. P. Gillin, IEICE. Trans. Electron., E87C (12), 2023, (2004).

Magnetoresistance and efficiency measurements of Alq3-based OLEDs
P. Desai, P. Shakya, T. Kreouzis, W. P. Gillin, N. A. Morley and M. R. J. Gibbs, Phys. Rev. B **75**, 094423 (2007).

The role of magnetic fields on the transport and efficiency of aluminum tris(8-hydroxyquinoline) based organic light emitting diodes
P. Desai, P. Shakya, T. Kreouzis and W. P. Gillin, J. Appl. Phys. **102**, 073710 (2007).

Magnetoresistance in organic light-emitting diode structures under illumination
P. Desai, P. Shakya, T. Kreouzis and W. P. Gillin, Phys. Rev. B **76**, 235202 (2007).

Magnetoresistance in triphenyl-diamine derivative blue organic light emitting devices
P. Shakya, **P. Desai**, T. Kreouzis and W. P. Gillin, J. Appl. Phys. **103**, 043706 (2008).

The magnetic field effect on the transport and efficiency of group III tris(8-hydroxyquinoline) organic light emitting diodes
P. Shakya, **P. Desai**, M. Somerton, G. Gannaway, T. Kreouzis and W. P. Gillin, J. Appl. Phys. **103**, 103715 (2008).

Intrinsic mobility limit for anisotropic electron transport in Alq_3

A. J. Drew, F. L. Pratt, J. Hoppler, L. Schulz, V. Malik-Kumar, N. A. Morley, **P. Desai**, P. Shakya, T. Kreouzis, W. P. Gillin, K. W. Kim, A. Dubroka, and R. Scheuermann, Phys. Rev. Lett. **100** ,116601 (2008).

Direct depth-resolved measurement of the spin polarisation of electrons injected into the transport layer of an organic spin valve

A. J. Drew, J. Hoppler, L. Schulz, F. L. Pratt, **P. Desai**, P. Shakya, T. Kreouzis, W. P. Gillin, A. Suter, N. A. Morley, V. K. Malik, H. Bouyanfif, K. W. Kim, A. Dubroka, F. Bourqui, C. Bernhard, R. Scheuermann, T. Prokscha, G. J. Nieuwenhuys, E. Morenzoni., submitted to Nature Physics.

Isolation of charge carrier effects in OMR of illuminated Aluminium tris(8-hydroxyquinolinate) organic light emitting diodes

N. Rolfe, **P. Desai**, P. Shakya, T. Kreouzis and W.P. Gillin, accepted for publication, J. Appl. Phys. (2008).

The effect of Magnetic fields on the photocurrent in polymer blend organic photovoltaic devices

P. Shakya, **P. Desai**, T. Kreouzis, W.P.Gillin, S.M.Tuladhar and J.Nelson, in preparation.

1 Introduction

1.1 The basics

Organic Light Emitting Diodes (OLEDs) have been widely studied for the best part of 25 years since the publication of the seminal paper demonstrating the first modern device [1]. There are many motivations that have driven forward the study of OLEDs that include device engineering, material properties and the fundamentals of device physics. In particular the study of OLEDs have led to a greater understanding of charge transport and photo-physics in organic semiconductors.

1.1.1 Organic molecules and molecular bonding

There are two key organic semiconductors and several other materials used throughout this thesis. Before this work can be understood fully, certain concepts concerning the semi-conducting nature of the organic materials must be explained first. Aluminium tris(8-hydroxyquinolinate) (Alq_3) and N,N'-diphenyl-N,N' -bis(3-methylphenyl)-4,4'-diaminobiphenyl (TPD) are the two materials used throughout this work. Both materials are part of a class of materials commonly known as “small molecules”. The term “small molecule” is used to distinguish low molecular weight organic semiconductors from relatively high molecular weight semiconducting polymers.

Figure 1.1-1 shows the molecular diagram for both Alq_3 and TPD. It is the intra-molecular bonding that gives rise to the semiconducting nature of these materials. Benzene is also shown in figure 1.1-1 and is a good example for explaining semiconducting behaviour in organics. Benzene is made up of six carbon atoms, with each carbon having the charge occupancy of $1s^2$, $2s^2$, $2p^2$. In order to form the bonds between the carbon atoms in benzene sp^2 hybridised bonds are formed. In the sp^2 hybridised scheme the 2s level mixes with two of the available 2p levels, which gives a configuration of $1s^2$, sp^2, sp^2, sp^2, p. For a given carbon atom in benzene the $1s^2$ is fully occupied and is screened from the rest of the electronic structure. The 3 separate sp^2 levels form σ bonds with two other carbons and a single hydrogen atom. These σ bonds lie in the plane of the molecule, while the

remaining p orbital is perpendicular to it. The p orbitals of each carbon overlap to form a π bond which extends above and below the ring, shown as blue rings in figure 1.1-1. The electrons within the π orbital are weakly bound and as such are delocalised throughout the entire ring.

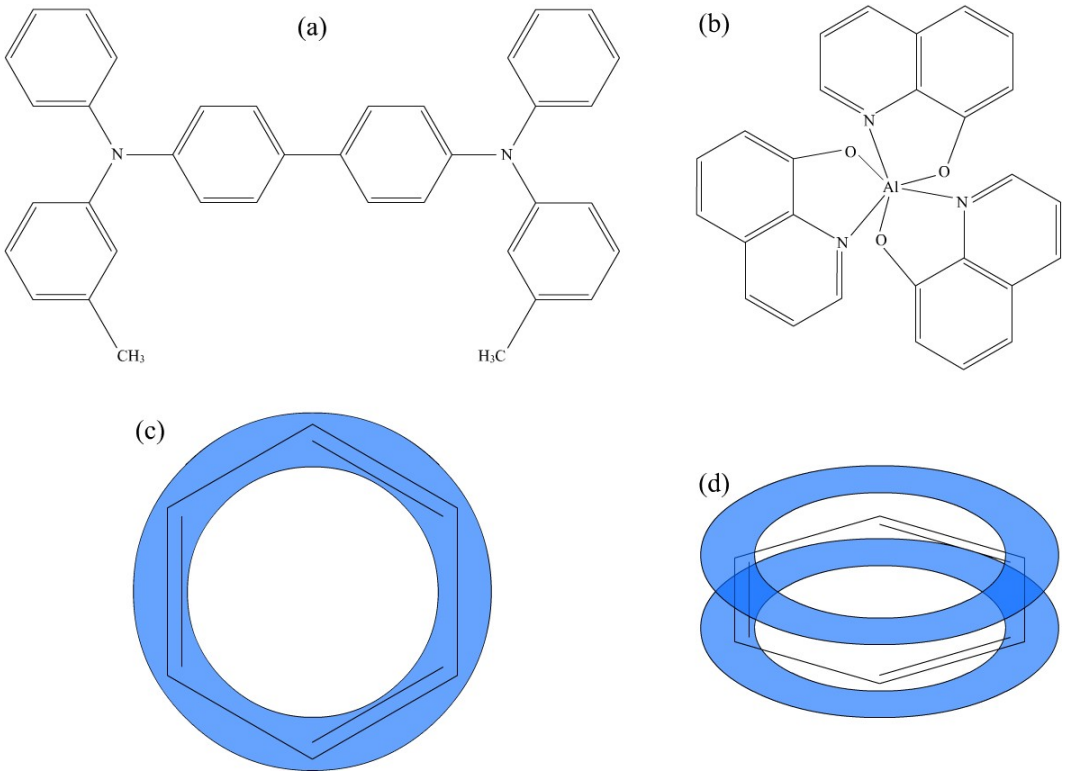

Figure 1.1-1: Molecular diagrams of TPD and Alq_3 and schematic of π-orbitals

The diagrams (a) and (b) show the molecular diagrams for the two organic semiconductors used throughout this work. The diagrams (c) and (d) show a shaded region to indicate the areas of π-orbital overlap and charge delocalisation in a benzene ring.

It is the π molecular orbital that give rise to the semiconducting nature of organic molecules. The π molecular orbital gives a significant wavefunction overlap between molecules, while the low energy π - π^* transition gives a low barrier to charge carrier hopping. The Highest Occupied Molecular Orbital (HOMO) is equivalent to the valence band of a traditional semiconductor. Similarly the Lowest Unoccupied Molecular Orbital (LUMO) is equivalent to the conduction band. The energy difference between the HOMO and LUMO is taken to be the band gap of the organic semiconductor.

1.2 The modern OLED

1.2.1 A brief history

The history of the modern OLED can be traced back to studies conducted on the organic semiconducting crystals in the 1960s. Some of the earliest organic electroluminescent devices were reported in anthracene crystal based devices. It was found that charge could be injected into these crystals with a subsequent luminescence. The first anthracene devices used liquid electrodes [2] or silver epoxy [3] these were later replaced by solid contacts that deliberately took advantage of tunnelling effect cathodes [4,5]. On the whole these devices required large operating voltages of >~100V, had low quantum efficiencies of 1~8% (photon/electron) and power conversion efficiencies of ~0.1%.

It took the work of Tang and Van Slyke [1] to reinvigorate interest in organic luminescent diodes in 1987. They produced a thin film device based on aluminium tris(8-hydroxyquinolinate) (Alq_3) as an electron injection/luminescent layer, which is shown in figure 1.2-1. This structure was created by thermally subliming/evaporating the various layers onto an indium tin oxide (ITO) coated glass substrate. ITO acts as a transparent anode; on top of this the organic layers were deposited and sandwiched with an Al cathode. This type of design is often referred to as a sandwich structure. The sublimation technique allowed for the growth of relatively thin films (~600Å) when compared to the crystals previously used in the 1960s (~μm-mm). The unique feature of this device was that it utilised a second organic material, diamine. The use of thin films and a second organic layer led to the improvement of electroluminescent characteristics when compared with the historical results of anthracene devices.

In 1990 the first polymer based OLED was demonstrated [6,7]. The device was single layer, using the polymer poly(p-phenylene vinylene) (PPV), with the device structure ITO/PPV/Al. This device spurred more intense research into polymer based devices.

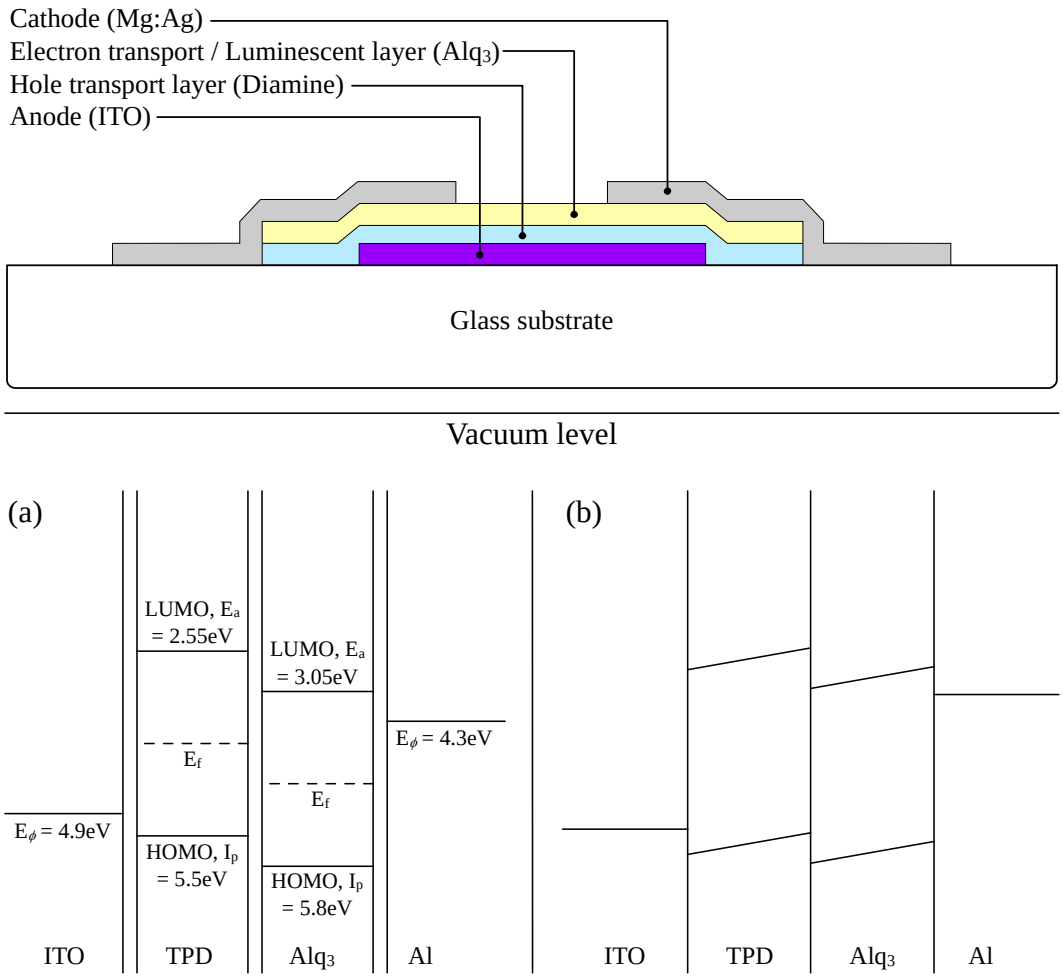

Figure 1.2-1: Schematic of first modern OLED and energy levels

Above shows the schematic of the first thin film OLED based on Alq_3. Below is a schematic of the energy levels in isolated pristine materials (a). E_ϕ denotes the work function of the metals, E_a the electron affinity, I_p the ionisation potential and E_f the Fermi energy. Pane (b) shows a device with an applied potential, the difference between the electrode work functions is the applied potential.

1.2.2 From charge injection to luminescence

Also shown in figure 1.2-1 is a basic schematic of the energy levels of a device structure analogous to that of Tang and Van Slyke, both the pristine materials (a) and a device with an applied voltage (b). These diagrams can be used to understand the basic way in which an OLED works.

Applying a voltage across the device gives rise to potential gradients in the layers. These gradients decrease the width of the potential barrier experienced by the charge carriers in the contacts. With the barrier width reduced it is possible for the wavefunction of a charge carrier to extend through the barrier into the organic

layer. Thus decreasing the barrier width increases the probability of charge tunnelling into the device. This principle of charge injection applies to both electrons and holes.

Once the charge is injected into the organic layers the potential gradients also drive charge towards the TPD/Alq_3 interface. At the interface the electrons face a large potential barrier caused by the large difference between the LUMO of TPD and the LUMO of Alq_3. This barrier effectively traps the electrons in the Alq_3 and prevents them from transiting into the TPD. The barrier experienced by holes between TPD and Alq_3 is much lower which allows for some holes to tunnel through into the Alq_3.

Exciton formation occurs once both types of charge are in the Alq_3, once here they will feel Coulombic attraction for one another. This attraction can lead to the formation of a correlated electron-hole pair state, (e…h), which is a precursor to exciton formation. When the electron and hole become close enough for their wavefunctions to significantly overlap an exciton is formed. Upon exciton formation there is a probability of radiative decay that is dependent upon the relative orientations of spin within the exciton.

1.2.3 Advantages of modern device architecture

In using the two layer approach Tang and VanSlyke were able to greatly improve the performance of OLEDs. Data presented for these devices show similar values of quantum efficiency to the earlier anthracene results, but had much lower drive voltages of <10V, which gave a much better power conversion efficiency of 0.46% [1].

The thin film structure of Tang and Van Slyke's design meant higher potential gradients could be achieved without having to increase the voltage applied to a device. Higher potential gradients at lower applied voltages meant that potential barriers to charge injection are much more easily overcome, which has an obvious benefit to device efficiency.

Using two organic layers improved the charge injection in a second way. Two layers allowed for optimisation of the barrier heights experienced by holes and electrons within the device. The HOMO of TPD is well matched to the work-function of ITO which gives a low injection barrier for holes into the device.

Likewise the LUMO of the Alq_3 is well matched to the work-function of the aluminium, which gives good electron injection into the device. So when a potential is applied across the device the high potential gradients of Tang and Van Slyke's design allow for better charge injection.

Aside from improved charge injection from the contacts the two layer structure has an added benefit: Trapping electrons at the TPD/Alq_3 interface increases the electron population in the Alq_3. A larger electron population increases the probability of electron/hole interactions, which increases subsequent exciton formation. An increase in exciton formation naturally leads to an increase in the luminescence of the OLED. So the increase in luminescence brought about by electron trapping at the TPD/Alq_3 interface is another positive outcome of Tang and Van Slyke's multi-layer design.

To this day this basic structure is still proving to be a useful blueprint for OLED fabrication and testing. While materials and fabrication techniques can vary, particularly spin-coating and drop casting for polymer based device [6,7], the fundamental structure and principles of operation are still rooted in the device demonstrated by Tang and Van Slyke.

While Alq_3 was used as the primary electron transport layer (ETL) and emission layer in Tang and Van Slyke's first design, Alq_3 has also become widely used in devices where its luminescent properties are not required. The high electron mobility in Alq_3 [8,9] means that the material is often used as an electron transport layer between the cathode and some other functional layer [10]. The good electron mobility and good work-function matching to conventional metal cathodes has also led to Alq_3 being used as a host for functional dopants [11], in particular for the enhancement of phosphorescence [12]. Due to the large number of studies involving Alq_3 it is comparatively well understood and as such is well suited to the exploration of new effects in organic semiconductors.

1.3 Luminescence in organic semiconductors

1.3.1 Excitons and their flavours

Luminescence in Alq_3 and other organic molecules requires the formation of excited states (excitons). Excitons can take on one of four forms that are grouped

into one of two manifolds, which are indicated by figure 1.3-1. The four excitons forms are a consequence of the possible spin configurations. The first configuration is when the electron and hole are orientated with spins anti-parallel; this kind of exciton forms the singlet state. The other manifold contains three possible spin orientations and as such is known as the triplet state. The three orientations that form the triplet state are when both electron and hole have spins up, secondly with both spins down and thirdly with spins opposite but with a non-zero resultant spin component. Formation of excitons can occur in one of two ways, photo-excitation that results in photoluminescence and electrical excitation which results in electroluminescence.

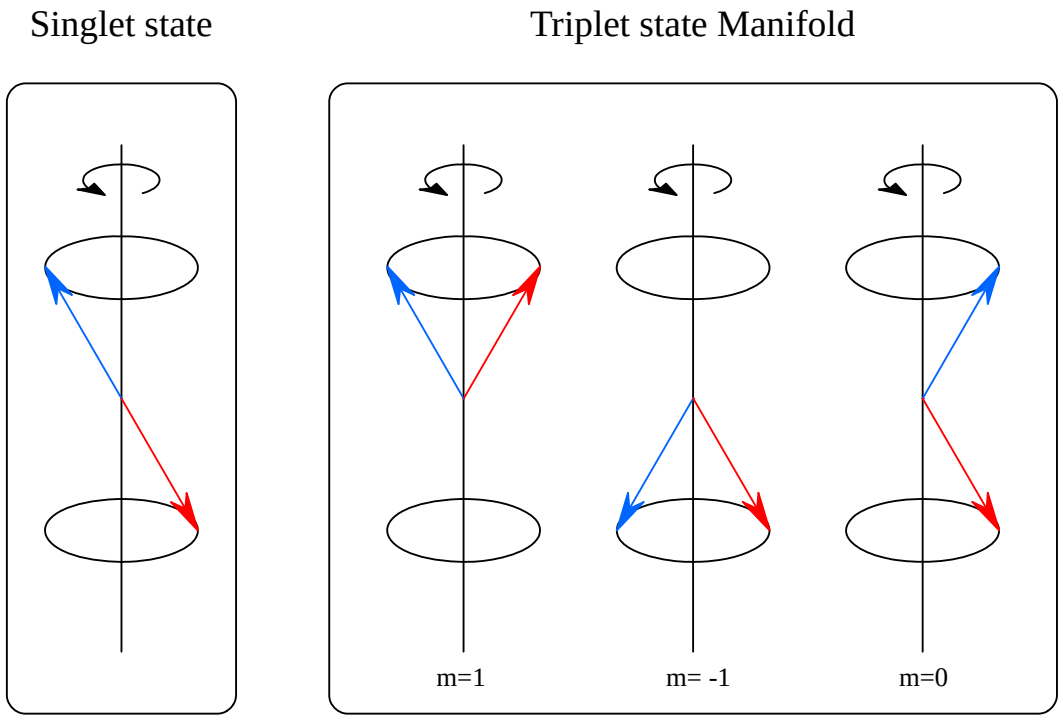

Figure 1.3-1: Exciton spin arrangements

The various arrangements of spin within an exciton are shown. Indicated on the triplet manifold is the orbital angular momentum number.

1.3.2 Photoluminescence

Photoluminescence (PL) is typically utilised in spectroscopic studies of organic molecules. Photo-excitation is usually achieved through the use of a laser. Light incident on the sample will be absorbed by an electron, which promotes the

electron into a higher energy state. The electron then looses energy through phonon emission before an exciton is formed. Due to spin conservation reasons excitons formed through photo-excitation are necessarily singlets. Photoluminescence studies have found the radiative lifetime of a singlet exciton in Alq_3 to be ~16ns [11,13]. Even small organic molecules have a complex structure compared to traditional semiconductors. This structural complexity will naturally be reflected in the energy level structure of the molecule. Phonons also have a major impact on range of possible energies for a charge/exciton. Since organic molecules are not locked into a rigid structure they have the freedom to deform. Taking a single molecule and exciting a single electron can greatly change the local potentials experienced by the molecule, which will in turn cause the molecule to deform in response to the change in local potential. This deformation and change in potential will also affect the possible energies of a charge/exciton. Figure 1.3-2 shows a representation of the photo-excitation, phonon emission and photoluminescence of an electron within an energy level structure that is affected by multiple vibrational levels and molecular deformation.

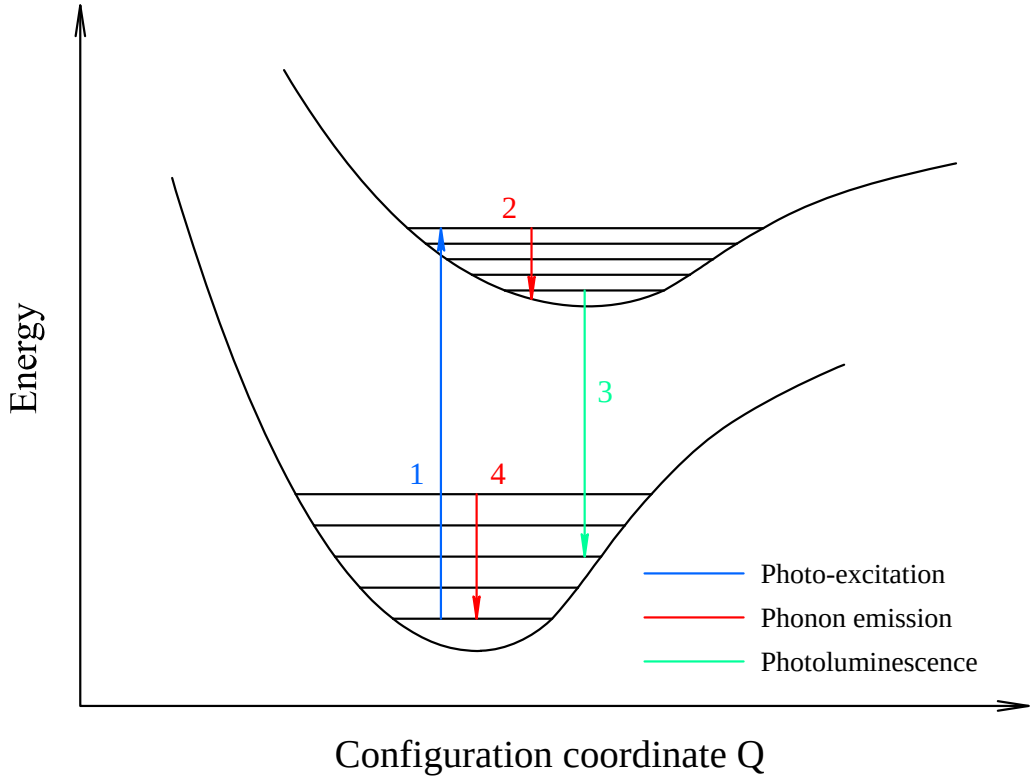

Figure 1.3-2: Schematic of Photoluminescence process

This figure represents (1) the photo-excitation from a ground state molecule to an excited state, (2+4) Phonon emission between vibrational levels, (3) Photoluminescence. The change in molecular potentials caused by the photo-excitation is indicated by the change in shape of the excited state potential and the shift along the configuration coordinate.

1.3.3 Electroluminescence

If a voltage is applied to an OLED electroluminescence (EL) is observed. Electroluminescence is subject to all the various considerations described in sections 1.2.2 and 1.2.3. Holes injected from the anode into the HOMO of the hole transport layer (HTL) meet with electrons that have been injected from the cathode into the LUMO of the electron transport/emission layer. Once both types of charge are present in the emission layer excitons may form. The orientation of spins within the anode and cathode are random, which means that the spins of the injected charge are also random. The random spin orientation of the injected charge means that exciton formation is solely governed by spin statistics. Spin statistics says that the formation of singlet and triplet excitons is equally probable under the condition that there are no external influences. So in the case of electroluminescence 25% of excitons formed are singlet and 75% of excitons

formed are triplets. This distribution of exciton populations has also been confirmed in Alq_3 OLEDs [14]. As with photoluminescence, electrically generated singlets will promptly recombine, emitting a photon. Due to spin conservation rules triplets cannot immediately recombine. As such triplets have a very long lifetime and are subject to quenching from non-radiative decay routes. The heavy quenching of triplet excitons means that luminescence from the triplet state is weak. Studies in the literature show that measurement of triplet luminescence can be observed when quenching is minimised through the use of a cryogen. Since quenching is seen to diminish with temperature the radiative lifetime of a triplet is also seen to vary with temperature [15]. As with the case of photoluminescence the large number of vibrational states is also important in electroluminescence, which is also reflected in electroluminescent spectra of organic molecules.

1.4 Magnetic field effects in OLEDs

Magnetic field effects in organic semiconductors have had a chronologically similar history to the development of OLEDs. Organic crystals such as anthracene and tetracene were studied using magnetic fields in the 1970s. During this period there was a flurry publications from various groups. This activity proved to be short lived and development largely diminished until the 1990s. While the development of modern OLEDs has seen wide spread research interest in modern organic semiconductors and electronic devices, research on the magnetic field effects of these materials and devices is still relatively immature. This section aims to provide the reader with a review of historical and current publications that are pertinent to magnetic field effects in OLEDs.

1.4.1 Early works on organic crystals

The effects of magnetic fields on organic semiconductors were first studied significantly in the late 1960s. Magnetic fields were shown to affect the luminescence from anthracene crystals by Merrifield [16] in 1967. In this study it was found that the intensity of delayed fluorescence was modulated when a magnetic field was applied. Fluorescence is radiative decay from singlet state

excitons, as such fluorescence is characterised by short lifetimes. Delayed fluorescence occurs when triplet-triplet annihilation (TTA) occurs to form an excited state singlet and a ground state singlet. The triplet-triplet annihilation and delayed fluorescence process is described by the following:

$$T_1 + T_1 \leftrightarrow (T_1 T_1) \leftrightarrow S_1^* + S_0 \rightarrow S_0 + \gamma \qquad \textbf{Equation 1.4-1}$$

Where T_1 is the first excited triplet state, S_1^* is the first excited singlet state, S_0 is the ground state singlet and γ is the energy lost through photon emission. While this process gives a photon from the singlet level, the decay lifetime is now dominated by the long-lived triplet precursors that went to form the singlet exciton. Hence this is why this type of decay is known as delayed fluorescence. In order to measure delayed fluorescence, Merrifield utilised long excitation wavelength photoluminescence techniques.

Merrifield found that upon the application of an external field the delayed fluorescence from anthracene would increase by up to 5% for fields of ~35mT. For fields greater than 35mT the delayed fluorescence was seen to decrease, by 500mT this decrease was 80%. It was said that there were four possible effects that could be the root of the modulation of the delayed fluorescence. One cause, the magnetic modulation of singlet decay, was ruled out because no magnetic field effect was seen on prompt fluorescence from the anthracene crystal. The magnetic field modulation of light absorption and triplet lifetime were ruled out through the measurement of transients when the magnetic field was pulsed. This leaves the magnetic modulation of triplet-triplet annihilation rate as the only viable cause. Despite this conclusion no mechanism was offered for how the TTA rate is modulated by an external field.

In 1968 work from this group reported that the lifetime of triplet decay could be increased upon the application of a magnetic field [17]. The experiment that led to this observation involved photoluminescence techniques to excite the anthracene. The photo-excitation of anthracene generates singlets, which are then able to undergo intersystem crossing into the triplet state. Paramagnetic centres (electrons or holes) were generated in the sample by exposing the organic crystal to x-rays.

Previous studies showed that x-rays could lower the triplet decay lifetime [18], Merrifield proposed that this occurs through the following interaction:

$$T_1 + D_{\pm 1/2} \xleftrightarrow{k_1} (T_1 \ldots D_{\pm 1/2}) \xrightarrow{k_2} D_{\pm 1/2} + S_0^* \qquad \textbf{Equation 1.4-2}$$

So the photo-excitation gave rise to a population of triplets and subsequent delayed fluorescence, while the x-rays gave rise to a population of paramagnetic centres ($D_{\pm 1/2}$). Merrifield found that applying a magnetic field to this system the delayed fluorescence lifetime and the inferred triplet lifetime was seen to increase. In order to explain this observation it was suggested that the interaction of triplet excitons with paramagnetic centres could be affected by an applied magnetic field.

The early 1970s saw further publications that demonstrated magnetic field effects on the photo-physics of organic crystals. Hyperfine effects on delayed fluorescence were also found to be significant in dye-sensitised anthracene crystals [19,20]. Again delayed fluorescence techniques were used; this time in combination with an organic dye that could greatly increase the triplet injection into anthracene. Data gathered on the delayed fluorescence as a function of applied field showed a similar form as the delayed fluorescence of non-sensitised anthracene [16]. A major difference, however, was that much lower fields were required to observe the same effects in a sensitised sample when compared to a non-sensitised sample. This smaller applied field scale was explained in terms of the hyperfine mixing between singlet and triplet states.

Local asymmetries experienced by the electron and hole in an exciton can lead to a mixing of the singlet and triplet states through the hyperfine interaction. In photo-excited, dye-sensitised anthracene it was found that the mixing of the singlet and triplet states was significantly increasing the triplet population and the subsequent delayed fluorescence. In these systems it was found that an applied field could diminish any asymmetry caused by the local environment upon the electron and hole within an exciton. Hence by applying an external field it was possible to diminish the transfer from singlets to triplets and see a subsequent drop in the delayed fluorescence.

1975 saw an early example of the magnetic field effects in an electrically pumped anthracene crystal by a group in Basle [21]. While previous studies demonstrated charge/exciton interactions with a single charge carrier, the Basle study was able to probe effects in a system with both holes and electrons. The simultaneous injection of electrons and holes gives a significant triplet population. As with the previous photoluminescence studies the triplets were studied through the measurement of delayed fluorescence. It was found that the application of a magnetic field was able to quench the delayed fluorescence, which is in agreement with the previous work of Merrifield. The cause of this was argued to be the enhancement of triplet-pair dissociation through charge carrier interactions.

These early works show how various field dependent mechanisms may affect exciton populations and exciton/charge-carrier interactions within organic materials, which gives a useful insight into charge transport within organic semiconducting materials. However, as previously mentioned, this early work remained largely undeveloped until interest in modern organic semiconductors was established.

1.4.2 Magnetic field effects on modern devices – A detailed survey

This section aims to provide the reader with a context for the research that is presented in chapter 3. As such, in this section a detailed review of the current literature on OMR and related magnetic field effects in modern OLEDs is presented.

In 1992 work by Frankevich [22] saw magnetic field effects on photo generated current in PPV derivatives. This work was not carried out on sandwich style devices but was instead configured with both contacts on one surface. Nevertheless, this study is an early example of magnetic effects in a modern organic semiconductor. The observed effect showed a sharp rise in photo current of ~3% for fields of ~4mT. For fields greater than 4mT the change in photocurrent was seen to plateau.

Magnetic field dependent mixing between charge pair states was used to explain the observed change in photocurrent, figure 1.4-1 shows the proposed energy level diagram that indicates the pair states possible above the ground state ($^1M_0$) and

rates between them. Excitonic states are described by $^1M_1$ and $^3M_1$ for singlet and triplet excitons respectively. Distinct from the excitonic states is a short range charge pair state ($p^+.p^-$). Above this lies a long range charge pair state ($p^+\ldots p^-$). At higher energies still, there are "well separated" charge pairs, which are effectively dissociated polarons. Each of the pair states, excitons, short range charge pair and long range charge pair has a singlet and triplet equivalent defined by the arrangements of spins within the pair. Frankevich states that hyperfine mixing of singlet and triplet pairs only occurs between long range polaron pairs. It is stated that in applying an external field the mixing between the long range pairs is reduced to the singlet and T_0 states, which reduces the population in T_{-1} and T_{+1}. It is argued this change in population actually increases the population of long range pairs that can go on to dissociate, hence the observed magnetically induced increase in photocurrent.

1996 saw an extension of this work where the magnetic field effects were used as a tool to study the nature of the photocurrent and dissociation mechanisms [23]. Frankevich reported that there were two dissociation mechanisms in play. One was electrically assisted thermalisation, as in the 1992 study, and was associated with "prompt" magnetic field effects. The second dissociation mechanism was associated with the discovery of a "delayed" magnetic field effect. This dissociation mechanism was attributed to the dissociation of singlets by molecular oxygen, photo-oxidation products and specially selected dopants. As such, this study did not greatly change the previously proposed model for magnetic modulation of photocurrent.

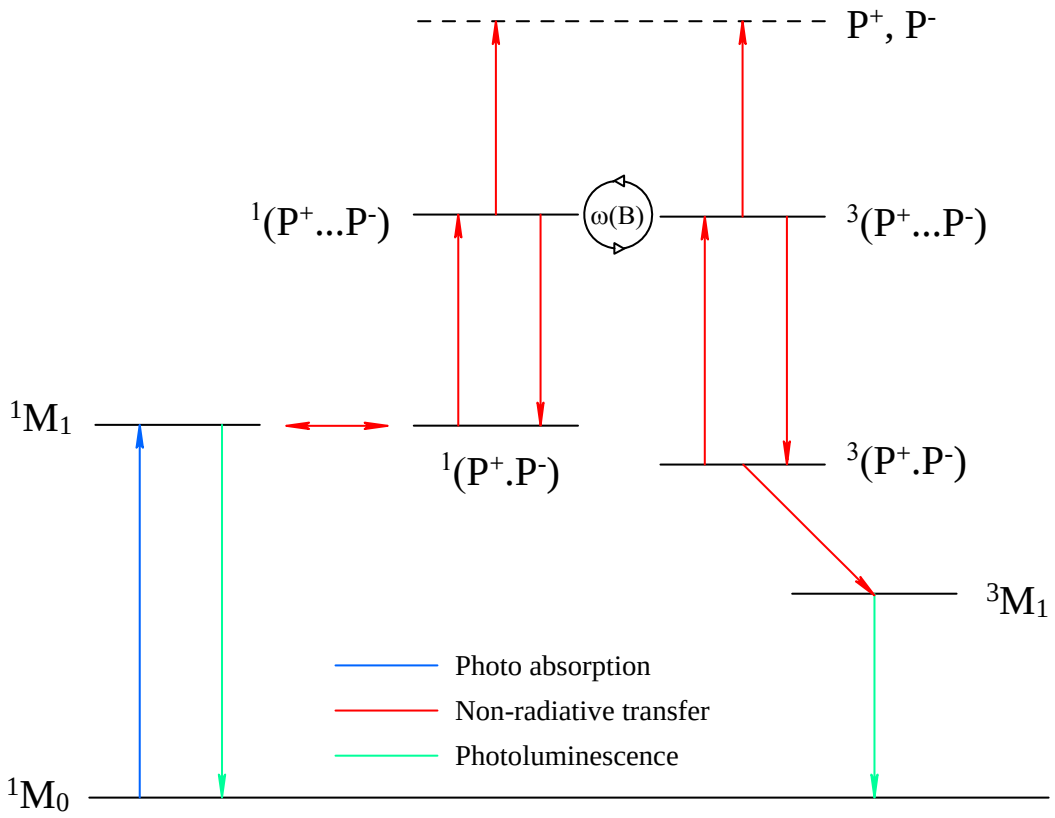

Figure 1.4-1: Frankevich schematic for magnetic modulation of photo-current

The schematic outlined above shows the various possible charge pair states and the transitions between them. Also indicated is the magnetic field dependent oscillation frequency (ω(B)) between the singlet-like long range pair state and the triplet-like long range pair state. This figure has been adapted from reference [22].

A similar model to that used by Frankevich was also used to explain the magnetic modulation of photocurrent in Al/Alq_3/Al sandwich devices by Kalinowski [24]. Photocurrents were found to sharply increase under fields of up to ~65mT and plateau or decrease for higher fields. The early work of Merrifield [20] formed part of the foundation of Kalinowski's proposed mechanism.

Kalinowski's view is summarised in the schematic shown in figure 1.4-2. In this scheme incident photons will lead to the formation of excited Alq_3 molecules, from which there is a branching into two pathways. One pathway is exciton decay, the excited Alq_3 molecules can either radiatively or non-radiatively decay, defined by k_{fl} and k_n respectively. Since the excited Alq_3 is photo-generated, it is naturally in the singlet state, which means there is no impediment to radiative decay. The other pathway for the excited Alq_3 state is to form a correlated pair state, ^{1}(e…h). Again this would naturally have a singlet characteristic due to the singlet nature of

the photo-generated Alq_3 excited state. From this pair state, Kalinowski states that there are three possible pathways. One is simply the reformation of an exciton and the associated excited Alq_3 state. The other is the dissociation of the pair state, defined by rate k_1, and giving rise to a free electron and hole. The third possibility is for the pair state to undergo some transition to a pair state with triplet character, ^{3}(e…h), which is defined by the rate k_{ST}. This triplet pair state can also dissociate with the rate k_3.

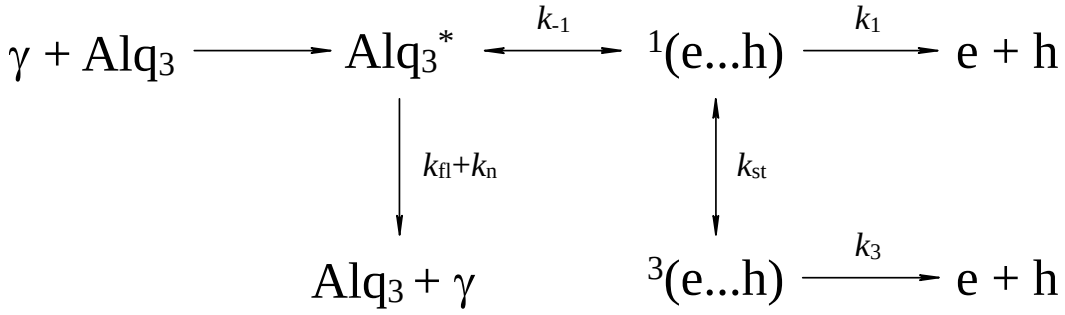

Figure 1.4-2: Kalinowski rate schematic for magnetic modulation of photo-current

The rate schematic outlined above is for a system in which charge carriers are being photo-generated. The various possible charge pair states and the transition rates between them are indicated. This figure has been adapted from reference [24].

Kalinowski argues that singlet pairs couple more strongly with charged molecules than triplets. Charged sites (i.e. polarons) could potentially act as dissociation centres, so if singlets are indeed coupled more strongly to charged sites they should have a higher dissociation rate. This leads to the assumption that $k_1 >> k_3$. Kalinowski does not acknowledge the role that the metal/organic interface might play in dissociation. The idea that singlets have a stronger coupling to charged sites seems to be based upon a theory which says that singlets are ionic in nature and triplets are covalent [25]. The theory was based upon polymeric systems and uses the term “ionic” for a (e…h) pair state or exciton that is bimolecular (i.e two oppositely charged molecules) and uses the term “covalent” for a pair that is monomolecular (i.e neutral).

Why singlets should be preferentially bimolecular and triplets monomolecular, is unclear and seems unintuitive. Indeed there are numerous studies where strong absorption and luminescence can be seen in organic solutions where there is a

large separation between molecules. If singlets are preferentially bimolecular then luminescence and absorption into these systems ought to be weak. It is possible that Kalinowski has misinterpreted and misapplied reference [25] or that the aspects of the theory in [25] concerning “ionic” and “covalent” excitons are erroneous. In either case, the conclusion drawn by Kalinowski that $k_1 >> k_3$ is somewhat dubious and any conclusions drawn from the assumption need to be analysed carefully.

In order to explain the observed increase in photocurrent with applied magnetic field Kalinowski used Zeeman and hyperfine effects to explain an increase in singlet population and their subsequent dissociation. In this model it is presumed that under null field the hyperfine mixing between the singlet pair state and the entire set of triplet pair states has a significant effect on the dissociation current. When a field is applied to the sample there is a splitting of the triplet pair state manifold into T_{+1}, T_0 and T_{-1}. Kalinowski states that at a high enough field the hyperfine mixing is reduced to associated energies and transfer rates. So it would be premature to assume a proof of principle without some quantitative evidence to show the transfer rates do proceed by Kalinowski’s model.

One particular question that is not addressed in the model is why it is assumed that transfer between the singlet and triplet manifolds occurs at the point of pair state formation rather than at the excitonic stage. If it is possible to transfer from a singlet exciton to a triplet exciton then it would then be necessary to factor in the effects of the decay rates from these two states, as well as the additional transfer from triplet exciton to triplet pair state. This obviously would make the model much more complicated.

Kalinowski’s group later extended this study to Alq_3 based OLEDs. This was the first reported observation that magnetic fields could modulate current in a non-ferromagnetic OLED and was presented in 2003 [26]. In this work it was shown that a magnetic field could modulate the light output by up to 5%, current through the device by up to 3% and efficiency by ~2%. The magnetic field was applied orthogonally to the current flow, but it was not stated if this was important. The device structure used in this study is very similar Tang and Van Slyke’s early example. The key difference between Kalinowski’s device and Tang and Van Slyke’s device is the use of a polymer matrix/Diamine derivative blend as the hole

transport layer [26,27]. Strangely the operating voltages used in reference [26] are significantly higher than the drive voltages used for seemingly identical devices in reference [27]. Despite this there is no reason to believe that the magnetic field effects and associated transport mechanisms in the OLEDs of reference [26] are significantly different to the photocurrent study of reference [24].

Since the exciton generation in an OLED is due to charge injection this naturally changes the rate schematic shown in figure 1.4-2 to the one shown in figure 1.4-3. The argument of hyperfine/Zeeman effects is again invoked to explain why an applied field increases the singlet like pair state and the hence increases the singlet exciton population. Kalinowski's data, which shows unequivocally that the luminescence and efficiency increase under an applied field, so it is natural that the view of an increase in singlet population is taken. Concluding that an increase in singlet population was the cause for increased luminescence naturally leads to the assumption that the magnetic field induced increase in current is also linked to the increase in the singlet population.

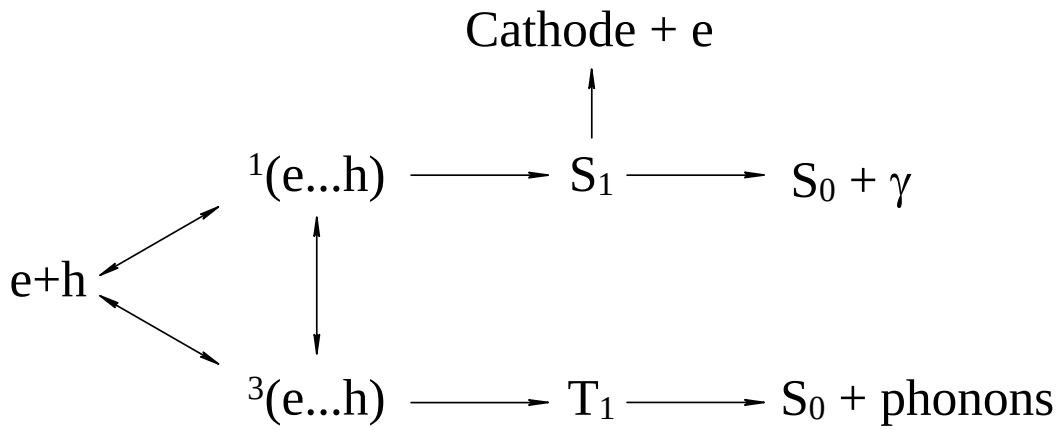

Figure 1.4-3: Kalinowski rate schematic for an Alq_3 OLED

The rate schematic outlined above is for a Alq_3 OLED in which injected charge carriers produce charge pair states. The various possible charge pair states and the transition rates between them are indicated. This figure has been adapted from reference [26].

Again, singlet dissociation and the subsequent release of charge is used to explain the increase in current. However, the nature of the singlet dissociation changed from the original reasons stated in reference [24]. Instead of using an argument based upon "ionic" or "covalent" pair states, Kalinowski states that it is exciton

diffusion to the cathode that leads to dissociation and a release of electrons back into the system. As stated earlier, dissociation at a cathode was completely neglected in the photocurrent study of reference [24] and it is not immediately clear why it should be relevant in an OLED but not in a photodiode. Since an increase in the singlet population is increasing at the expense of the triplet population, Kalinowksi takes the simple and logical view that it must be singlet dissociation that gives the increase in current.

When we take this idea of singlet exciton dissociation in combination with the rate schematic presented in figure 1.4-3 and reference [24], there are some peculiar omissions from the scheme. First, the scheme clearly states that a charge pair state is formed before exciton dissociation but neglects the dissociation rates that were so significant in the photo generation study scheme of figure 1.4-2 and reference [24]. There is no obvious structural or environmental reason why this is the case. Secondly, the photo generation scheme clearly states that there is mutual transfer between excitonic and charge pair states, which is neglected in the OLED scheme. Thirdly, as mentioned in reference to the photo generation scheme, there is no reason given as to why intersystem crossing only occurs between charge pair states, not excitonic states. Fourthly, the radiative decay rates from the singlet (k_s) and triplet (k_t) states have been neglected. Under the condition that either or both points two and three are valid, the decay rates k_s and k_t could prove to be significant since they will have a large impact upon the population of the singlet and triplet state.

In mid 2004 a publication from Davis and Bussman showed the magnetic field effects on electroluminescence for various Alq_3 based devices with the hole transport material N,N'-Di(napthalen-l-yl)-N,N'-diphenyl-benzidine (NPB) and differing anode/cathode combinations [28]. They were able to access a range of magnetic fields up to ~2T and stated that the observed effects were independent of angle for this entire range. Testing over this large range showed that for a device structure (ITO/NPB/Alq_3/Li/Al), similar to Kalinowski's, a positive effect on luminescence was seen. This proved to be the exception, for all other device structures, the measured trend was positive for low fields of <100mT, but then negative for increasing fields. The most remarkable of these devices was a device that only differed in anode material (Au/NPB/Alq_3/Li/Al) but showed a large

negative change in luminescence. Since the work functions of ITO and gold only differ by ~0.3eV it is not clear why this should have such an effect on the luminescence from Alq_3. The interpretation of Davis and Bussman's data is made complicated due to the large variety of electrode combinations and the randomness with which they appear to be presented.

The measured curves showed a trend towards saturation but this was not confirmed due to the experimental limitations. These negative trends in luminescence are very similar to the trends in luminescence seen for anthracene crystals. Naturally this led Davis and Bussman to propose that modulation of TTA was the cause as in the anthracene studies of Merrifield [16,19].

In order to test the effect of TTA transient measurements were performed. Comparing their results to a room temperature measure of the triplet lifetime [29] they argued that the response of the magnetic field effect was ~10 times too fast to be caused by TTA. It is important to note that all of the data presented in reference [28] was measured at 100K and it was acknowledged by the authors that the triplet lifetime at these temperatures was likely to be longer. Indeed this was confirmed shortly afterwards; the triplet lifetime is approximately three orders of magnitude longer [30]. This means that Davis and Bussman's measurements are more than $\sim 10^4$ times too fast for TTA. TTA was not ruled out; instead it was argued that short lived triplet entities could be playing some role.

Interestingly the low field effects seen by Davis and Bussman showed no temperature or drive condition dependence. To date this is the only study known by the author that shows negative changes in luminescence in a modern OLED, upon the application of a magnetic field.

The current interest in OMR began to take off following the work by Kalinowski with the publication of a study on poly(9,9-dioctylfluorenyl-2,7-diyl) (PFO) sandwich devices [31] in 2004 by Wohlgennant and his Iowa based group. Soon after the publication of the PFO study was published a similar study was published by the same group on Alq_3 based OLEDs [32]. These early studies are analogous and complimentary in their attempts to characterise OMR, and as such they will be presented here together.

In both of these early publications OMR was presented as the percentage change in resistance, given by:

$$\frac{\Delta R}{R} = \frac{R(B) - R(0)}{R(0)}$$

Equation 1.4-3

Where $R(B)$ is the device resistance at a given magnetic field and $R(0)$ is the device resistance at zero magnetic field. No indication was given regarding the transformation of the measured currents to resistance. This is significant considering that an OLED is non-Ohmic, which excludes the use of Ohm's law. Despite any possible misapplication of Ohm's law, or any other mistake in current to resistance conversion, it is safe to say that the shape of the OMR traces reported is accurate. However, the magnitudes of the traces could be incorrect and the polarity will be opposite to $\Delta I/I$ curves.

Figure 1.4-4 shows OMR scans for both PFO and Alq_3 that are taken from references [31,32]. It was stated that the OMR for both materials showed dependence on the angle of the magnetic field, which was in agreement with Davis and Bussman's results. To this date OMR is found to be independent of the angle of the magnetic field, which is unsurprising given the amorphous nature of the organic layers used in these OLEDs.

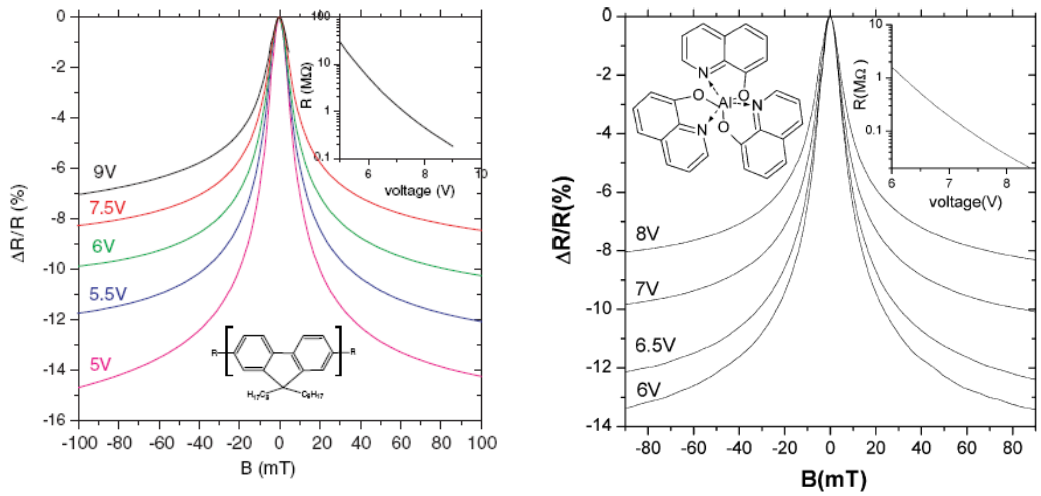

Figure 1.4-4: Literature results for OMR in PFO and Alq_3 OLEDs

Both of the above graphs show the OMR results for a device based on the structure ITO/PEDOT (~100nm)/working layer)/Ca (~50nm). The working layers are denoted by the molecular diagrams in each pane, PFO (left), Alq_3 (right). The thickness of the PFO and Alq_3 layers is ~100nm and ~50nm respectively.

Comparing the shapes of Alq_3 OMR results from Iowa and Kalinowski a clear pattern emerges concerning the nature of OMR response. Both groups report OMR data that shows a sharp rise, which is followed by a flattening for fields greater than ~40mT. The Iowa group showed that the magnitude of OMR in both Alq_3 and PFO devices was ~10%. This is much higher than the results published by Kalinowski, who only observe OMR of ~2.5%. The device structures used by the two groups do vary slightly in that Kalinowksi uses an organic hole transport layer while the Iowa group uses an organic anode. This difference in device structure between the two groups could account for the discrepancy in OMR results.

In the PFO study, data is presented that shows no appreciable difference in the functional form or magnitude when compared with the Alq_3 data of reference [32]. This study also compared devices with differing PFO thicknesses, again relatively little difference was found. Similar results were claimed, but not presented in the Alq_3 study. Aside from thickness, the only other difference between the Alq_3 and PFO devices was the voltage regime that the devices were operated under. If correct this means the discrepancy between Kalinowski's Alq_3 results and the Iowa group's results is due to the operating voltage or the choice of hole transport/anode material and not due to the Alq_3 thickness. The results gained from varying the device thickness led to the conclusion that OMR must be due to bulk effects and not electrode interface.

As well as studying the effect of the organic layer thickness, both of the Iowa studies on Alq_3 and PFO presented results on the effects of varying the electrode materials. The Iowa group states that the OMR in PFO results show that in changing the anode there is little difference in between the use of an ITO or Au contact when either is compared with a poly(3,4-ethylenedioxythiophene) poly(styrenesulfonate) (PEDOT) anode. The use of Al, Au and Ca cathodes on PFO was also studied but not fully presented and it was merely stated that changing the cathode had no appreciable effect. Since changing the anode had an effect and the changing the cathode had no effect it was argued that OMR in PFO is due to an effect related to the hole current.

The results of an ITO/PFO/Au device were highlighted as evidence for the view that the OMR in PFO was due to holes. Since Au has a work-function that is more suited to hole injection it makes a poor cathode, as such the ITO/PFO/Au device

was described as “hole only”. OMR was still measurable in these devices, hence it was argued that OMR must be due to hole transport. Strangely it was also argued that the device demonstrated “very weak electroluminescence”. How a “hole only” device can demonstrate any electroluminescence was not addressed. Further questions are raised when comparing these results to the analogous results in Alq_3. Alq_3 has opposite charge transport properties compared with PFO, specifically relating to the hole mobility (μ_h) and electron mobility (μ_e). In Alq_3 $\mu_h << \mu_e$ [8], whereas the opposite is true in PFO, where $\mu_h >> \mu_e$ [33]. Since the mobilities in these two materials have the opposite relation it was expected that Alq_3 devices would be largely dependent upon electron current and not the hole current like in PFO. Thus, Alq_3 devices should show variance of OMR when changing the cathode material, and should show little change in OMR when changing the anode. This rationale neglects that the majority/minority carriers in a sandwich device are determined by the potential barrier defined by work-function of the cathodes.

The results for the cathode study on Alq_3 show that OMR is observed with cathodes of Ca, Al and Au. Similar magnitudes of OMR are observed for Ca devices operated at ~10V and Al devices operated at ~30V. The OMR for Au devices was diminished and required operating voltages of ~55V. These results were described by the Iowa group as showing that “OMR responses critically depend upon the choice of electron-injecting cathode material”. In changing the anode material similar results were found. PEDOT/Alq_3/Ca devices and ITO/Alq_3/Ca devices showed similar OMR, but ITO required higher operating voltages to achieve this. Confusingly it then stated that OMR is independent of anode material, despite the direct comparison that can be drawn with the cathode results.

To add to this confusion, in the same paper, within the same paragraph it is said that “holes also play a role [in OMR], at least in determining the onset voltage”. The acknowledgement that holes play a role in Alq_3 OMR is again reiterated in the conclusion of this paper. So, despite comparable results for PFO and Alq_3 it was concluded that PFO OMR was due to holes and Alq_3 OMR was due to electrons and holes.

As well as studying the effect of various electrodes on Alq_3 OMR, reference [32] also presented the percentage change in electroluminescence with magnetic field. This change in electroluminescence was studied in two operating modes, which were constant current and constant voltage. For simplicity the percentage change in electroluminescence under constant current/constant voltage will be denoted by $\%EL_I$ and $\%EL_V$ respectively. Both of these quantities were measured in order to "directly measure the magnetic field effect on η_{EL}", where η_{EL} is the electroluminescent quantum efficiency. It was stated that $\%EL_I << \%EL_V$ and as such it was stated that the change in luminescence was a direct consequence of the change in current. The implication of this is that magnetic field does not effect efficiency. Again there appears to be a discrepancy between the published results and the conclusion. If indeed $\%EL_I << \%EL_V$, this does not mean that $\%EL_I$ is zero. In fact, closer inspection of the published results shows that $\%EL_I$ is only a factor of ~5 different from $\%EL_V$. In measuring I, V and EL the group had enough information to calculate the external efficiency, which directly relates to the quantum efficiency. Hence there was a direct way to show the precise nature of a magnetic modulation of efficiency, but it was either not done, or not presented. Also, Kalinowski showed that there is a clear change in the efficiency of an Alq_3 OLED. So it is possible that efficiency and associated excitonic effects have been prematurely neglected in references [31] and [32].

Another observation made by the Iowa group was noting the remarkable similarity between Alq_3 and PFO OMR traces. Example data from both materials was normalised with respect with one another and showed well matched traces with negligible deviation. This matching was referred to as "universality". It was rightly pointed out that it was not obvious why Alq_3 (small molecule) should display functionally identical OMR to PFO (polymer). Alq_3 and PFO have very different chemical structures, which gives rise to very different local environments and subsequent charge transport. This is borne out by the differences in charge mobilities between the two materials. Given these differences the Iowa group states that there must be a general mechanism for OMR in which material properties are not significant.

Following these two early works from Iowa, another broader study of OMR was published by the same group [34]. One notable aspect of this paper was the discussion of positive and negative OMR. While the group had previously shown that both directions of OMR were possible [32], it had not been discussed to any significant degree until the publication of reference [34].

Under the $\Delta R/R$ definition of magnetoresistance, a negative trend is usually observed, as was the case in the previous studies [31,32]. Positive OMR was observed in several polymeric systems, with the transition from negative to positive OMR occurring as applied voltage was increased. Careful study of the transition region was not carried out for PFO devices because "irreversible changes often occurred to the devices at the large current densities usually needed for crossover". This can be surmised as an admission that, for a given device, this cross over behaviour was not reproducible. It is well known that organic semiconductors will indeed undergo irreversible and even catastrophic changes if they are driven too hard. Interestingly no transition is observed when PEDOT is used instead of ITO, so possibly the negative OMR is due to the change in interface or charge balance.

In the same publication data on regio-regular poly(3-hexylthiophene-2,5-diyl) (RR-P3HT) is presented with greater resolution in the crossover region between positive and negative OMR. For RR-P3HT devices the transition seems to occur opposite of PFO, i.e. as voltage is increased OMR goes from positive to negative. However this is not completely consistent or conclusive since data is also shown at 100K where the negative OMR response appears to reduce towards zero with increasing voltage, which is similar to the 300K PFO results.

It is suggested that the observation of positive/negative OMR in RR-P3HT is largely due to temperature. However, the work presented shows data at several temperatures with each in a different voltage regime, so it is not certain whether temperature or current density is crucial. This ambiguity is further compounded by the inconsistency of the 100K data. Also it is not mentioned if the RR-P3HT devices suffer from the same reproducibility problems of the PFO devices.

The lack of reproducibility casts great doubt over the validity of the data after the crossover from negative to positive. Despite this the Iowa group were confident

enough to say that any theory for OMR will have to be able to explain both positive and negative OMR traces.

Within reference [34] the effects of spin-orbit coupling in OMR is also studied. This was achieved through the use of polyphenylene ethynelene (PPE) diodes in comparison with heavy metal containing Pt-PPE devices. The inclusion of platinum in Pt-PPE is stated as having no effect on the conjugation of PPE. Also the platinum does show good phosphorescence, hence a greater crossing from singlet to triplet state. So in studying the effect of increased spin orbit coupling, the comparison of PPE and Pt-PPE is a good one.

It was found that the OMR of Pt-PPE was lower then that of PPE. Despite a diminished OMR it was concluded that there was no effect due to spin and thus no effect due to intersystem crossing between excitons. Again, the presented data was seemingly random and showed no consistency between temperatures or current density. This is not to say that the conclusion drawn is incorrect, but merely that the reasoning is inconclusive, especially given the stronger evidence for excitonic conversion effects presented by Kalinowksi and Frankevich.

Reference [34] also expands on the concept of universality that was first highlighted in reference [32]. Normalised OMR traces of seven different organic semiconductors were compared and all were found to have one of two shapes. These shapes were categorised into “fully saturated” and “weakly saturated”. Accompanying the identification of these OMR types was an attempt to model the functional form. Two equations are given to fit the two functional forms:

$$\frac{\Delta I}{I} = \left(\frac{\Delta I}{I}\right)_{\max} \cdot \left[\frac{B}{B + B_0}\right]^2 \qquad \textbf{Equation 1.4-4}$$

$$\frac{\Delta I}{I} = \left(\frac{\Delta I}{I}\right)_{\max} \cdot \left[\frac{B^2}{B^2 + B_0^2}\right] \qquad \textbf{Equation 1.4-5}$$

Where $\Delta I/I$ is the percentage change in current through the device (the subscript max indicates the change at infinite field), B is the applied field and B_0 is the quarter saturation field. Unlike the experimental data these equations are presented in terms of current rather than resistance. Both of these curves are empirical and no physical significance is implied. Figure 1.4-5 is taken from

reference [34] and shows normalised examples of “weakly” and “fully saturated” $\Delta R/R$ curves for several materials.

Figure 1.4-5: Example of “fully saturated” and “weakly saturated” OMR.

Figure is taken from reference [34] and demonstrates how OMR for various molecules fall into one of two categories; “weakly saturated” and “fully saturated”. Regio-random/regular are in reference to P3HT. “Weakly saturated” and “fully saturated” curves are said to be described by equation 1.4-4 and equation 1.4-5 respectively.

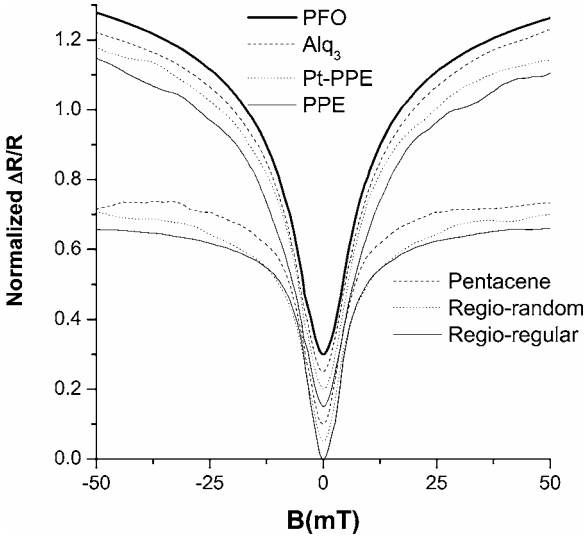

Equation 1.4-4 was shown to fit a PFO OMR curve that weakly saturates, however equation 1.4-5 was shown to fit a RR-P3HT curve that fully saturates. Both fits are presented on a log/log plot and appear to show good fits to ~300mT. However the nature of the log/log plot is to display a wide range of magnitudes at the expense of resolution. So the quality of the fits cannot be verified. None of the OMR plots presented contain fine structure that is separated by orders of magnitude so why a log/log plot was chosen is unclear. Neither of these two equations is capable of fitting OMR curves that show a transition from negative to positive OMR. So the conclusion drawn from equation 1.4-4 and equation 1.4-5 is that the “universality” of OMR is described by two curves that do not fully apply to all of the observable OMR.

In 2006 Prigodin published a study in which the role of spin-orbit coupling on OMR was studied [35]. The motivation for this study was to test a model for OMR that is similar to the model proposed by Kalinowski. In this model intersystem crossing between singlet like charge pairs and triplet like charge pairs is limited to $S_0 \rightarrow T_0$ under the application of a magnetic field. The argument is that the reduction in intersystem crossing reduces the recombination rate of the pairs, which ultimately increases dissociation. If spin-orbit coupling is increased then this should restore the intersystem crossing between the singlet state and the

entirety of the triplet manifold. Thus, increasing spin-orbit coupling should mitigate the effect of the magnetic field and reduce OMR.

The devices used by Prigodin for the study were identical to the Alq_3 devices (PEDOT/Alq_3/Ca/Al) used by the Iowa group. In order to vary the spin-orbit coupling the heavy metal dopants Iridium tris(2.phenylpyridine) ($Ir(ppy)_3$) and Platinum 2,3,7,8,12,13,17,18-octaethyl-21*H*,23*H*-porphine (PtOEP) were co-deposited with the Alq_3. The OMR traces for these devices did indeed show that for heavier dopants the OMR response decreases. As such it was concluded that spin-orbit coupling is indeed relevant to OMR. The implication of Prigodin's model is that singlet dissociation is responsible for the increase in current. So the same questions that are raised by Kalinowski's model are also applicable to Prigodin's view.

Prigodin also concludes that negative OMR ($\Delta R/R$ definition) is more probable than positive OMR since the proposed model requires the suppression of the singlet channel to achieve positive OMR. This is obviously inconsistent with the results of the Iowa group, who showed positive/negative OMR is easily achieved with the right combination of temperature and drive voltage. However, as previously indicated, the Iowa study was not conclusive, so it is not clear if either view is correct. Another major disparity between Prigodin's conclusions and other published data concerns OMR as a function of voltage. It is stated that they expect OMR to "increase with electric field and experimentally this type of dependence is observed". Prigodin presents no data that is relevant to this statement meaning that it must be in reference to the literature. However the Iowa study explicitly demonstrates devices in which OMR peaks and decreases, as well as devices in which OMR decreases as a function of voltage.

Shortly after Prigodin's publication the group from Iowa released another publication on the role of the hyperfine interaction in OMR [36]. In this paper is a more thorough presentation of the empirical equation 1.4-4 and equation 1.4-5. As such, OMR data in this paper is presented as $\Delta I/I$, as are subsequent publications from this group.

The equations are compared to the results of several groups who have published data on magnetic effects on current, electroluminescence and delayed

fluorescence in various organic systems. On first glance the fits to the data appear to be good. However on closer inspection the reader will realise that equation 1.4-4 and equation 1.4-5 have been arbitrarily applied based on quality of fit rather than on physical reasoning.

Also shown in this paper is the derivation of equation 1.4-5 from the hyperfine Hamiltonian. An origin for equation 1.4-4 is conceded as a problem that is yet to be solved. The B_0 term in equation 1.4-5 is linked by the authors to theoretical work in radical chemistry. The resulting relation given by the Iowa group is:

$$B_0 = \sqrt{3}\left(\sum_i a_{H,i}^2\right)^2 \qquad \textbf{Equation 1.4-6}$$

In this relation $a_{H,i}$ is the hyperfine splitting constant.

The comparison between B_0 and $a_{H,i}$ is made so that measured B_0 values can be compared with B_0 values calculated from published values of $a_{H,i}$. The paper then states that there is disagreement between the measured and calculated values. However, in order to justify this statement only one set of data for pentacene is actually compared.

Another discrepancy between the measured values for B_0 and theory that is highlighted in the paper is that theory predicts dissimilar values of B_0 for small molecules and polymers. Results in the literature to this point have already established that the OMR response of small molecules and polymers is similar. If we take this comparison of B_0 and $a_{H,i}$ and subsequent analysis at face value then the logical conclusion would be that the role of hyperfine effects in OMR is questionable. However these conclusions are based upon equations that have no physical explanation. While equation 1.4-5 is shown to stem from the hyperfine Hamiltonian this does not constitute a physical mechanism because there is no link provided by the authors that shows how hyperfine effects could affect OMR. So to then take terms from this equation and make physical conclusions seems optimistic. This is especially true when the equations seem to be applied on criteria based upon convenience rather than physical reasoning.

Since the hyperfine interaction plays such an important role in models proposed by Frankevich and Kalinowski (referred to as the pair mechanism model) it was also natural for the Iowa group to also address this. Calculations are presented that

form the basis of a claim that the pair mechanism model yields only a small and necessarily positive effect, which contradicts the data presented in previous publications. Another key argument against the pair mechanism model is made with the presentation of a comparison of $\Delta I/I$ with the internal quantum efficiency. The internal quantum efficiency (η_1) is defined as the exciton/charge carrier ratio. If OMR is dependent upon excitonic pairs then it would be expected that OMR should scale with the internal quantum efficiency. Data was presented showing that $\Delta I/I$ does indeed with rise with efficiency, with the following relation:

$$\Delta I/I \propto \eta_1^{\alpha}$$ **Equation 1.4-7**

Where α is a numeric value that ranges from 1/3 to 1/2. Despite the trend the conclusion drawn was that the relation was not linear and thus too weak for OMR to be excitonic. Again this seems to be an over extension of the presented data, due to several inconsistencies. First, it is stated that the internal quantum efficiency is taken from an electroluminescence versus current plot. The measured electroluminescence was presented in arbitrary units, which is by no means an absolute measure of emitted excitons. So to make a quantitative conclusion from this measure is dubious. Secondly, the views on OMR mechanisms presented by Kalinowski, Frankevich and Prigodin are qualitative. So it is seems to be an assumption that $\Delta I/I$ should be linear with efficiency. However, as previously noted there are flaws with the views of Kalinowski, Frankevich and Prigodin. This brings us to a third flaw with the conclusions of the Iowa group. If their conclusions concerning the magnitude, polarity and efficiency relationship of OMR are correct, this is only evidence to say that the pair mechanism model is incorrect. Their data does not conclusively rule out all excitonic effects.

Early in 2007 another publication was released by the Iowa group [37] that detailed the results of magnetic field effects in current, electroluminescence and photoconduction of both Alq_3 and PFO based devices. Asides from the photocurrent results, the data and subsequent arguments presented in this paper are identical to what had already been published in reference [31,32,36]. The photocurrent data showed that results of Kalinowski were correct insofar as the

magnetic response of current, electroluminescence and photocurrent were functionally similar. In addition to the previous arguments made against excitonic OMR mechanisms, it was also argued that the magnetic field affected the mobility of charge carriers rather than carrier recombination. This argument followed from the idea that current, electroluminescence and photocurrent are functions of mobility. Another important reference in this paper is the first mention of a proposed mechanism for OMR by the Iowa group. Few details are given, other than the mentioning that it involves the formation of sites that are occupied by two like carriers. No further details were given in this paper.

Another paper from the Iowa group was published in parallel with reference [37]. In this paper [38] spin orbit coupling is probed. This paper is superseded by the publication of another paper by the same group the following month. In this later publication [39] identical data to that found in reference [38] is presented with greater discussion and comparison to other materials. As such reference [38] will not be discussed in detail here. In an extension of the hyperfine study in reference [36] reference [39] is a further study on hyperfine and spin-orbit effects in OMR and was published by the Iowa group in February 2007.

In order to probe hyperfine effects several devices were fabricated using fullerenes (C_{60}), which due to their structure contain no hydrogen atoms. No OMR was found in C_{60} devices with Au or ITO used as the anode. When a PEDOT layer is used as the anode a small positive OMR is observed. The natural question to this is whether or not this OMR is caused by the hydrogen in the PEDOT. To address this OMR data on identical structures without the C_{60} is presented. OMR curves for the PEDOT only devices are of a similar magnitude but negative rather than positive. If the PEDOT is responsible for OMR in both the PEDOT/C_{60} and PEDOT only device it would be expected that the OMR responses should have a similar magnitude and polarity. This switch in polarity is dismissed by a referral to their previous OMR data that shows a switch in OMR polarity can be achieved merely by varying the driving conditions. Besides the flaws previously stated with this view, the data published for both the PEDOT/C_{60} and PEDOT only device show remarkably similar variations with temperature and drive voltage. So the inconsistency between OMR in PEDOT only and PEDOT/C_{60} devices cannot be dismissed by a drive condition argument. Also if it the polarity switch in OMR

was due to drive conditions then it should be trivial to test for this. Data from any such testing is not presented. One possibility that is overlooked is the role of C_{60} in the switch from positive to negative OMR. While it is not conclusive whether C_{60} has an intrinsic OMR or not, it seems likely that it is playing some role, possibly related to interfaces.

The PEDOT results also raise the question of how the usage of PEDOT may have affected the OMR results in references [31-34, 36-38]. It is possible that instead of measuring intrinsic OMR of single organic layers, the Iowa group was actually measuring the combined OMR of the primary organic layer plus the OMR of PEDOT.

In order to probe spin-orbit effects the Iowa group used the same heavy mass molecules as Prigodin. Instead of using $Ir(ppy)_3$ and PtOEP as dopants they were used purely as the functional layer. As before these devices were based on PEDOT anodes and Ca cathodes giving a structure of ITO/PEDOT/heavy metal complex/Ca. Strangely, the results did not agree with the results of Prigodin. Instead of showing a diminishing OMR for increased spin-orbit coupling, there was a completely different and previously unseen magnetic field response. Both the $Ir(ppy)_3$ and PtOEP showed OMR traces with what appeared to be a sum of at least two different curves.

Previously the group had stated that equation 1.4-4 and equation 1.4-5 could describe all observed OMR. The new results showed traces that seem to follow these functional forms at low magnetic fields but then deviate against the initial trend at high magnetic fields. This data is not addressed in the context of equation 1.4-4 or equation 1.4-5. Clearly the results for $Ir(ppy)_3$ and PtOEP devices show that the mechanisms for OMR are not as simple as previously implied by the Iowa group.

Interestingly the same $Ir(ppy)_3$ data published in reference [38] is fitted with a linear combination of equation 1.4-4 and equation 1.4-5. Good fits to the data were achieved and it was suggested that the low field process was due to hyperfine effects, while the large field process was due to spin-orbit effects. While these conclusions were repeated in reference [39], the fitting of the curves was not. This is likely because the high field process in PtOEP looks linear and could not be fitted in the same way as the $Ir(ppy)_3$ data.

One major conclusion to come from these two works [38,39] is that the results of C_{60} devices implies that "hydrogen, specifically hyperfine coupling" is a necessary pre-requisite for OMR. A second major conclusion is that "experiments prove that OMR is caused by spin-dynamics".

Late 2007 saw the publication of a new model for OMR based on spin-dynamics [40]. This work was a collaborative effort from the Iowa group and researchers from the "Technische Universiteit Eindhoven". Their model was based around the principle of bipolaron formation. Charges hopping throughout an organic semiconductor can either hop onto an empty site, forming a polaron, or hop onto an occupied site, forming a bipolaron. In the case of polaron formation/hopping there is no barrier to movement beyond the normal energetics. For bipolaron formation there are spin selection rules that determine whether or not a charge can hop onto a site with an existing polaron. It is stated that in order to satisfy Pauli's exclusion principle bipolarons can only be formed in a singlet configuration, i.e. that the spins are oppositely aligned [37]. These criteria for bipolaron formation are in effect a spin blocking mechanism that will ultimately hinder charge transport. Reference [37] also mentions that under the application of a magnetic field the Zeeman states become mixed due to hyperfine interactions. This mixing partially lifts the exclusion due to Pauli's principle; hence applying a field reduces the spin blocking mechanism, which leads to an increase in current.

In this model the OMR will ultimately be dependent upon the probability of forming a singlet like bipolaron. It is stated that the probability of singlet bipolaron formation is defined by the local field experienced by the individual carriers. The local field is the sum of the fields due to hydrogen dipoles and the external field. Hence the probability of singlet bipolaron formation is ultimately a function of the applied external field. So, external field affects singlet bipolaron formation, which in turn affects current; by definition this is OMR.

Monte Carlo simulations were performed in order to generate OMR curves from this model. The results were able to simulate both positive and negative OMR curves that could be fitted with either equation 1.4-4 or equation 1.4-5. It is obviously encouraging that the Monte Carlo results can be fitted with the same functions as actual measured OMR. However the study does not perform the logical step of comparing the model with actual data. Also, from this study it is

not clear how the model accounts for OMR traces that show multiple components, such as the $Ir(ppy)_3$ or PtEOP results. Another possible flaw with this model is that you would only expect bipolaron formation to be a significant factor when the polaron density is comparable to the molecular density of the device. If they are not comparable you would expect there to be too many competing transport routes for bipolaron formation to be significant.

Also in early 2007, a group from the University of Tennessee released a paper that explored several ways in which OMR could be affected [41]. Their devices were based on a weak spin-orbit coupling polymer poly(N-vinyl carbazole) (PVK) and the heavy spin-orbit coupling $Ir(ppy)_3$. One of the first things that were investigated was the role of device structure. The PVK and $Ir(ppy)_3$ devices were fabricated with either the materials blended with various levels of concentration, or with the materials arranged in a sandwich structure. In agreement with the results of Prigodin it was found that OMR decreased as the concentration of $Ir(ppy)_3$ was increased in the blended devices. Zero OMR was seen for a 100% $Ir(ppy)_3$ OLED of structure ITO/$Ir(ppy)_3$/Al; however it is not clear if this structure produces good diodes. If the structure does not yield a good diode then the lack of OMR could be coincidental.

The results of the sandwich layer device showed that for a constant thickness of $Ir(ppy)_3$ changes in the PVK thickness could also change the overall OMR of the device. It was found that decreasing the PVK thickness also decreased the OMR. Since the OMR dropped towards zero for thinner layers of PVK these results are in agreement that OMR is a bulk effect. The results of the blended films and sandwich devices were used to argue that some intermolecular effect at the interface of the two materials is actually affecting the OMR of the device. Two mechanisms were identified that could be having an effect on the OMR, namely energy transfer and spin-orbit coupling between the two materials. Both mechanisms were studied and both were found to have an individual effect on OMR. It was stated in the paper that excited states significantly contribute to OMR, which is in agreement with the views of Kalinowski, Prigodin and Frankevich.

At the end of 2007 the Eindhoven group published a letter distinguishing between the nature of positive and negative OMR [42]. In this study devices were fabricated with a structure of ITO/PEDOT:PSS/Alq_3/LiF/Al. Using low frequency admittance measurements it is claimed that the presence of "minority" charge carriers could be determined. Their results show that the transition voltage (V_{tr}) from positive to negative OMR is coincidental with an upward inflection in the IV characteristics of their devices. It is also claimed that V_{tr} is coincident with the onset of minority charge carrier observation determined using the low frequency admittance technique. The conclusion drawn was that V_{tr} is also the point at which charge transport moves from unipolar to bipolar. This evidence obviously contradicts OMR models based on excitonic effects and is used by the authors to support the bipolaron model. This study not only appears to contradict excitonic models but also a large body of literature that shows PEDOT:PSS to be an efficient hole injector. The values quoted for V_{tr} and associated minority charge injection is remarkably high. PEDOT:PSS is shown to have very efficient hole injection in many systems including Alq_3 OLEDs, which ultimately leads to low turn-on voltages [43,44]. A more direct and obvious technique for bipolar charge injection is luminescent measurements. This was either not done or presented with the low frequency admittance results. As such the conclusions drawn from this study are highly dubious.

In February 2008 the Ohio group of Prigodin published a paper analysing the effects of drive voltage, device thickness and temperature on OMR [45]. As with reference [35] they found that through the modulation of these three variables it was possible to see a wide range of OMR shapes, transitions from positive to negative OMR and vice versa. While data of this kind has been seen before, the unique thing in this publication was the presentation of these results with a comparison to existing Space-Charge Limited Current (SCLC) equations.

Crucial to this analysis is the concept of recombination mobility (μ_r) modulation through the inter-conversion of singlets and triplets. Hyperfine interactions and Zeeman splitting were cited as the mechanisms through which an applied magnetic field can affect the intersystem crossing. Current density was linked to μ_r through the following equation that was originally adapted from reference [46]:

$$J = \frac{3\varepsilon}{4}\left[\frac{2\pi\mu_e\mu_h(\mu_e+\mu_h)}{\mu_r}\right]^{1/2}\left(\frac{V^2}{d^3}\right)$$ **Equation 1.4-8**

Where J is the current density, ε the dielectric constant, V is the potential across the organic layer, d is the layer thickness, while μ_e, and μ_h are the electron and hole mobilities respectively. It was stated that for small changes in μ_r there is a linear dependence between J and μ_r which gives:

$$J = \mu_r dnp\left(\frac{2e^2}{\varepsilon}\right)e^{(eV/k_bT)}$$ **Equation 1.4-9**

Where n and p are the negative (electron) and positive (hole) carrier densities respectively. These two current regimes are said to cross over at some critical value of μ_r that is derived from equation 1.4-8 and equation 1.4-9. It is obvious from these equations that changing applied voltage, device thickness and temperature will naturally change the shapes of curves that follow the relations set out in equation 1.4-8 and equation 1.4-9 and hence change the crossover between the two. Figure 1.4-6 shows J versus μ_r for several different crossover values, with a shaded region giving an example of a change in μ_r.

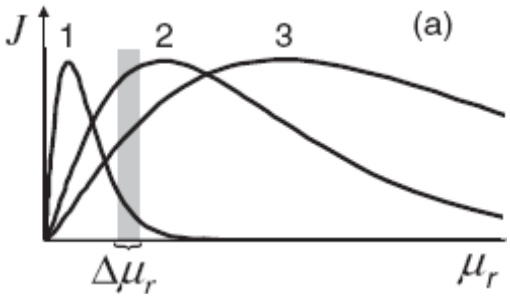

Figure 1.4-6: OLED current density versus recombination mobility

This figure shows how a specific change in μ_r can give a negative OMR (curve 1) or a positive OMR (curve 3). The shape of each curve is determined by a crossover between equation 1.4-8 and equation 1.4-9.

Taking this small magnetically induced change in μ_r, it is argued that the parameters V, d and T will determine whether $\Delta\mu_r$ will lie in the current region described by equation 1.4-9, the crossover region or the region defined by equation 1.4-8. Equation 1.4-9 is linear with a positive gradient so this will give a positive change in current, hence a positive OMR; this is indicated by the overlap of shaded region and curve 3 in figure 1.4-6. Equation 1.4-8 is nonlinear with a

negative gradient so will give a drop in current, hence a negative OMR; this is indicated in figure 1.4-6 by the overlap of the shaded region with curve 1. For $\Delta\mu_r$ that lies in the crossover region a small OMR with a transition between positive and negative is possible.

1.5 Synopsis and motivations

So in synopsis we can see that despite the relative youth of OMR research there is much activity, publication and contention. Even the basic nature of OMR is unclear, with some groups pointing to bulk effects, while others demonstrate that interfaces play some role. Questions regarding the polarity of OMR are also contested; with some showing either is easily achievable, while others claim the contrary.

Related magnetic field effects concerning luminescence are also disputed. Arguments are put forward that state changes in luminescence are merely a consequence of the magnetic change in current. At the same time some groups show that the external efficiency clearly modulates with magnetic field. These two views are clearly incompatible.

With the very nature of OMR and related effects so poorly agreed upon it is no surprise that there is even greater contention of the fundamental mechanisms of OMR. There are studies that claim excitonic effects, particularly concerning singlet dissociation, are the root cause of OMR. There are also studies that claim excitonic mechanisms are necessarily excluded. More recently the bipolaron model has been promoted as an alternative to excitonic mechanisms.

Despite the disagreements that are evident in the literature there do appear to be common views held between the small number of groups active in OMR research. All the mechanisms and effects relating to OMR are argued in terms of spin dynamics. To date all the publications on OMR seem to be consistent with the view that studies on OMR could lead alternate insights into charge transport mechanisms in organic semiconductors. In particular OMR in OLEDs seems to be providing an insight into charge transport in the presence of excited states. This is significant for two reasons, first, charge transport in the presence of excited states is another area of organic electronics that has received relatively little attention

since the 1970s. Secondly the understanding of charge transport in the presence of excited states is crucial to the understanding of charge transport through OLEDs. Asides from these significant and fundamental motivations for the study of OMR there is also the possibility of novel device applications that utilise OMR effects.

2 Experimental methods

In this section the processes for both sample preparation and experimental methods are described. As the techniques for sample preparation are well established and not unique to this document, only the basic steps will be explained with reference. In the later part of this chapter the experimental setups will be explained with detailed emphasis on the relevance to OLED structures.

2.1 How to make an OLED

2.1.1 Substrate preparation

OLEDs are prepared on Indium-Tin-Oxide (ITO) substrates (purchased from Merck) with a sheet resistivity ~13Ω/□. Substrates are cut to 20mm x 20mm and cleaned through the following empirical method prior to device fabrication:

1. Scrubbed with detergent and distilled water.
2. 20 minute sonication in detergent/distilled water solution.
3. 3x 5 minute sonication in distilled water.
4. 2x 5 minute sonication in acetone.
5. 2x 5 minute sonication in chloroform.

Once cleaned, the substrates are lithographically patterned; this process is graphically represented in figure 2.1-1. The first step in this process is to spin coat a layer of Shipley 1818 photo-resist onto the surface of the ITO. In order to create the desired pattern of ITO the photo-resist covered substrates are then exposed to UV light through a mask. After UV exposure the substrates are submerged into a sodium-hydroxide developer solution to remove the photo-resist that has been exposed to the UV light. The substrates are then placed into a ~50°C solution of hydrochloric acid, nitric acid and distilled water (48%:2%:50%). The acid bath etches away the unwanted ITO to form the correct pattern for the anode. The substrates are given a final rinse in order to remove the photo-resist that is protecting the anode.

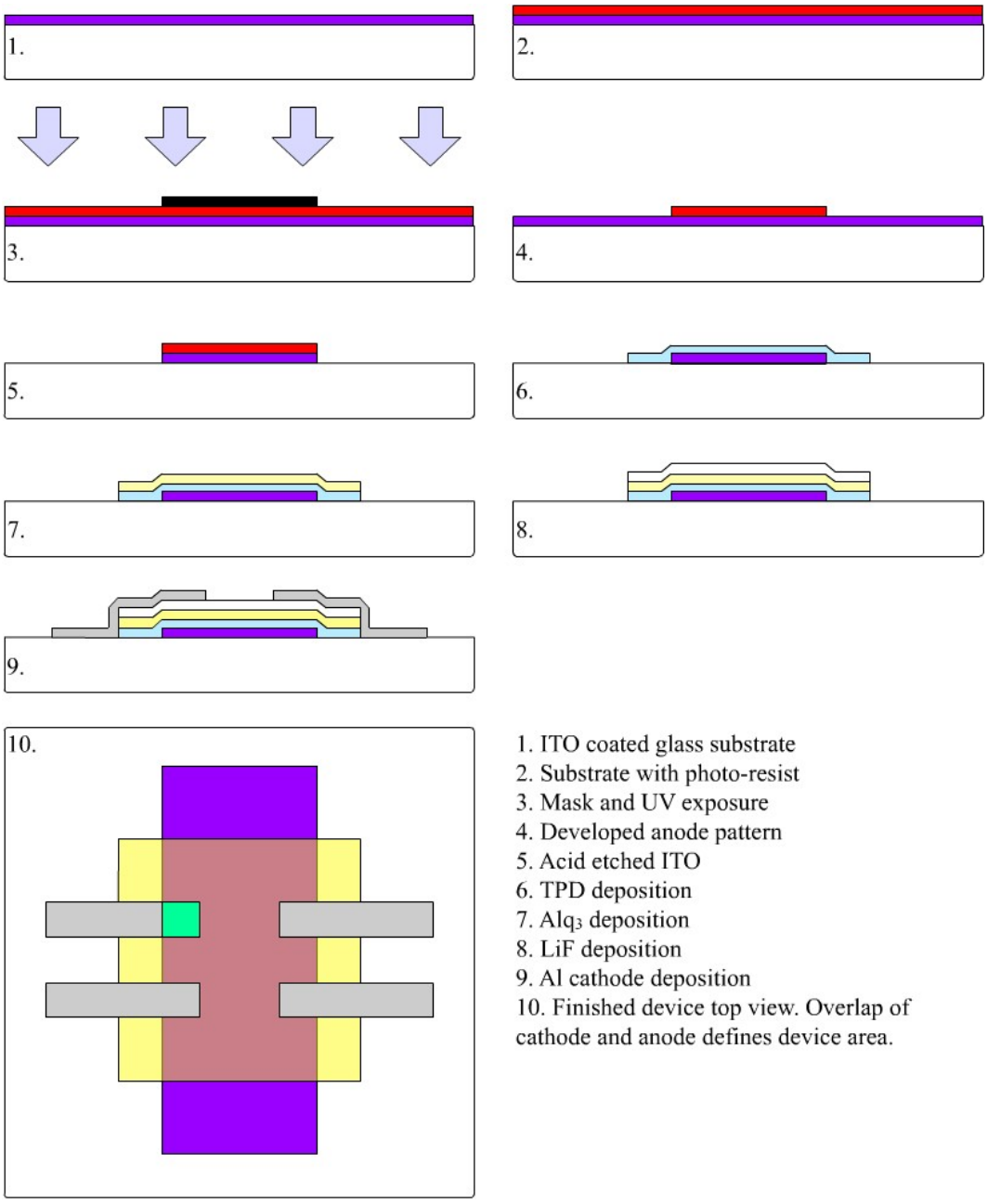

Figure 2.1-1: OLED fabrication procedure

An outline of the key steps in substrate processing using photo-lithography and device growth using sublimation. Also shown is the top view to indicate how multiple devices can be grown on one substrate. The area shaded in green indicates the active device area.

The lithographic process leaves the substrates contaminated, so it is necessary to put them through the entire cleaning process again. After cleaning the substrates are taken in the final beaker of Chloroform to an oxygen plasma chamber. It is widely reported that a short exposure to oxygen plasma lowers the device turn-on and increases efficiency due to an increase in the ITO workfunction [47,48]. From an empirical approach it was found that an exposure time above five minutes and below three minutes gave worst results, so exposures of four minutes are used. Once the treatment is complete the substrate is moved under-cover to a laminar flow bench and loaded into a sample holder. From here the substrate is ready for vacuum sublimation.

2.1.2 Organic and metallic deposition

A Kurt J. Lesker SPECTROS evaporation system is used for device growth. The system consists of two vacuum chambers one acts as a load lock, while the other contains the equipment for both organic and metallic sublimation. Figure 2.1-2 (page 53) shows a schematic for the system. The substrate sample holder is loaded onto a transfer arm in the load lock, which is evacuated using scroll and turbo-molecular pumps. The main chamber is evacuated using a scroll and helium cryo-pump. Typically the pressures in the load-lock are 10^{-7} mBar, while the main chamber is 10^{-8} mBar going up to ~10^{-7} mBar during evaporation. Inside the main chamber are six Boron-Nitride crucibles for organic sublimation and two sources for metal deposition. LiF requires relatively high temperatures for sublimation, so layers are deposited from an alumina crucible in one of the sources designed for metallic deposition. Titanium-diboride crucibles are typically used for metal sublimation.

Above the crucibles is a cassette that the substrate holder can be loaded into. The cassette can be moved in height and contains the masks needed for the organic and metallic layers. During sublimation/evaporation the cassette is rotated in order to improve the uniformity of the layers. This arrangement of crucibles and masks allows for all layers but the ITO to be grown without breaking vacuum. Both metallic and organic crucibles are resistively heated. Deposition is controlled through a calibrated quartz crystal monitor. Once the all the layers bar the cathode have been deposited the masks are changed so that the correct pattern for the

cathode can be generated. Following the cathode deposition the device is complete and can be returned to the load lock for access.

Depending upon the device structure different preparation of materials is required. The most common device structure consists of 500Å of TPD sublimed onto the ITO substrate. On top of this goes 500 Å of Alq_3, both of which are purchased from Aldrich. The Alq_3 is train purified before loading into a crucible within the evaporation chamber. Lithium-fluoride is used as an interface layer between the Alq_3 and the cathode; it is found to provide more efficient charge injection into the device [49,50]. After a change of masks the Aluminium cathode is ready to be evaporated. The overlap area of the ITO and cathode layers defines the shape of the OLED, which is indicated in figure 2.1-1. Variations on this basic structure such as cathode material, interface layer and layer thickness are commonly used; however the basic methods for construction are constant.

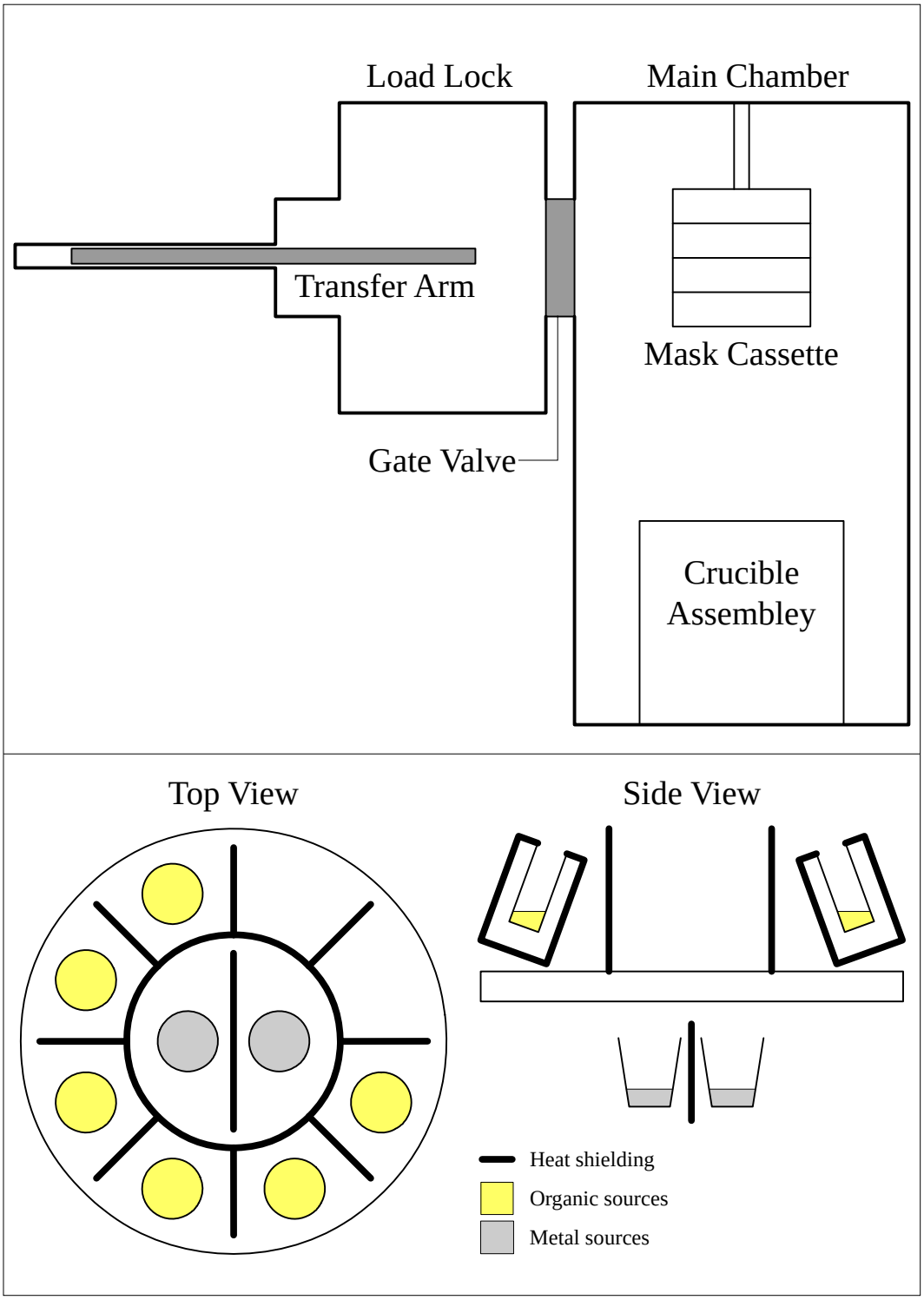

Figure 2.1-2: OLED growth system schematic

The top pane shows a schematic of the whole system. The bottom pane shows a schematic of the crucible assembly.

2.2 Experimental apparatus

2.2.1 Electrical and luminosity measurements

Once fabricated the device is placed in an electrical sample holder for testing, which is shown in figure 2.2-1a. The sample holder is constructed in a manner that gives electrical access from one side via a LEMO connector, while the other side gives optical access for luminescent measurements. The sample holder is able to be evacuated using a Leybold PT50 pumping station giving pressures of ~10^{-5}.
A Keithley 236 source-measure unit was used in constant voltage mode to make IV measurements. From the source-measure unit a triax cable leads to an adapter to connect to the LEMO connector on the sample holder. The adapter from the triax lead to LEMO connector is kept as short as possible in order to minimise noise. This setup allows for measurements of current from 10^{-12} to 10^{-1} Amps.
Luminosity was measured using one of two methods. Both methods involved the use of a Newport 1830C optical power meter. The first set of apparatus for measuring luminosity is a silicon photo-diode (818-SL) and matching integrating sphere (819M). This setup comes pre-calibrated and allows for absolute measurements of luminosity at a single wavelength. As the luminescent spectra of OLEDs are broad the power meter is not capable of giving absolute power measurements for these devices. In order to get a useful measurement the power meter is set to the peak wavelength of the emission spectra of the OLED. As this work is mainly centred on Alq_3 OLEDs the problems regarding power measurements are negligible since the devices are not being compared to other devices with different emission spectra. The second arrangement of apparatus for measuring luminosity is arranged so that the photo-diode is placed directly in front of the substrate, as indicated in figure 2.2-1b. By using this setup the measurement apparatus is kept to as small a size as possible, which is necessary in order to allow the setup to be used within the available magnetic equipment. The response of the detector was found to be invariant to magnetic fields. Due to the geometry of the detector and sample holder, some light is not detected by the silicon diode. Again since the measurements using the second method are compared with like measurements any discrepancy from the absolute luminosity is considered negligible.

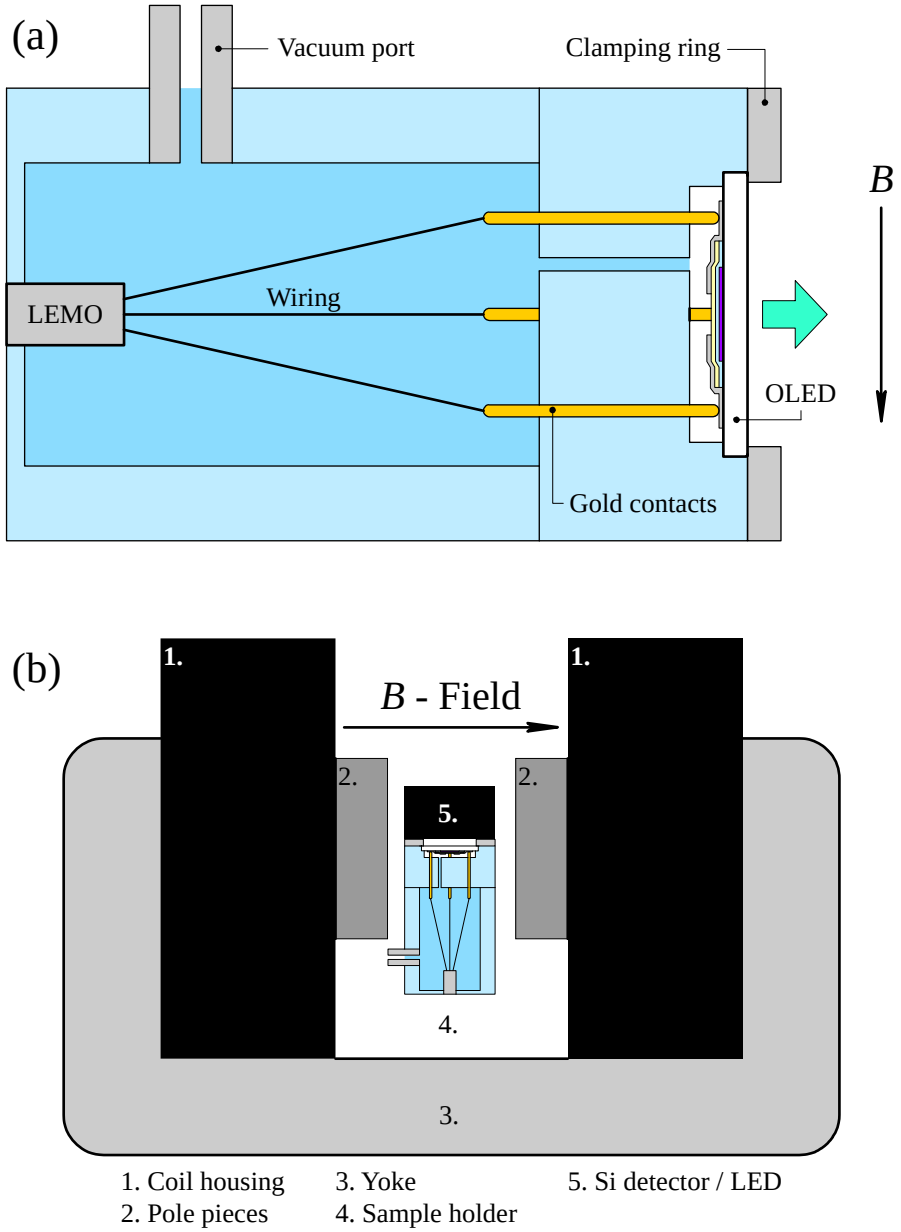

Figure 2.2-1: OLED sample holder and magnetic measurement schematics

The schematic of the sample holder used for all electrical and luminosity measurements is shown in (a). Indicated on the schematic are the channels for evacuating the holder and orientation of the OLED sample. Also shown are the electrical connections, including spring loaded, gold contacts, which are used to maintain a gentle but constant contact to the electrodes of the sample. The clamping ring ensures that the sample is held securely and that a good vacuum seal is achieved. Also indicated is the direction of the light emission and the magnetic field. (b) Shows the sample holder in between the pole pieces of the magnet, with the sample kept along the central axis of the pole pieces. The Si detector can be replaced by an LED in a similar shaped housing for the purpose of illumination experiments.

2.2.2 Measurements in a magnetic field

For studies in the presence of a magnetic field a Newport electromagnet type A was used. The magnetic field direction is horizontal with the field lines running parallel to the sample and perpendicular to the current flow, a schematic of the setup is shown in figure 2.2-1 (page 55). Variable pole spacing allows for a further method of varying field strengths. The size of sample holder and optical detector limited the poles to a spacing of 5 cm, which gave field strengths of up to ~300mT at an operating current of 3A. Field strength is measured by using a Hirst GM05 Gauss meter. Figure 2.2-2 is a graph of operating current versus field strength at the pole spacing used, from it a small hysteresis can be seen. Since dynamic measurements of magnetic field were not possible the current through the magnet was only switched on for the time it took for the field to stabilise and the current measurement to be made. After a single measurement the current to the magnet was then turned off before the software controlling the experiment stored the data and changed the necessary parameters for the next measurement. This pulsed measurement technique minimised the time the magnet was on and thus minimised any error due to hysteresis. As can be seen from the inset in figure 2.2-2, it was necessary to apply a negative current to the magnet in order to achieve null field and small values of B. The inset shows a remanence of ~6mT and the coercivity of ~0.07A.

The most basic way to conduct magnetoresistance measurements is to set the OLED to a given voltage and gradually increase the magnet current to a maximum while measuring the OLED current at each step (I_B). The magnetoresistance can then be calculated with reference to the OLED current that is obtained at null-field (I_0) using the following equation:

$$\frac{\Delta I}{I} = \frac{I(B) - I(0)}{I(0)}$$ **Equation 2.2-1**

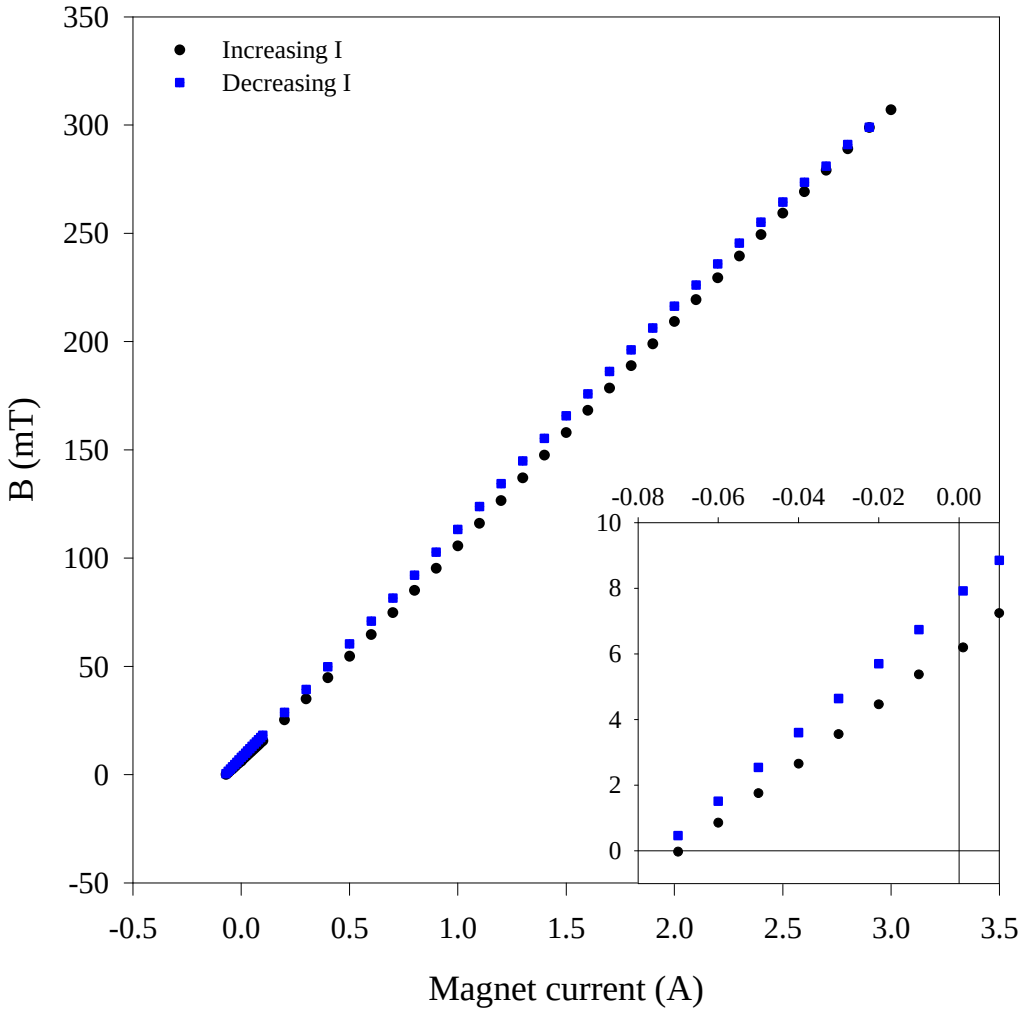

Figure 2.2-2: Magnet current versus magnetic field

This figure shows the measured magnetic field for a given current through the magnet. The black circles represent the measured magnetic field while increasing the current; the blue squares represent the magnet field measured while decreasing the current. The inset shows the region around zero field and zero current more clearly.

However a common problem with OLEDs is that the device can degrade during the course of a series of measurements. Degradation is visibly obvious in the form of pin-holes; where small areas of the device stop operating hence reducing the area of the device. This leads to a decrease in the current through the device at a given voltage. Since the drift in current is not necessarily constant between successive measurements it is necessary to account for this drift when taking measurements. This is especially true when taking measurements for magnetoresistance as the effect can be very small, while drift can be comparatively large.

The solution adopted in this work is to take a null-field measurement before and after every step in magnetic field. So for a given OLED current measurement, the null-field device current is then taken to be the mean of the null-field currents measured either side of that point. Figure 2.2-3 shows how the magnetoresistance can be affected by various ways of taking the null-field. From the figure it can be seen how the consideration of null-field current is especially important at low fields. Figure 2.2-3a shows an example of OMR curves calculated when the null field device current is taken to be a single value measured at the beginning of the scan, a single value measured at the end of the scan and a curve corresponding to the averaged method described above. Figure 2.2-3b shows what effect is seen on OMR curves when the null field device current is taken immediately prior to each data point, immediately after each data point and again the average either side of a data point.

The inset in figure 2.2-3 shows the raw current data used to calculate all the curves shown in figure 2.2-3; blue triangles show the device current with an applied magnetic field, while black circles show the device current taken at intermediate steps with zero applied magnetic field. From the inset it is clear to see that variations in current of ~0.07mA can be seen between the first null field measurement and the last null field measurement. This is relatively large to the maximum magnetic field induced change in current of ~0.02mA, which further highlights the necessity for a rigorous calculation of OMR.

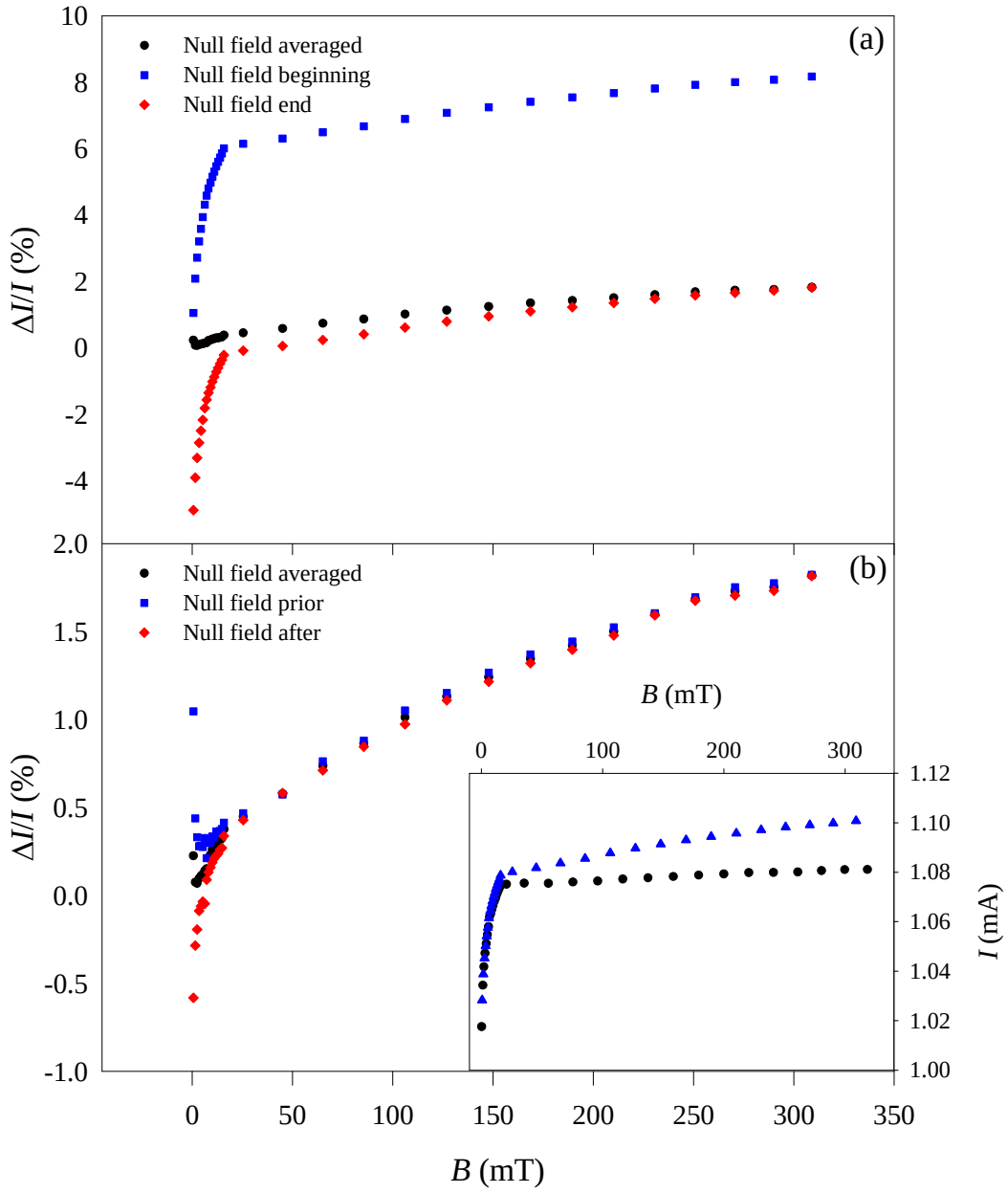

Figure 2.2-3: Alternative Null field OLED current measurement comparisons

Panel (a) shows the resultant OMR curves when the null field device current is taken before or after an entire scan. Panel (b) shows the OMR curves when null field device current is taken immediately before or after a measurement. Both panels show the result of the averaged null field device current method that is used throughout this document. Inset in (b) is the raw data that is used to calculate the curves in (a) and (b); blue triangles represent magnetic field on values, while black circles represent the intermediate null field device current measurements.

3 Results and discussion

3.1 Effects of charge injection on magnetoresistance

This section will present the results of a study on the effects of various cathode materials on magnetic field effects in OLEDs. Changing the cathode material changes the barrier height for electron injection in an OLED, which has effects on current-voltage characteristics, charge balance and luminescence. Ultimately these parameters affect device efficiency. Thus in changing the cathode we can probe how OMR changes as the current injection and efficiency of the device is altered. In this study a basic OLED structure of ITO/TPD (500Å)/Alq_3 (500Å) was used. On top of this structure one of three different cathodes were deposited: Al (1000Å), Mg:Ag (90%:10%, 1000Å) or LiF (~10Å)/ Al (1000Å). All three cathode types are well documented in the literature [51].

3.1.1 Current, voltage and luminescence characteristics

Upon fabrication of a device, current, voltage and luminescence (IVL) data was taken prior to magnetoresistance testing. Figure 3.1-1 shows the current density versus voltage (JV) and voltage versus luminescence (VL) curves for the three cathode combinations used. Both the JV and VL curves show three distinct regions that define the overall trends. These regions are; a relatively flat low current/luminescence region, a region of sharp rise in current/luminescence and a region of high current/luminescence that flattens. Also indicated on the plot are the device turn-on voltages, the data points corresponding to these values are encircled.

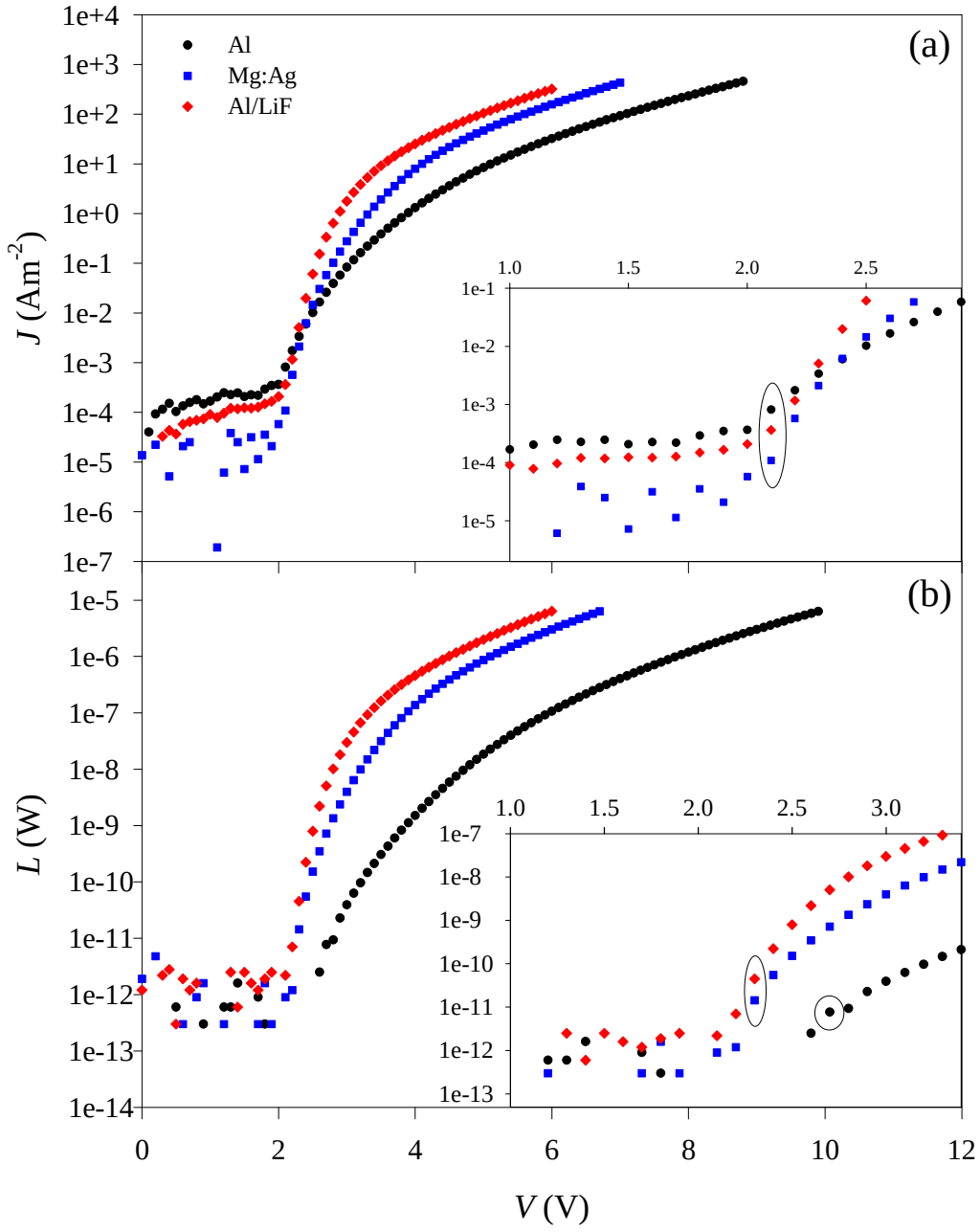

Figure 3.1-1: V against J and V against L curves for Alq_3 OLEDs with various cathodes

Pane (a) shows the voltage against current density. Pane (b) shows the voltage against luminescence. The insets show a close up of the turn-on limits for the corresponding curves, with turn-on limits indicated by circles.

The first two regions are of particular importance since they define the turn-on of the device and the injection efficiency. The low current region is not well defined in the literature and is often considered to be a “leakage” current due to the slight scaling with voltage. However, it is not clear why there should be a “leakage” current when the applied voltage is below the potential barrier for charge injection. The region of sharp rise is obviously due to the injection of charge carriers from the metal contacts. As such the electrical turn-on of the device is often defined as the point at which the current goes from the low leakage region to the sharp rise region. However, it is possible that the region of sharp rise starts at currents below the leakage current, thus the leakage region could be masking the true turn-on limit of the device.

Similarly there is a point of optical turn-on defined by the point at which light output is observable above the flat region. In the VL plots this flat region is simply due to the minimum sensitivity of the detection equipment. While the optical turn-on is slightly better defined than the current turn-on, it is still ambiguous since it ultimately depends on the sensitivity of the detection apparatus.

In the JV plots the region of sharp rise tells us about the injection efficiency. A rise with a high slope indicates that there is a large rise in current for a small change in the potential. A rise that has a low slope indicates that a bigger change in potential is required to achieve the same current; hence a lower slope indicates lower injection efficiency. The shape of the VL curve is a consequence of the shape of the IV curve, this is demonstrated by the linear trend when current is plotted against luminescence, figure 3.1-2.

By looking at the insets of the JV and VL plots it can be seen that by 2.2V all three devices have turned on electrically, with the initial slopes indicating that the Al cathode has the worst injection efficiency while LiF/Al has the best with Mg:Ag marginally lower. The plot of voltage versus luminescence shows that light can be detected for voltages greater than 2.3V for the LiF/Al and Mg:Ag devices, whilst it is 2.7V before light can be seen from the Al device. These two voltages define the optical turn-on limit for the respective devices.

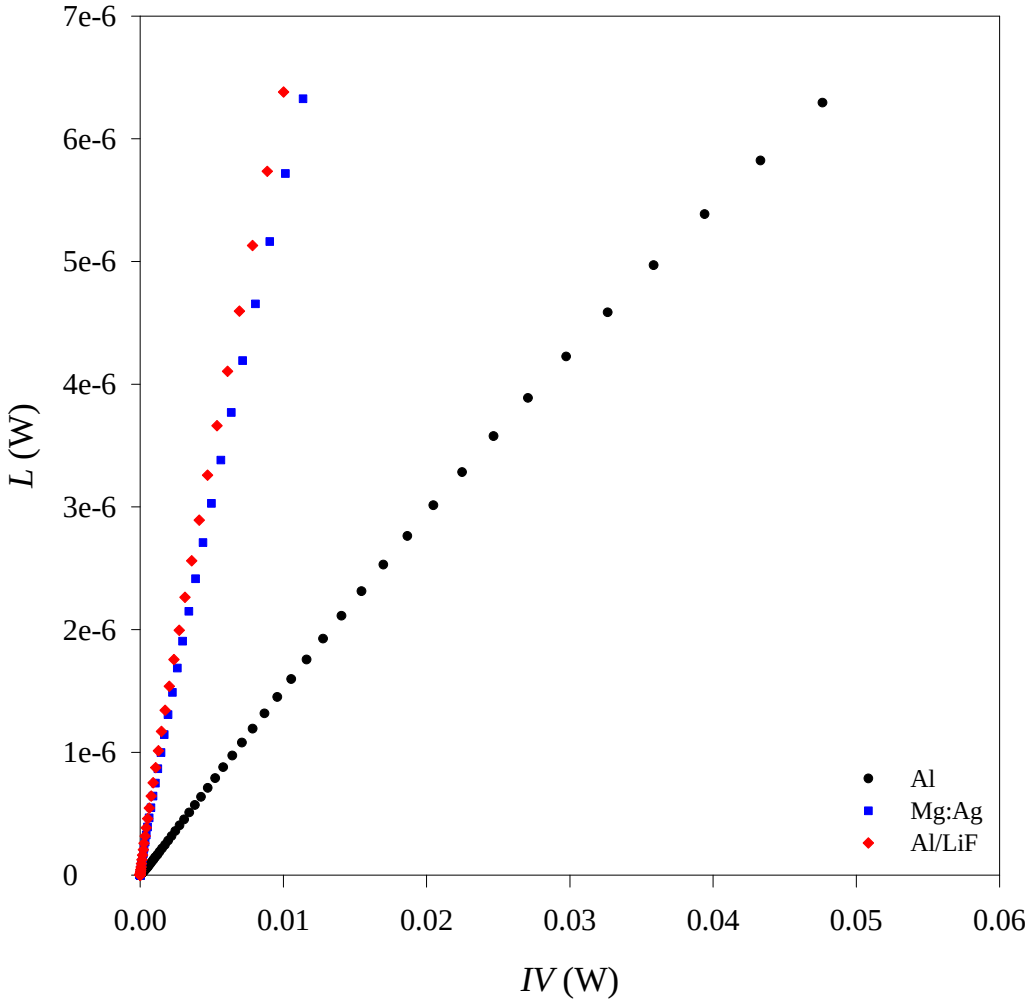

Figure 3.1-2: IV versus Luminescence for OLEDs with various cathodes

This plot shows the input power versus the output power for Alq_3 OLEDs with three different cathodes. The gradient represents the efficiency. The LiF/Al cathode demonstrates the highest efficiency, while Al the lowest.

3.1.2 Effect of magnetic field on device current at turn-on voltage

OMR was studied around the optical turn-on voltage by applying small voltage steps around the optical turn-on limit determined above. Figure 3.1-3 shows the current through the OLEDs with Al and LiF/Al cathodes as the applied magnetic field is altered. Included in the plot are the intermediate null field measurements, which are represented by circles while the triangles show current as field is increased. In order to show each data point clearly the data is presented on an arbitrary x-axis.

For the lower voltages shown in both plots, both the field on and null field measurements appear to follow the same trend. This obviously indicates that there is no effect of magnetic field on current, hence no OMR. Once the operating voltage gets to the point where light is measurable the field-on data points are clearly higher than the null-field data points. As the voltage increases this difference becomes more obvious. The point at which the OMR first becomes visible defines the onset of the effect. Since the onset of OMR appears after the device has electrically turned on and is coincident with the optical turn-on, it is clear that whatever the mechanism for OMR, bipolar charge injection and excitons are present within the system. This result provides us with our first piece of experimental evidence that excitons are a prerequisite for the observation of OMR.

It could be argued that OMR merely requires injected current and that the observation of OMR with luminescence is simply coincidence. However if we take the Al device as an example, there is a clear distinction between the electrical turn-on (2.2V) and optical turn-on (2.7V), this defines a region where there is significant increase in current with no luminescence. Also, in this region the "leakage" current is higher than the current at which OMR is seen in the other two devices, so the lack of OMR is not due to a lack of current. The fact that no OMR is observed in this region is a contradiction to the publications showing OMR in "unipolar" devices.

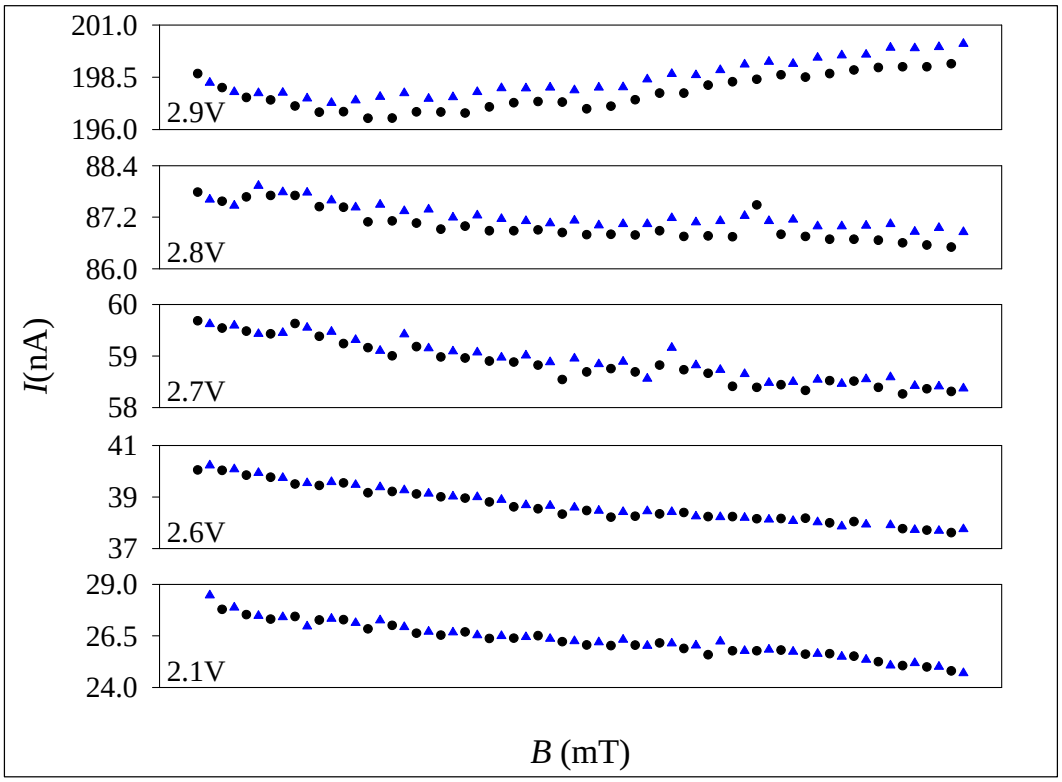

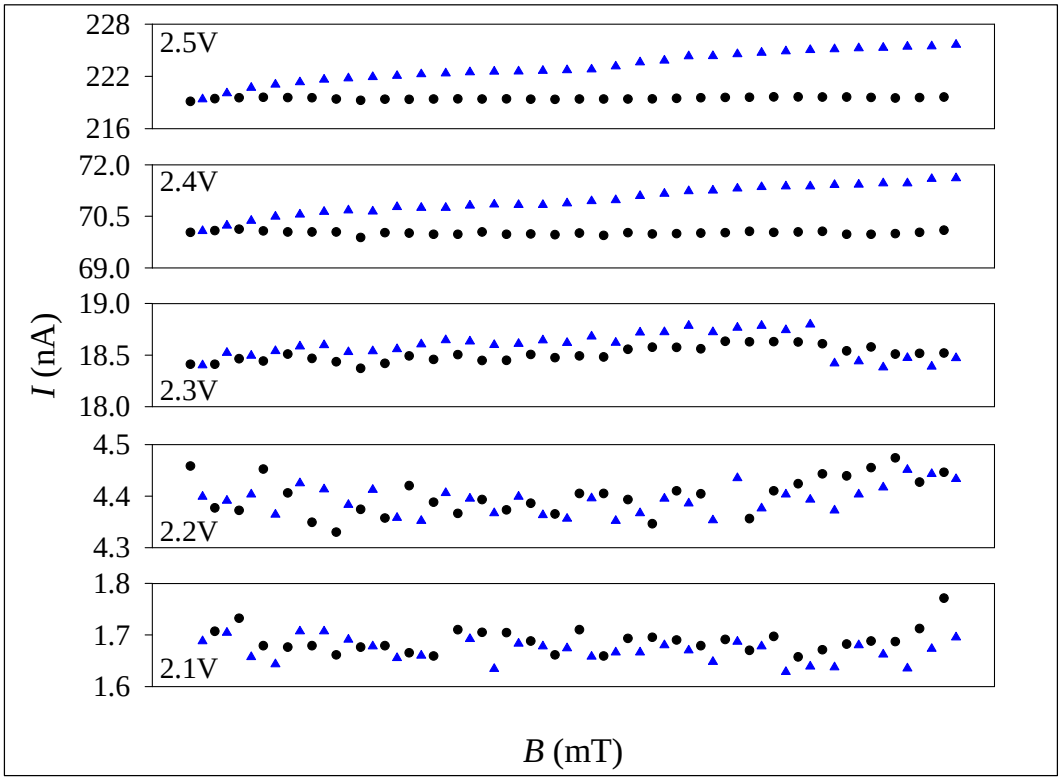

Figure 3.1-3: Raw current measurements for OLEDs in an applied field

Top presents the raw current data for an OLED with Al cathode, while the bottom pane is the analogous data for a LiF/Al device. While the abscissa is arbitrary, the magnetic field increases from left to right. Black circles show the null field device current, while blue triangles show the device current with applied magnetic field.

3.1.3 Comparison of OMR results with literature

As stated in the introduction much emphasis was placed on the equation 1.4-4 and equation 1.4-5 and their consequences in terms of possible models for OMR. As such, in order to compare the results published in the literature with the data presented here, it is important to fit these empirical equations to the OMR data obtained for the three cathodes. The two equations were used to describe two types of OMR that were labelled “fully saturated” and “partially saturated”. The Alq_3 data published in reference [36] was fitted with equation 1.4-4 since the trace was judged to be of the “partially saturated” type. In order to draw comparisons with the literature results the OMR data obtained for the three different cathodes has been fitted with the equation that describes partial saturation. Fits were calculated using free fitting parameters, without any constraints applied.

Figure 3.1-4 shows a sample of these results at low and high operating voltages. First equation 1.4-4 was fitted to OMR data for the entire range of magnetic fields available (~300mT). As the reader will see, the results for the Al device look encouraging at first glance with seemingly accurate fits. However, there is a great deal of noise on the results for Al, which could be masking any discrepancy between the fitting and the measured results. In particular, under close examination, the fit at high applied voltage seems to be following a different trend to the data at higher magnetic fields. The fits for the LiF/Al and Mg:Ag devices show a somewhat more obvious discrepancy. It has been noticed from the literature that while OMR data has been published with fields as high as ~300mT, the fittings are only ever shown for data up to ~50mT.

In order to identify the inconsistency between measured and literature results, fits were repeated while restricting the dataset to <50mT. The corresponding results of this restricted fitting are shown in figure 3.1-5. By restricting the dataset to <50mT much more positive fitting results are achievable. There is a slight deviation at ~50mT for all devices, however it is easy to see how this could be dismissed if there was no other evidence to cast doubt upon the fit.

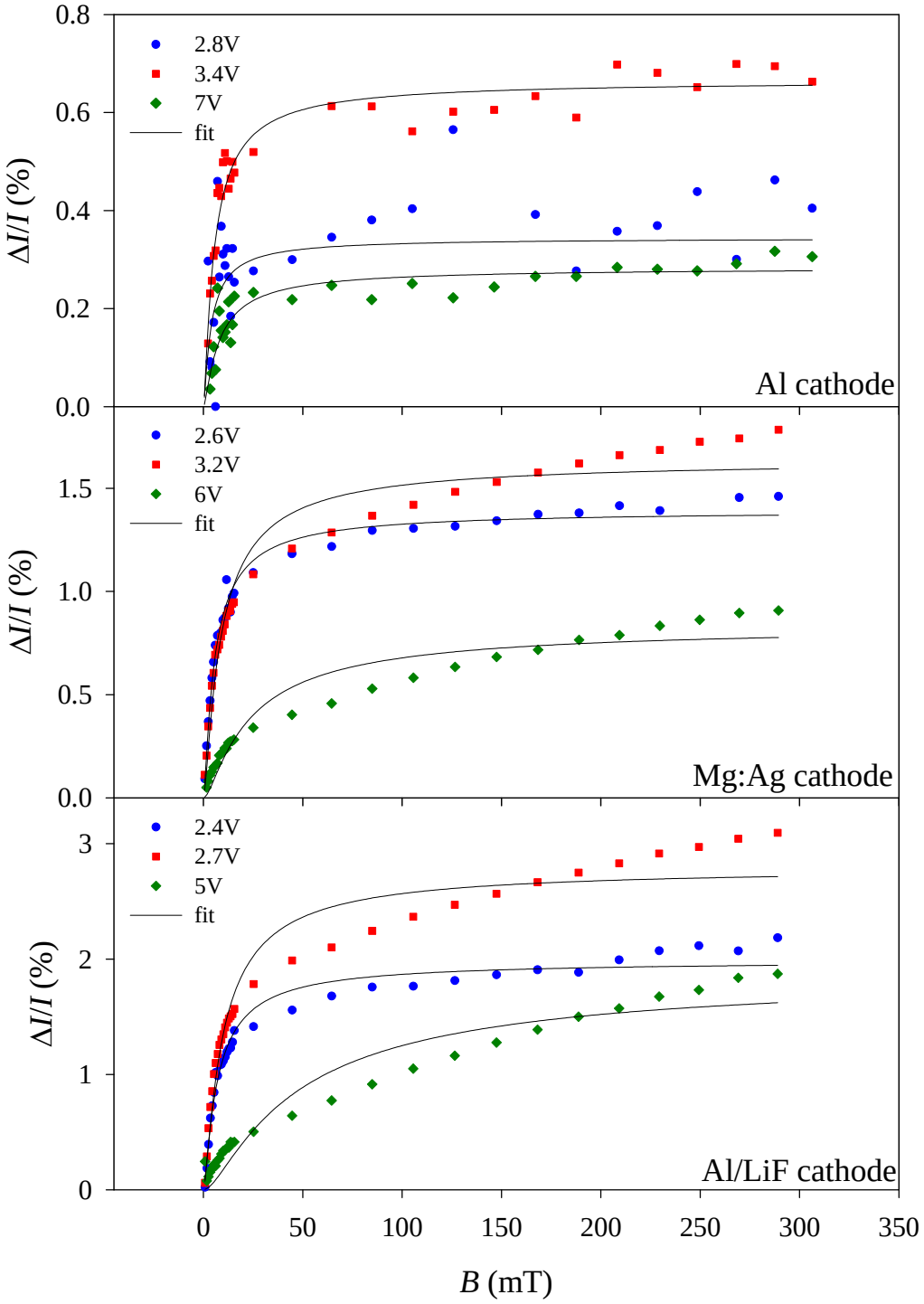

Figure 3.1-4: OMR fitting results using "partially saturated" equation from literature

This figure shows the fitting results for the full range of data available. Within each pane the data corresponding to three individually selected voltages is presented to give a broad representation of fitting quality over a wide range of current densities.

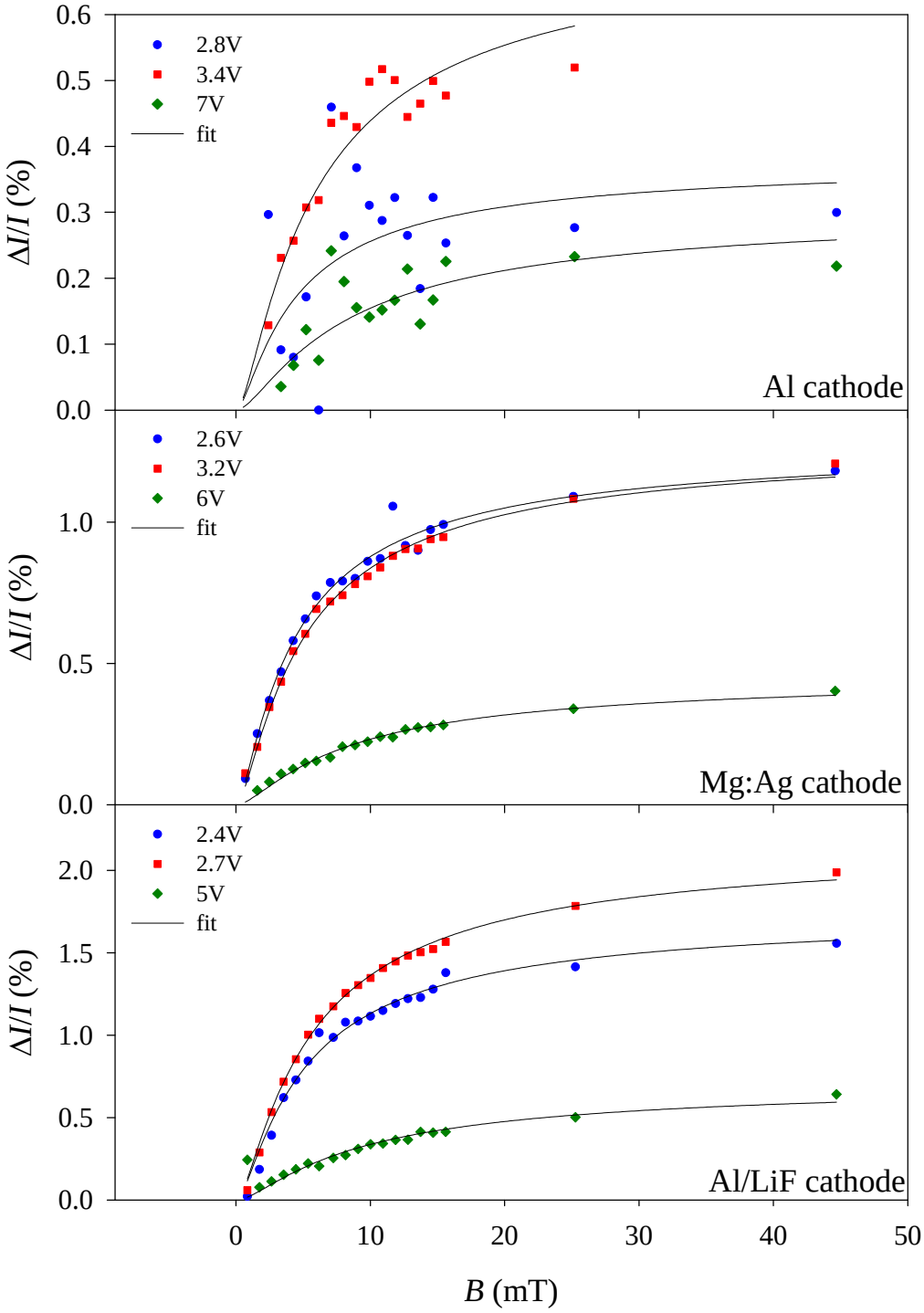

Figure 3.1-5: Restricted OMR fitting results using "partially saturated" equation from literature

This figure shows the fitting results for a restricted range of data available. This method matches the data presented in the literature. Again a selection of results over a wide range of applied voltages is presented.

It is not only the fittings to the unrestricted dataset that shows a flaw in the validity of equation 1.4-4. The published results of this fitting method gave a B_0 term of 5.4mT; however the values of B_0 obtained for the three different cathodes show further contradictions with results in the literature. Table 3.1-1 summarises the values of B_0 obtained from fitting equation 1.4-4 to the OMR data for the three cathodes. Since the fits over the entire range of ~300mT are clearly nonsense, table 3.1-1 only shows the fitting results to the restricted dataset of <50mT, so that legitimate comparison can be made with the literature result.

	B_0 parameter (mT)		
	Cathode type		
Applied Voltage	**Al**	**Mg:Ag**	**Al/LiF**
2.4			2.4 ± 0.2
2.6		2.1 ± 0.1	2.6 ± 0.1
2.7		2.1 ± 0.1	2.6 ± 0.1
2.8	2.1 ± 1.5	2.3 ± 0.1	2.7 ± 0.1
3.2		2.4 ± 0.1	
3.4	2.8 ± 1.1	2.2 ± 0.1	
5	3.2 ± 1.1	2.5 ± 0.1	4.6 ± 0.8
6	3.3 ± 1.4	4.1 ± 0.2	9 ± 2
7	4.1 ± 2.5		

Table 3.1-1: B_0 parameters obtained from fitting "partially saturated" OMR equation 1.4-4 to measured results <50mT

Comparing the data in table 3.1-1 with the literature result highlights a more serious discrepancy. While the literature published value for Alq_3 is 5.4mT for B_0, the results obtained from this study show much lower values. There are notable differences between the Alq_3 devices presented here and the devices used in reference [36]. The key differences are structural, with Alq_3 thickness, hole transport material, and cathode all differing. There are also likely to be experimental differences. While the alternating field/null-field method was used to gather the data presented above, there is no indication of how the experiments were conducted in reference [36]. Despite these differences in device structure and likely differences in experimental methods, the discrepancies between B_0 parameters and the fittings for high magnetic fields shows that there is good reason to be dubious of the "universality" of OMR and the empirical equation 1.4-4 and equation 1.4-5.

3.1.4 Magnetic field effect on luminescence and efficiency

Examining the features of the magnetic field effects on current, luminescence and efficiency further shows interesting differences between their respective curves. Figure 3.1-6 (page 72) shows the percentage change in luminescence versus applied field for similar operating voltages as used in the OMR curves of figure 3.1-4. The percentage change in luminescence is defined as:

$$\Delta L\% = \frac{L(B) - L(0)}{L(0)} \qquad \textbf{Equation 3.1-1}$$

Where L(B) is the luminescence in an applied magnetic field and L(0) is the luminescence at null-field. From figure 3.1-6 we can see that the magnetic field effect on the luminescence shows similar shapes to the corresponding OMR curves taken at the same voltage. Both sets of data rise sharply and show a shallower rise from ~45mT. At first glance the similarity between the OMR and luminescence curves is in agreement with the idea that the magnetic modulation of luminescence is simply a consequence of the change in current. However, there are differences between the curves that warrant a closer look at the relationship between OMR and luminescence curves.

An obvious difference is that the overall magnitudes of the curves are not the same, with the luminescence curves displaying a magnitude that is ~3-4 larger than the OMR curves. A more subtle difference is seen in examining the slow rise from ~45mT and comparing it to the total magnetic effect. The slow rise in OMR appears to form a greater proportion of the total OMR when the analogous comparison is made with the luminescence data. These differences in the shapes between the percentage change in luminescence and OMR is the first indication that the change in luminescence is not simply a consequence of the increasing current seen in the OMR. As stated in the introduction an obvious method to quantify whether magnetic effect on luminescence is dependent upon the change in current is to calculate the change in efficiency. Calculating the magnetic effect on efficiency is a trivial task since the OMR and luminescence data gives us current and luminescence of as a function of applied field. So the magnetic field effect on efficiency will simply be given by:

$$\Delta\eta\% = \frac{\eta(B) - \eta(0)}{\eta(0)}$$ **Equation 3.1-2**

Where η, the device efficiency is given by:

$$\eta = \frac{L}{IV}$$ **Equation 3.1-3**

Where L is the luminescence in Watts and IV is the input power of the device with current I and applied voltage V. Combining and simplifying equation 3.1-2 and equation 3.1-3 gives:

$$\Delta\eta\% = \frac{\frac{L(B)}{I(B)} - \frac{L(0)}{I(0)}}{\frac{L(0)}{I(0)}}$$ **Equation 3.1-4**

So clearly the percentage change in efficiency is defined by the magnet field effects on luminescence and current. Figure 3.1-7 shows the percentage change in the device efficiency. If the change in luminescence was a direct consequence of the change in current then one would expect the change in efficiency to be zero. Figure 3.1-7 clearly shows that this is not the case. This implies that an applied field also affects the luminescent process at some point. However, by itself the efficiency data shown in figure 3.1-7 cannot tell us if the luminescence is affected at the stage of exciton formation, excitonic interactions or exciton dissociation.

The one concrete thing the efficiency data tells us is in relation to the population of excitons within the device. As mentioned previously the efficiency data tells us about the luminescent output without the concern of changes in current. It is known that Alq_3 OLEDs do not display phosphorescence and hence radiative triplet decay at room temperature. So, the luminescence from an Alq_3 OLED at room temperature is exclusively from singlets. So if the efficiency of the OLED increases upon the application of a magnetic field the singlet population must be increasing. Given that the efficiency measurements factor out the effect of current, the only way singlet population can increase is at the expense of the triplet population. So the magnetic field acts to increase the singlet population and decrease the triplet population.

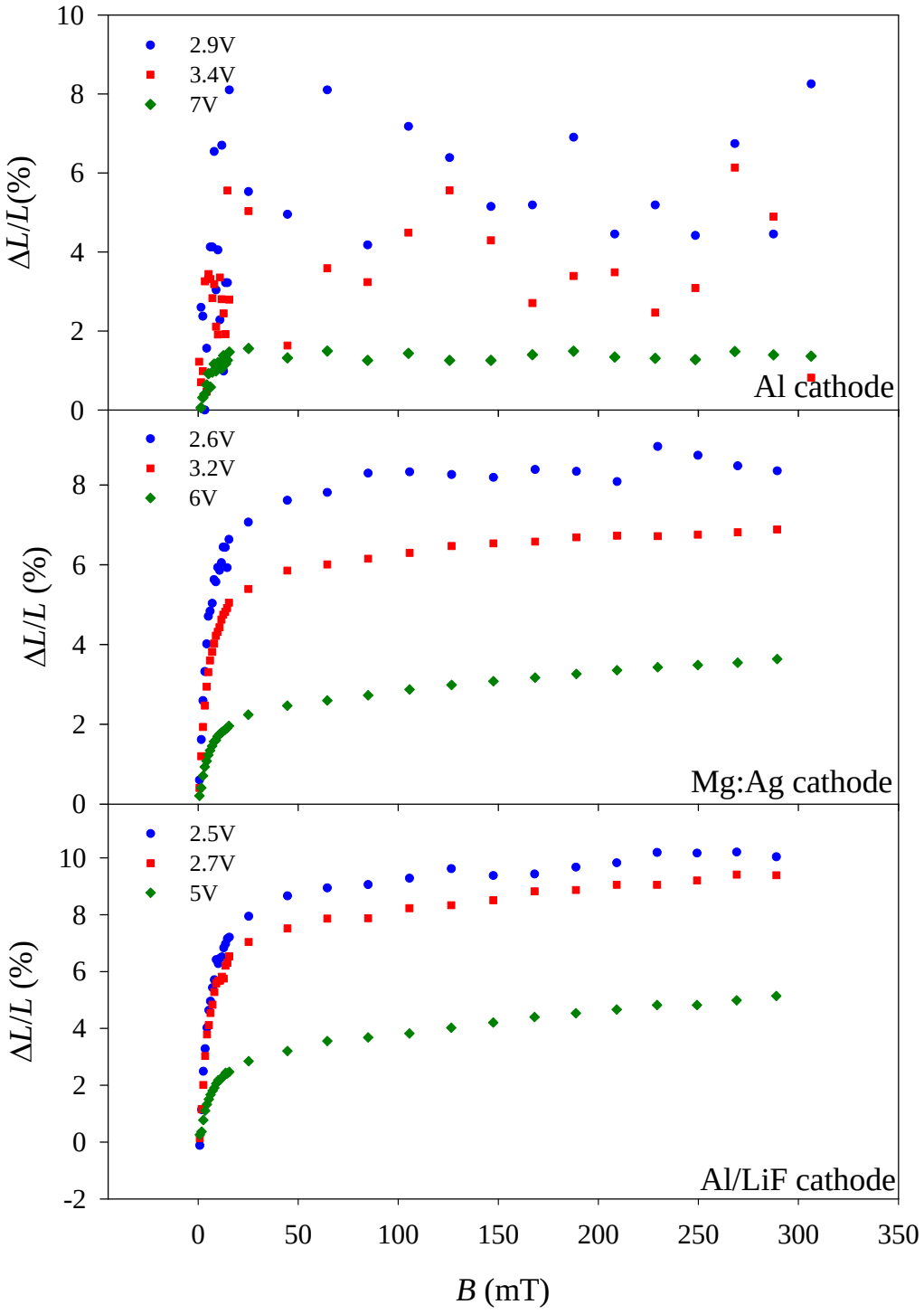

Figure 3.1-6: ΔL/L curves for OLEDs with various cathodes

The three panes above show the percentage change in luminescence for the three different cathodes used. The three voltages in each pane give a representation of the results over a wide range of current densities.

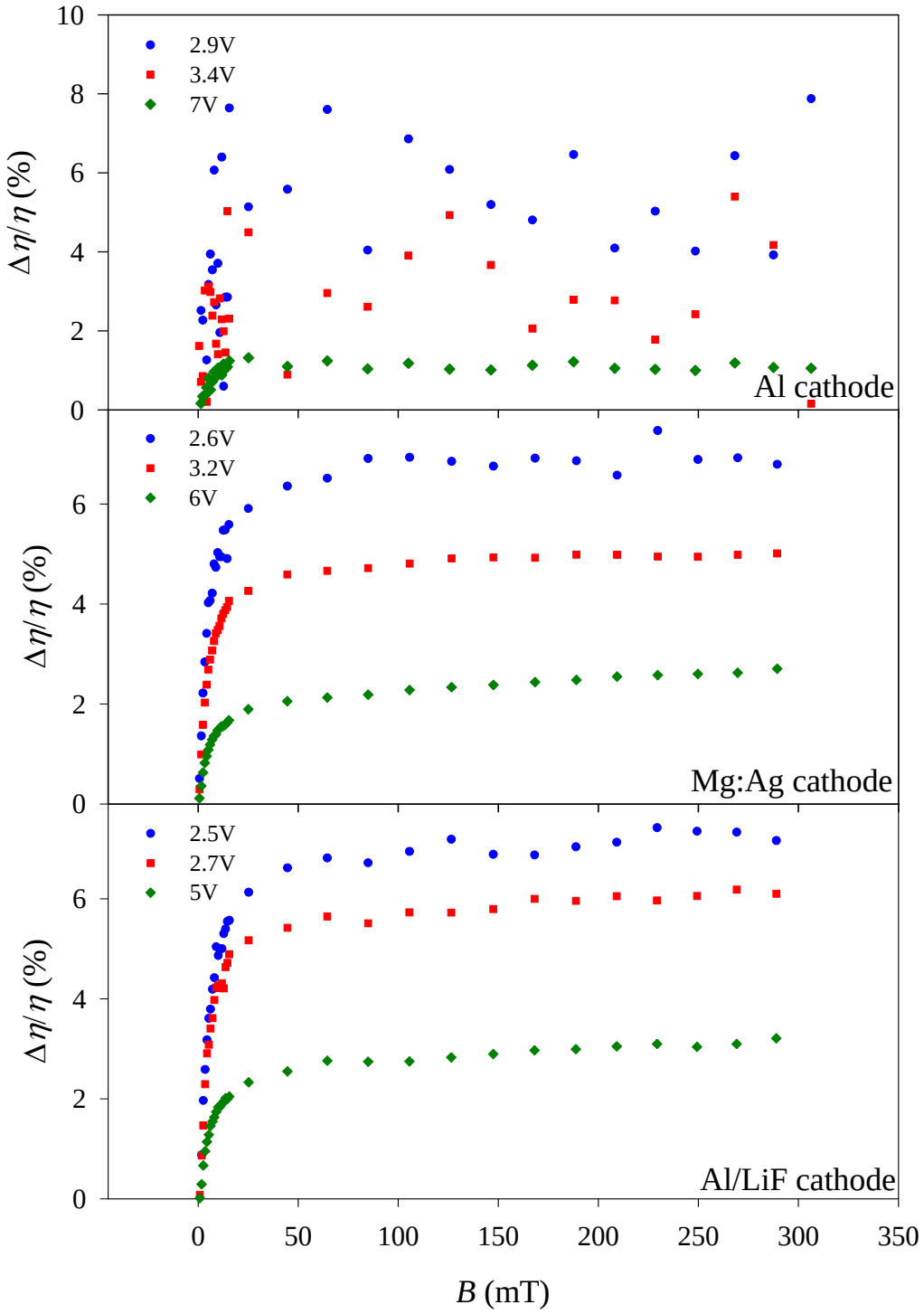

Figure 3.1-7: Δη/η curves for OLEDs with various cathodes

The three panes above show the percentage change in device efficiency for the three different cathodes used. The three voltages in each pane give a representation of the results over a wide range of current densities.

3.1.5 Cathodes and device efficiency – implications for possible mechanisms

As indicated by the historical review in the introduction, relatively little attention has been given to the magnetic field effects on excitons in OLEDs. Efficiency is essentially the luminescent output normalised for the input current, so it allows for the measurement of magnetic field effects on luminescence without the concern of how the magnetic field is also affecting the current.

As would be expected, changing the cathode charge injection efficiency is also reflected in the magnetic field effects measured with different cathodes. Efficiency is effectively a measure of the number of excitons generated for a given amount of injected charge. Figure 3.1-2 compares the luminescent output and input power of devices with the three different cathodes. The gradient of a luminescence versus IV plot gives the external efficiency of the device, with efficiency increasing from small to large gradients. From figure 3.1-2 it is evident that the efficiency of these devices increases as we go from Al to Mg:Ag to LiF/Al. So for a fixed current density the exciton concentration also increases as we go from Al to Mg:Ag to LiF/Al.

Figure 3.1-8 shows the OMR and magnetic field effect on efficiency for the three devices taken with approximately the same current density. As we can see from this figure the magnitude of the OMR also increases in the same order as the efficiency increases for the three devices. Since the OMR increases as the device efficiency increases it implies that OMR is increasing with an increased exciton density. This also indicates that the occurrence of OMR and associated mechanisms are linked to the presence of excitons within the device.

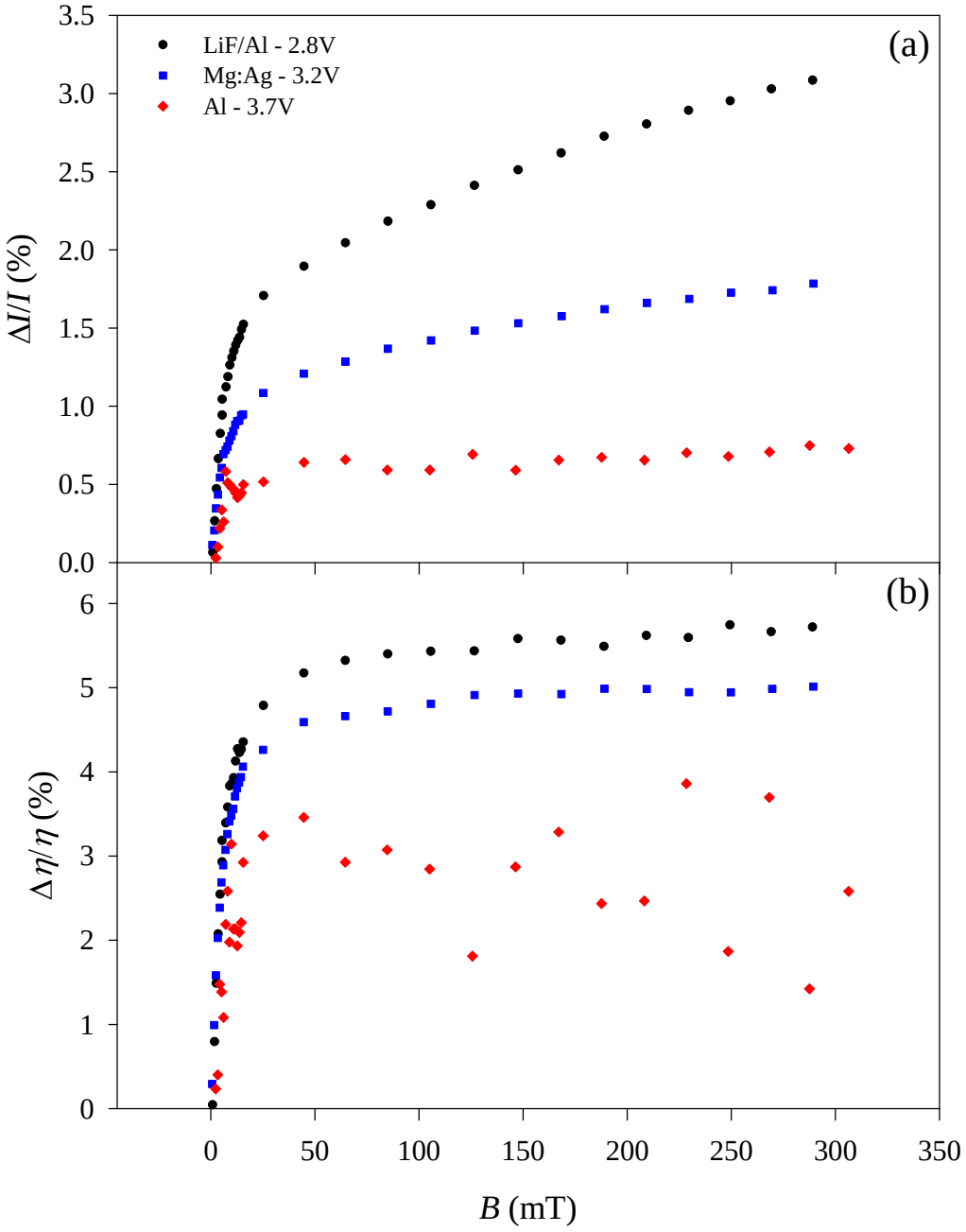

Figure 3.1-8: OMR and $\Delta\eta/\eta$ curves at ~0.65Am^{-2}

Pane (a) shows the OMR curves for Alq_3 OLEDs with different cathodes at approximately the same current density. Pane (b) shows the corresponding results for $\Delta\eta/\eta$.

3.1.6 Excitonic model for OMR – The role of triplets

So far the data presented shows that previous studies have been premature to exclude excitonic processes from any possible mechanisms for OMR. The magnetic effect on device efficiency clearly implies that singlet population increases with an applied magnetic field. This is in agreement with several publications [22,24,26] that went on to propose models for OMR that were dependent upon dissociation of the singlet state. Reasons to be dubious of the singlet dissociation view have already been stated in the introduction. Since there is good evidence to suggest that OMR and the magnetic effects on luminescence and efficiency are related to excitons it seems logical to search for some other way in which excitons may be able to explain the observed data.

From the magnetic field effect on efficiency data we have established that enhanced luminescence is most likely due to the increase in singlet population at the expense of the triplet population. Due to the similarities observed between the magnetic effects on luminescence and current traces, it is natural to ask whether triplet to singlet conversion can explain OMR as well as magnetic changes in luminescence. Following this rationale we come to one of two possibilities. The first possibility is that a magnetically induced increase in singlet population leads to increased current. This conclusion is ultimately what led to the proposal of the singlet dissociation models for OMR. Secondly, the magnetically induced decrease in triplet population leads to increased current. As highlighted in the introduction there are good exciton diffusion reasons to doubt the singlet dissociation model, hence the effect of decreasing triplet population on current needs to be examined further.

Drawing analogy from the singlet dissociation model it can be concluded that triplet dissociation cannot be the cause of an increase in current. A triplet dissociating would certainly release charge back into the system. However, the overall effect of the magnetic field would have to increase the triplet population in order to see an increase in the overall current through a device. This possibility is obviously ruled out by the magnetic field effect on efficiency data, which shows triplet population decreases with applied field.

Another way in which triplets might affect current in the manner observed is if there is some current limiting interaction between charge carriers and triplets. If there was such a limiting interaction then lowering the triplet population by applying a magnetic field would also see a drop in the interaction. The drop in the rate of interaction would naturally see the current increase with magnetic field also.

As highlighted in the introduction, the role of triplets in organic materials and the associated magnetic phenomena was studied greatly when large organic crystals such as anthracene and tetracene were of broad interest. The effects of triplets, under magnetic fields or otherwise, has not received the same level of attention since the development of modern amorphous small-molecule/polymeric thin film organic devices. Looking back at the older literature it is possible to draw parallels between historical magnetic effects on organic materials/devices and modern thin film devices. It is possible that these older studies can provide plausible explanations to the observed magnetic phenomena in modern devices. In reference [17] a description of free carrier (paramagnetic centre) interactions with triplets is given. This description can be summarised by the following:

$$T_1 + D_{\pm 1/2} \xleftrightarrow{k_1} (T_1 \ldots D_{\pm 1/2}) \xrightarrow{k_2} D_{\pm 1/2} + S_0^* \qquad \textbf{Equation 3.1-5}$$

Where T_1 is the triplet state, $D_{\pm 1/2}$ is a free carrier (paramagnetic centre), ($T_{1\ldots}$ $D_{\pm 1/2}$) is a paired state, S_0^* is an excited vibrational level of the ground state, while k_1 and k_2 are rate constants. It is clear that the process governed by rate k_1 will act as a scattering mechanism, both delaying and altering the path of the free carrier and triplet alike. So if these interactions are occurring then it is likely to be a significant factor affecting the mobility of the free carriers through the organic layer.

Spin statistics dictate that excitons will be formed in the ratio of 1:3 (singlet to triplet). The radiative lifetime of the spin forbidden triplet decay is several orders of magnitude above the singlet. From these two facts it is reasonable to assume that the steady state population of triplets is significantly greater than that of singlets. For every exciton formed there are at least two free carriers required, which in steady state, must be entering the luminescent layer at the same rate that

all excitons are decaying. These devices are not 100% efficient, which leads to the conclusion that the system also has an abundance of free carriers passing through the device. Given the relatively large numbers of triplets and free carriers it is not an unreasonable possibility that the mobility of free carriers in Alq_3 devices is indeed dependent upon the interaction defined by Ern and Merrifield [17].

Comparing this model of triplet/free-carrier interactions to the data in figure 3.1-8 there is good consistency. The percentage change in efficiency data for all cathodes shows that there is clearly a conversion of triplets to singlets. If triplets are acting as a scattering site for free carriers then removing triplets from the system would decrease the scattering events. Any decrease in scattering events would mean an increase in the mobility, which would naturally mean an increase in the current through the device. Obviously this matches with the observation that the current increases as the applied field increases.

3.1.7 Magnetic field effects with varying voltage

The charge/triplet interaction model can qualitatively explain why a positive increase in current, luminescence and efficiency can be seen with the application of a magnetic field. However there is nothing within the simple view described above to explain the specific shape of the trends observed. There is also nothing in this model that will quantify exactly how OMR would be expected to change as drive conditions such as voltage or temperature change.

Figure 3.1-9 shows the OMR and magnetic field effect on efficiency at several voltages for a LiF/Al device. Broadly speaking the traces do not significantly vary in shape with increasing voltage, insofar as they all show a sharp rise at low fields and a slower rise at high fields. However, there are differences that can be seen between the various OMR traces in figure 3.1-9a. Looking closely at the 2.4V OMR data a relatively shallow rise at magnetic fields above ~45mT can be seen, which is similar to the magnetic field effect on efficiency traces in figure 3.1-9b. As the applied voltage increases from 2.5V the contribution of the high-field OMR increases. At 2.7V and above the high-field component of the OMR is very prominent and appears to have a consistent shape. This implies some other effect occurs and saturates at high current densities.

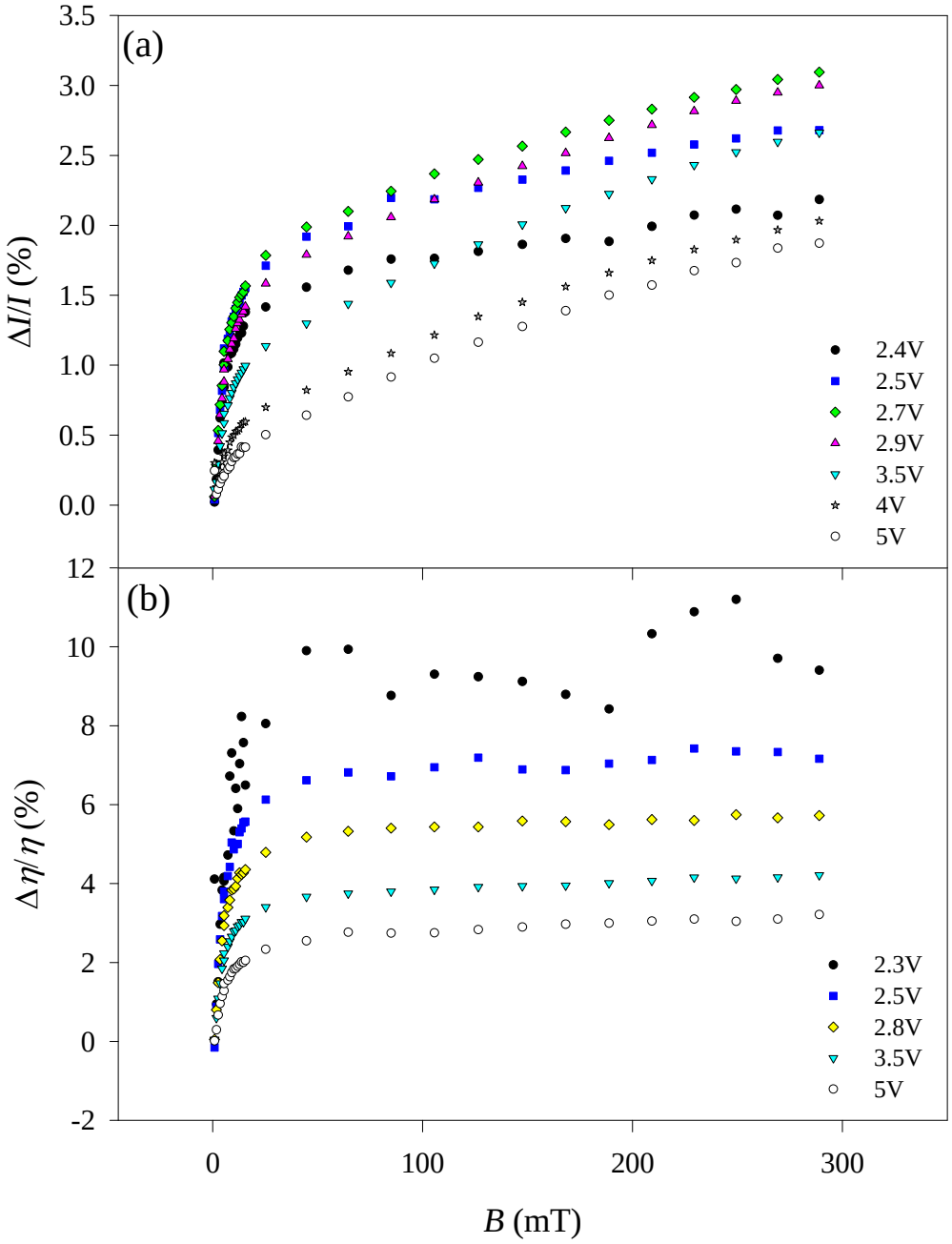

Figure 3.1-9: OMR and $\Delta\eta/\eta$ curves for an OLED with a LiF/Al cathode

The top pane (a) shows the OMR at a wide range of applied voltages, showing how OMR changes with current density. In the bottom pane (b) the corresponding data for $\Delta\eta/\eta$ is shown.

The magnitudes of both OMR and magnetic field effect on efficiency clearly vary greatly with applied voltage. Efficiency seems to simply decrease with increasing voltage, while OMR seems to reach a peak before decreasing with increasing voltage. Figure 3.1-10 shows these trends more clearly; the data is presented for several fixed fields as a function of voltage. Here the decay in magnitude of the magnetic effect on efficiency as applied voltage increases is clear. Also evident is the peak in OMR as voltage increases. If charge/triplet interactions are responsible for OMR it would naively be expected that the magnitude of OMR should increase with current density/voltage, since at high current densities the population of free carriers and excitons is higher. Figure 3.1-10a shows that this clearly not the case. This in itself is not contradictory to the proposed model. Since both the charge carrier density and triplet population are functions of different quantities it would be logical that the OMR would be dependent upon a balance of the charge carrier and triplet populations rather than on the sheer magnitude of either the free carrier or triplet population. This concept has been demonstrated for the luminescent efficiency of OLEDs. It has been shown that the balance between holes and electrons is crucial to the overall efficiency of the device [51].

Comparing OMR versus voltage at a given field for devices with the three different cathodes shows different trends. Figure 3.1-11a (page 82) shows OMR as a function of applied voltage for a field of ~45mT. It is seen that while all the cathodes show a peak in the OMR, the peak occurs at different voltages. Also shown in figure 3.1-11b is the OMR plotted against current density from which we can see that all three curves actually peak at current density of ~0.1-1Am^{-2}. Why OMR for different cathodes should peak at similar current densities is not clear. From the data of figure 3.1-2 we know that efficiency increases as the device cathode is changed from Al to Mg:Ag to LiF/Al. OMR versus current density confirms that high OMR is coincident with an increased device efficiency brought about by the change in cathode. The device efficiency is a measure of exciton population for a given amount of injected charge. So OMR versus current also tells us that OMR varies as the ratio of excitons to free-carriers changes. However, this data does not tell us the precise details of how OMR is affected by the exciton/ free-carrier ratio.

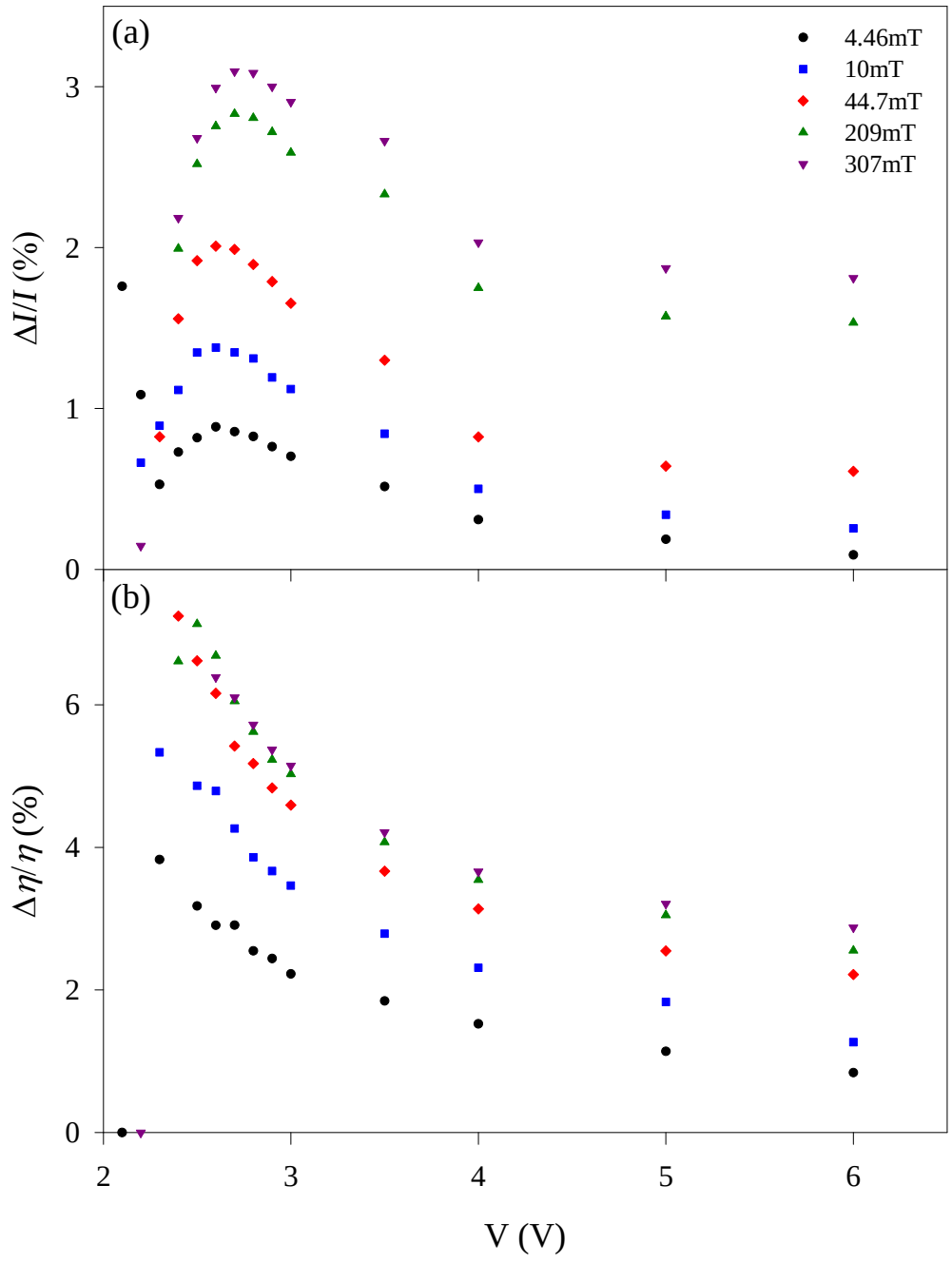

Figure 3.1-10: OMR and $\Delta\eta/\eta$ versus voltage for an OLED with a LiF/Al cathode

The top pane shows the OMR at several applied fields plotted against applied voltage, showing how OMR changes with current density. In the bottom pane the corresponding data for $\Delta\eta/\eta$ is shown.

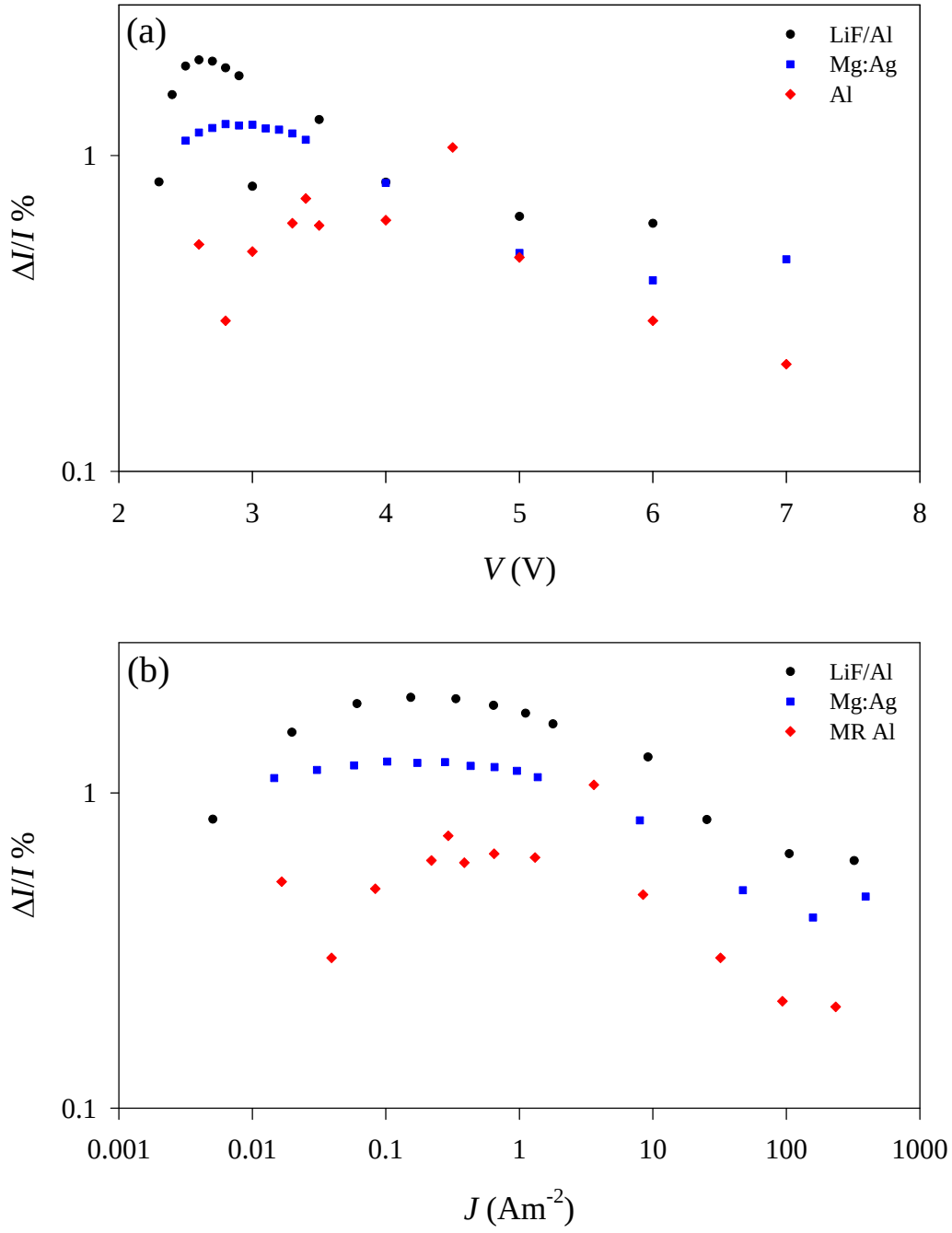

Figure 3.1-11: OMR versus applied voltage and current density

Pane (a) shows OMR versus applied voltage for three cathodes at an applied magnetic field of 44.7mT. The bottom pane (b) shows this same data plotted against current density.

3.1.8 Triplet population modulation – possible causes

The triplet/free-carrier interaction provides us with a model that qualitatively could explain all the observable magnetic effects on current, luminescence and efficiency. However the mechanism by which the singlet population increases at the expense of the triplet population is not established. There are several processes that occur in organic semiconductors that are known to affect the balance between singlet and triplet populations. Indeed as highlighted in the introduction hyperfine scale effects were used to explain the modulation of triplet-triplet annihilation. Both hyperfine scale effects and triplet-triplet annihilation alter the relative populations of singlet and triplet states. Also mentioned in the introduction is how spin orbit coupling effects have been used to change singlet/triplet ratios to achieve phosphorescent diodes.

Reference [38] showed a theoretical analysis which concluded that both spin-orbit and hyperfine effects were likely to be significant. As such, the results of fittings were presented in this publication where a linear combination of equation 1.4-4 and equation 1.4-5 was used to fit the measured OMR data and to try and quantify the different contributions from hyperfine and spin-orbit effects:

$$\frac{\Delta I}{I} = A_0 \frac{B^2}{B^2 + B_0^2} + A_1 \frac{B^2}{(|B| + B_1)^2} \qquad \textbf{Equation 3.1-6}$$

The pre-factors $A_0 + A_1$ gives the maximum OMR at infinite magnet field. B_0 and B_1 are the constants as covered in the discussion of reference 34 on page 36. There was no rationale given for why the fit should be performed in this way. Perhaps not surprisingly it was noted that there were some peculiarities in the fitting results. Spin-orbit and hyperfine effects change excitonic populations, however the attempts to fit the measured data were only performed on OMR data. The more direct method to quantify changes in exciton populations would have been to fit the magnetic field effect on efficiency data as that represents changes in exciton population more accurately. Since the Iowa group argue that luminescent effects are secondary to current effects there is no reason why equation 3.1-6 should not also apply to $\Delta\eta/\eta$ data.

It was noted that equation 1.4-5 could be derived from the Hyperfine Hamiltonian [36]; it was also shown that considerations of spin-orbit coupling gives a similar form [38]. So it is logical to use equation 1.4-5 as part of any potential fitting solution. Using equation 1.4-5 to fit the $\Delta\eta/\eta$ data for both the Mg:Ag and LiF/Al devices shows very poor fits, as is demonstrated in figure 3.1-12 (page 86), which shows fit to a selection of data over a wide range of applied voltages. Only the 2.6V LiF data shows a good fit, however this is likely due to the level of noise producing a coincidental result. Given that equation 1.4-5 does not produce good fits and that the evidence shows that magnetic field effects in OLEDs is likely to be multi-faceted, it is not surprising that a single parameter equation such as equation 1.4-5 does not work. So some multi-parameter approach should be considered.

It is assumed that both spin-orbit and hyperfine effects might be occurring simultaneously and acting independently. So in order to try and quantify the trend of magnetic field effect on efficiency a linear combination of 2 instances of equation 1.4-5 were used to fit the measured data:

$$\frac{\Delta\eta}{\eta} = A_0 \frac{B^2}{B^2 + B_0^2} + A_1 \frac{B^2}{B^2 + B_1^2} \qquad \textbf{Equation 3.1-7}$$

The terms in this equation are as in equation 3.1-6. At low current densities the change in efficiency is well described by equation 3.1-7; however this relation is not adequate at higher current densities. Figure 3.1-13 (page 87) shows a selection of $\Delta\eta/\eta$ data and corresponding fits for both the LiF/Al and the Mg:Ag devices. Table 3.1-2 shows the parameters given from fitting equation 3.1-7 to the measured data. Comparing the results in table 3.1-2 and the corresponding traces from figure 3.1-13 (page 87) it is apparent that there is a trend in the fitting parameters up until the point at which the quality of the fits break down. At low current densities the magnetic widths described by B_0 are ~3.7mT and ~2.7mT for the LiF/Al and Mg:Ag devices respectively. The B_0 values are reasonably stable showing variation on the 0.1mT scale. The B_1 values are less stable with average values of ~34mT and ~22mT for the LiF/Al and Mg:Ag devices respectively. The variation in the B_1 values is on the 10mT scale.

	V	A_0	A_1	B_0	B_1
LiF	2.5	5.5 ± 0.2	1.7 ± 0.2	3.8 ± 0.2	30 ± 7
	2.6	4.7 ± 0.5	1.7 ± 0.5	3.6 ± 0.4	19 ± 7
	2.7	4.9 ± 0.1	1.2 ± 0.1	3.9 ± 0.1	53 ± 11
	2.8	4.3 ± 0.1	1.3 ± 0.1	3.8 ± 0.1	32 ± 4
	2.9	4.1 ± 0.1	1.2 ± 0.1	3.8 ± 0.1	33 ± 4
	3	2.6 ± 0.1	0.9 ± 0.1	3.9 ± 0.1	56 ± 7
	3.5	3.1 ± 0.1	1 ± 0.1	3.8 ± 0.1	48 ± 7
	4	2.7 ± 0.1	0.9 ± 0.1	3.8 ± 0.1	51 ± 7
	5	2.1 ± 0.1	1 ± 0.1	4.1 ± 0.2	54 ± 7
	6	1.9 ± 0.1	1.2 ± 0.1	5.2 ± 0.4	135 ± 30
Mg:Ag	2.6	5.0 ± 0.2	1.9 ± 0.2	2.9 ± 0.2	24 ± 6
	2.7	3.8 ± 0.2	2.5 ± 0.2	2.2 ± 0.2	13 ± 1
	2.8	4.2 ± 0.1	1.9 ± 0.1	2.8 ± 0.1	19 ± 1
	2.9	3.9 ± 0.2	1.9 ± 0.2	2.7 ± 0.2	21 ± 3
	3	4.2 ± 0.1	1.3 ± 0.1	3.0 ± 0.1	37 ± 5
	3.1	3.3 ± 0.2	1.8 ± 0.2	2.4 ± 0.2	16 ± 2
	3.2	3.2 ± 0.2	1.8 ± 0.2	2.6 ± 0.2	15 ± 2
	3.3	3.4 ± 0.1	1.3 ± 0.1	2.7 ± 0.1	23 ± 2
	3.4	3.4 ± 0.1	1.2 ± 0.1	2.9 ± 0.1	27 ± 3
	4	2.6 ± 0.1	0.9 ± 0.1	2.9 ± 0.1	30 ± 4
	5	2.0 ± 0.1	0.8 ± 0.1	3.5 ± 0.1	50 ± 7
	6	1.7 ± 0.1	0.9 ± 0.1	3.9 ± 0.2	77 ± 8

Table 3.1-2: Fitting parameters obtained from fitting equation 3.1-7 to $\Delta\eta/\eta$ data.

For the change in efficiency at higher current densities there is a clear sign of a slower rise from ~45mT. It is this slower rise that hinders the fitting of this data with Equation 3.1-7. The fact that this shallow rise only appears at high current densities could be explained by triplet-triplet annihilation. Triplet-triplet annihilation is a bi-excitonic process hence the probability of this process goes as the square of the triplet population. Triplet population will increase as the current density increases, hence the greater likelihood of seeing TTA at higher drive voltages. From equation 1.4-1 we know that TTA goes to increase luminescence through the generation of a singlet exciton. If all other effects are constant then any magnetic field effect on TTA should go to increase the efficiency, however figure 3.1-13 shows that the percentage change in efficiency actually decreases with increasing voltage. This does not necessarily rule out any potential significance of TTA, but it does mean that the potential impact of TTA on OMR is limited to the high-field component.

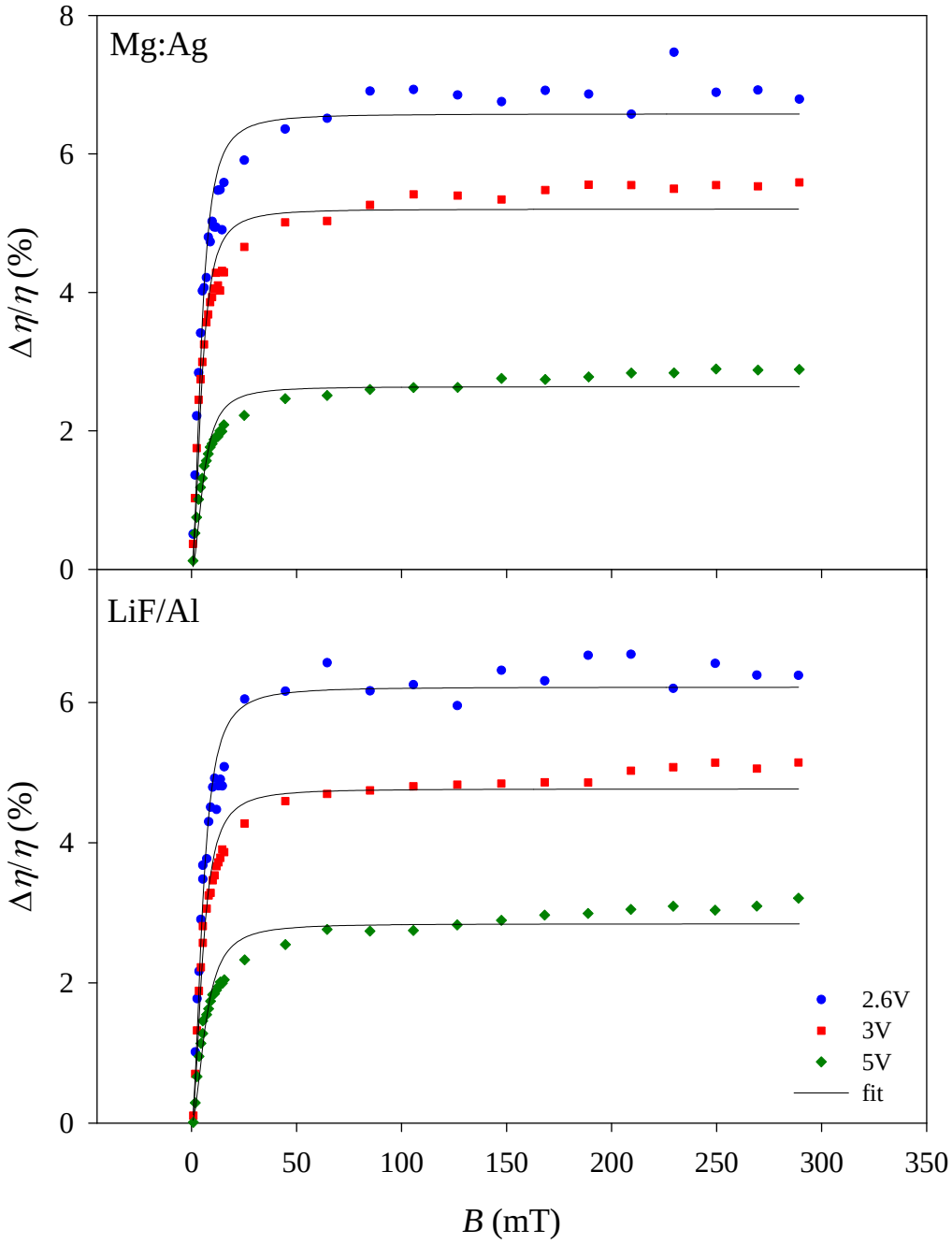

Figure 3.1-12: Single term fits of $\Delta\eta/\eta$ curves

The two panes show the results of fitting equation 1.4-5 to the $\Delta\eta/\eta$ curves of devices with an Mg:Ag cathode and a LiF/Al cathode.

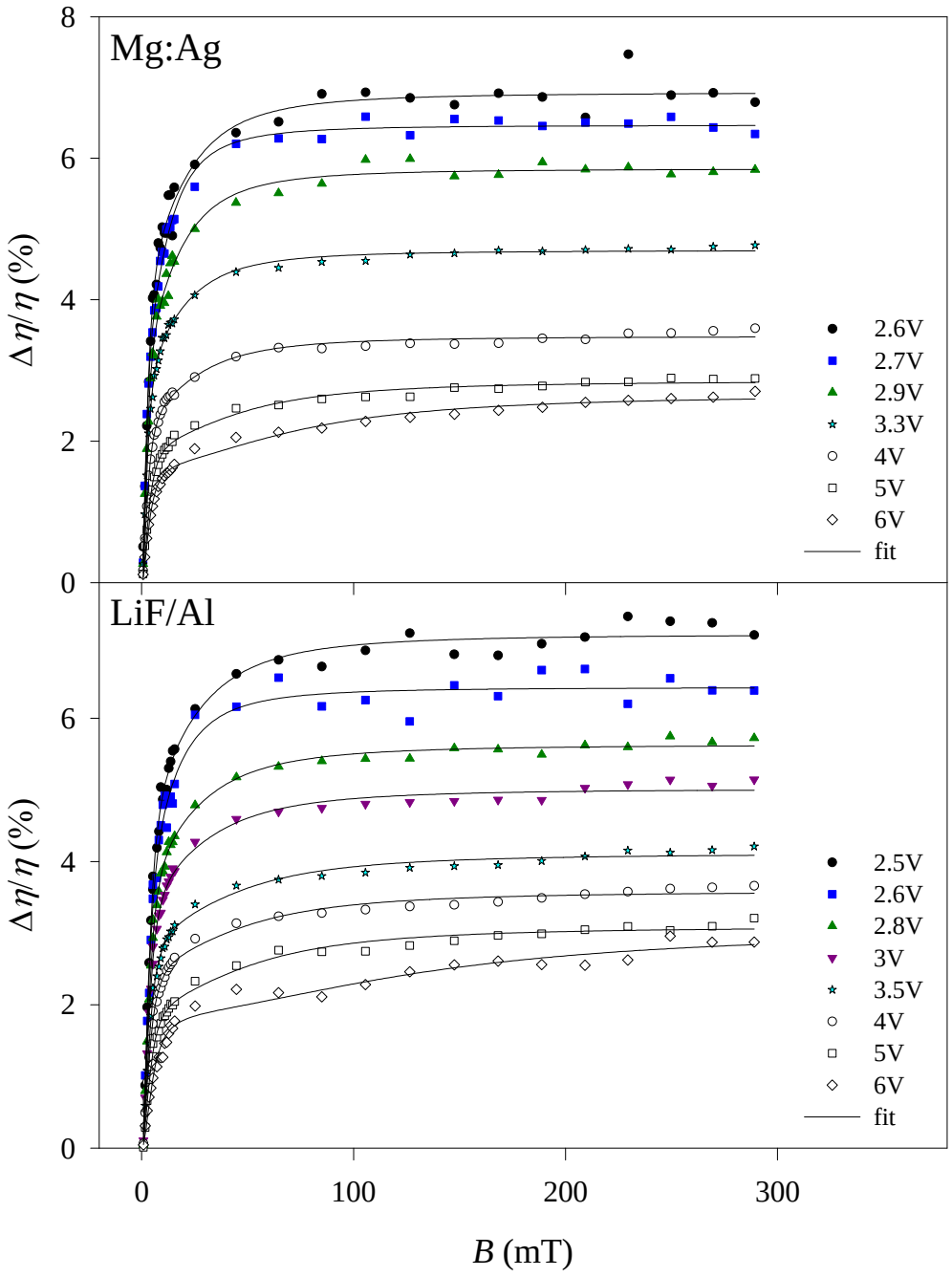

Figure 3.1-13: Double term fits of $\Delta\eta/\eta$ curves

The two panes show the results of fitting equation 3.1-7 to the $\Delta\eta/\eta$ curves of devices with an Mg:Ag cathode and a LiF/Al cathode.

Looking at this overall analysis of change in efficiency shape an adequate description of the observed effects has not been found. What certainly can be said is that at low fields the change in efficiency does show “Lorentzian” like behaviour. At higher fields there are subtle differences between the traces at different current densities. There is possibly a linear component which is poorly defined by the data presented here. Since the nature of the change in efficiency cannot be well defined as a function of current density, effects such as triplet-triplet annihilation cannot be conclusively eliminated as a cause or contributor to the magnetic effects observed. Triplet-triplet annihilation can also lead to an increase in singlet luminescence, but as we have shown while this cannot be conclusively eliminated it is not likely to have a dominant effect on luminescence or OMR.

3.1.9 Synopsis – Cathode study

Through the simple method of changing the cathode material of a basic Alq_3 OLED a number of interesting effects have been observed. The comparison of this data with literature shows a large number of inconsistencies when analysis is made of the functional form of the magnetic field effects. The discrepancies between the functional forms is in contradiction to the simplistic ideas of “universality” and shows that device structure can be an important factor in determining the shape of the measured traces.

Perhaps most importantly is that excitonic effects cannot be dismissed as they have been in many publications. Indeed the data presented here shows that excitonic effects are likely to be the root cause of magnetic field effects in OLEDs. The triplet/free-carrier interaction that was first proposed by Ern and Merrifield provides a mechanism that qualitatively explains the observed phenomena.

Triplet-triplet annihilation is also highlighted as having a possible significance. If TTA is a significant process that affects triplet population and luminescence then the data obtained here would suggest that the magnetic field modulation of TTA is in addition to the triplet/free-carrier interaction and is seen for increasing magnetic fields.

3.2 The effect of device thickness on magnetic field effects

As has been indicated in the literature the changing of device thickness appears to affect the measurable OMR. OMR in PVK was seen to decrease as the PVK thickness was decreased, which was taken as a sign that OMR in PVK was a bulk effect [41]. However the device structure used in reference [41] contained a heavy spin-orbit coupling material $Ir(ppy)_3$ layer, which has been shown to quench magnetic field effects in organic semiconductors. So the high spin-orbit coupling could be the reason that OMR decreased as the PVK thickness was decreased and the total device thickness became dominated by the $Ir(ppy)_3$ layer. There are other references to the effect of varying device thickness [31], although these are for polymer systems where there are difficulties in accurately controlling the thickness over a wide range. As such the effect of Alq_3 thickness on OMR requires further investigation.

Most of the published studies on magnetic field effects on OLEDs appear to focus exclusively on OMR. Magnetic effects on luminescence are covered to a small degree while effects on efficiency receive even less attention. In the cathode study the efficiency data helped to identify the charge/triplet interaction as a possible mechanism for OMR. Since the efficiency data from the cathode study proved to be insightful it is natural to ask how changing thickness will affect the magnetic field induced change in efficiency.

3.2.1 IVL and excitonic correlation of OMR

The basic device structure used was ITO/TPD/Alq_3/LiF/Al, with various thicknesses of Alq_3. From this basic structure various samples were made with Alq_3 layers of 115Å to 900Å. In the study of different cathode materials the coincidence of optical turn-on and measurable OMR was taken as a sign that OMR is dependent upon the presence of excitons within the system. The same comparisons were made for all the thicknesses tested here to check whether this trend continues. Table 3.2-1 shows the voltage for optical turn-on compared with the voltage for the onset of OMR:

Alq_3 thickness	I turn-on	L turn-on	OMR onset
115Å	2.1 ± 0.1V	2.1 ± 0.1V	2.1 ± 0.1V
150Å	2 ± 0.1V	2.1 ± 0.1V	2 ± 0.1V
195Å	2.2 ± 0.1V	2.2 ± 0.1V	
300Å	2.2 ± 0.1V	2.2 ± 0.1V	2.3 ± 0.1V
500Å	2.2 ± 0.1V	2.3 ± 0.1V	2.3 ± 0.1V
700Å	2.2 ± 0.1V	2.3 ± 0.1V	2.7 ± 0.4V
900Å	2.2 ± 0.1V	2.5 ± 0.1V	2.6 ± 0.1V

Table 3.2-1: Alq_3 OLED turn-on and OMR-onset voltages

The first thing to note is that the electrical turn-on limit is fairly consistent, whereas the optical turn-on seems to increase as Alq_3 thickness increases. Comparing the OMR onset voltage to the electrical and optical turn-on we can see the data shown is still consistent with the idea of excitons being necessary for OMR. With the exception of the 150Å data all the OMR onset voltages are equal to or just above the optical turn-on limit. Some peculiarities seen in the OMR onset values are the omission of a value for the 195Å device, the high value for the 700Å device and low value for the 150Å device. The 150Å data showed some noise at low voltages which made it hard to determine the turn-on values, which could explain the discrepancy. The high value for the 700Å device is due to the absence of data between 2.4V and 2.7V; the 2.4V data shows no OMR while the 2.7V data does, so the onset is definitely above 2.4V but cannot be confirmed below 2.7V. The lack of a clear OMR onset value for the 195Å device cannot be understood without a more detailed presentation of the OMR and efficiency data of all the device thicknesses. This is covered in section 3.2.6.

3.2.2 Device thickness effects on efficiency

OMR and magnetic effects on efficiency were measured for a wide range of voltages for all device thicknesses. Operating voltages were taken from the point at which OMR was first detectable to voltages that were as high as possible without risking device degradation. This degradation limit obviously varies from device to device, however over time a good idea of this limit could be determined by comparison of IVL data. IVL data was compared before and after magnetic measurements as well as between devices. Data that showed irreversibility like that of reference [34] was discarded as unreliable.

Figure 3.2-1 shows two plots for the magnetic field effect on efficiency for all thicknesses. The two plots displayed are for data taken towards the extremes of the current densities used; they are separated by three orders of magnitude, 0.1A m^{-2} and 100A m^{-2}. For current densities in between 0.1A m^{-2} and 100A m^{-2}, other than magnitude, no significant variation was seen in the magnetic field effect on efficiency. From figure 3.2-1 we can see that for all thicknesses the magnetic field effects on efficiency are consistent with the previously observed trends witnessed in the study of different cathodes. For fields of up to ~45mT there is a rapid rise in device efficiency followed by a flattening for fields greater than ~45mT. Again this indicates that there is conversion from triplets to singlets within the device.

Another trend that is observed is that the percentage change in efficiency appears to decrease as device thickness is increased. Not only is this evident for the 0.1A m^{-2} and 100A m^{-2} data in figure 3.2-1, but is also evident for all current densities between the two extremes. There is one exception to the trend of lower $\Delta\eta/\eta$ for thicker devices. This exception is with the 300Å or 195Å data. For the low current density data it can be seen that the percentage change in efficiency is higher for the 195Å device. However for the higher current densities the percentage change in efficiency is now higher for the 300Å device. Why this is the case is not immediately clear, however, since all the other data shows such a clear trend it is likely that this inconsistency can be neglected as a random effect. Importantly this inconsistency does not affect the conclusion that all the magnetic effect on efficiency data shows a positive trend and thus shows that triplet to singlet conversion is occurring within devices of all thicknesses.

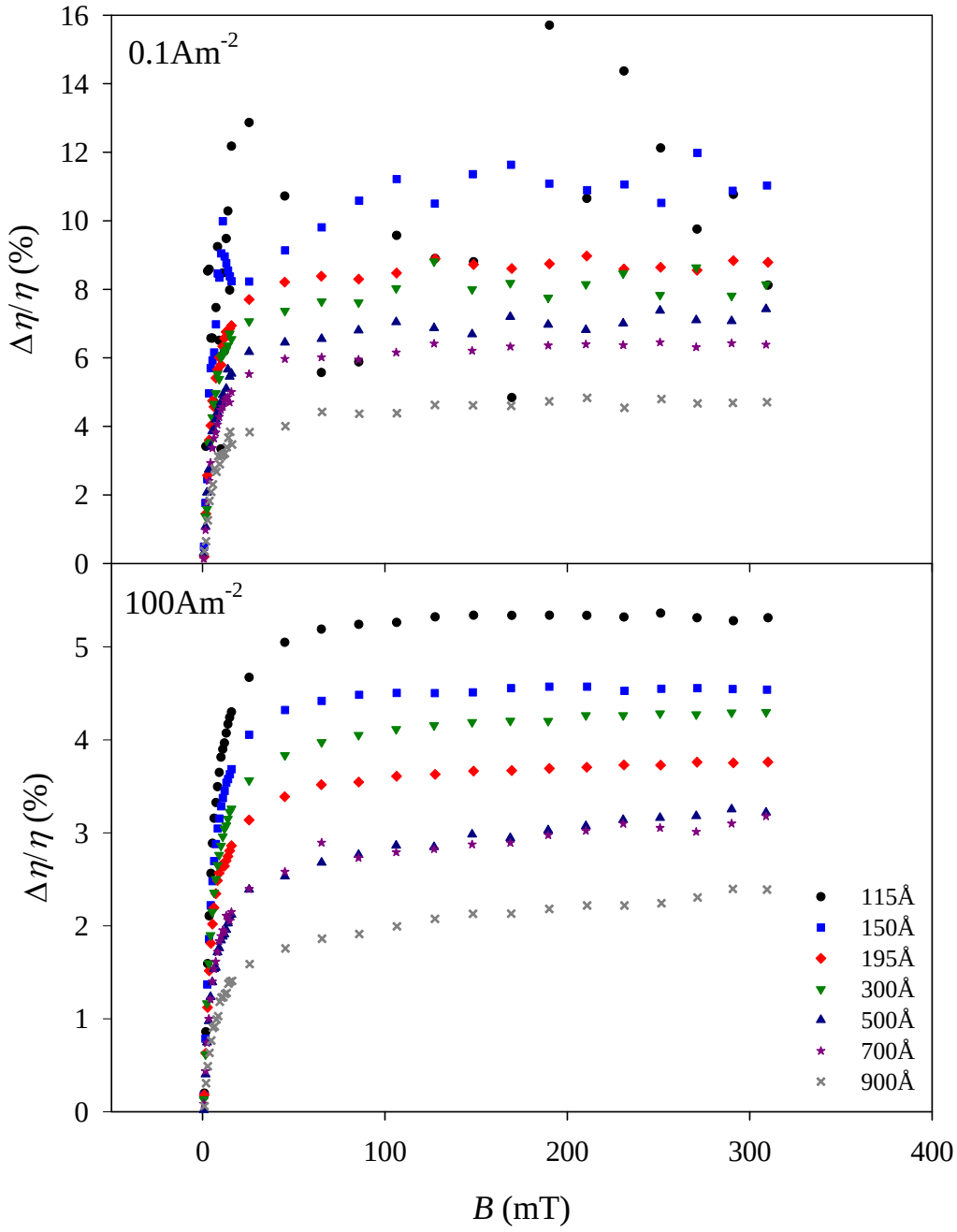

Figure 3.2-1: $\Delta\eta/\eta$ at low and high current density for various thicknesses of Alq_3 OLEDs

$\Delta\eta/\eta$ curves at taken at constant drive voltages corresponding to currents of ~0.1Am^{-2} are shown in the top pane for various thicknesses of Alq_3. The bottom pane shows the corresponding data for devices with currents of ~100Am^{-2}.

3.2.3 OMR – Thin devices, new effects

Looking at the OMR data corresponding to the same current densities of Figure 3.2-2 a more complicated situation is observed. If we first look at the ~100A m^{-2} data then it is apparent that there is a difference when compared to the corresponding $\Delta\eta/\eta$ data. Figure 3.2-3 (page 95) shows the results for $\Delta\eta/\eta$ data taken for all thicknesses at ~1Am^{-2}, normalised to 1. It is clear from figure 3.2-3 that there is very little variation in the shapes of the $\Delta\eta/\eta$ traces, the only significant difference is the absolute magnitude. For OMR, even without normalisation, it is clear that the data at 100A m^{-2} does not scale in the same way as the efficiency data, as thickness is altered. As the device thickness is lowered it appears that the low field rise up to ~45mT decreases relative to the high field effect.

If we now look at the ~0.1A m^{-2} OMR that is shown in figure 3.2-2 then the picture becomes more complicated still. It is clear to see that thinner devices at low current densities the OMR observed is negative. The only difference between the traces in figure 3.2-2 is the thickness of Alq_3, which implies that the switch from positive to negative OMR must be attributed to effects within the Alq_3 layer. These negative OMR traces do display a similarity with the positive OMR insofar as there is a sharp low field change in OMR followed by a flattening for fields greater than ~45mT. Negative OMR has been observed in Alq_3 devices before. As indicated in the introduction, negative OMR was only observed at very high applied voltages and was often not reproducible [34]. Negative OMR has not been previously observed at currents that are so low and close to the turn-on of the device as they are in figure 3.2-2. Indeed this is the first observation that negative OMR is witnessed for low current densities rather than high current densities. This observation is a clear indication that there are other processes that contribute towards the overall shape of the OMR traces. Before these possible effects can be addressed there is a need to understand the OMR traces more thoroughly, this is covered in section 3.2.4.

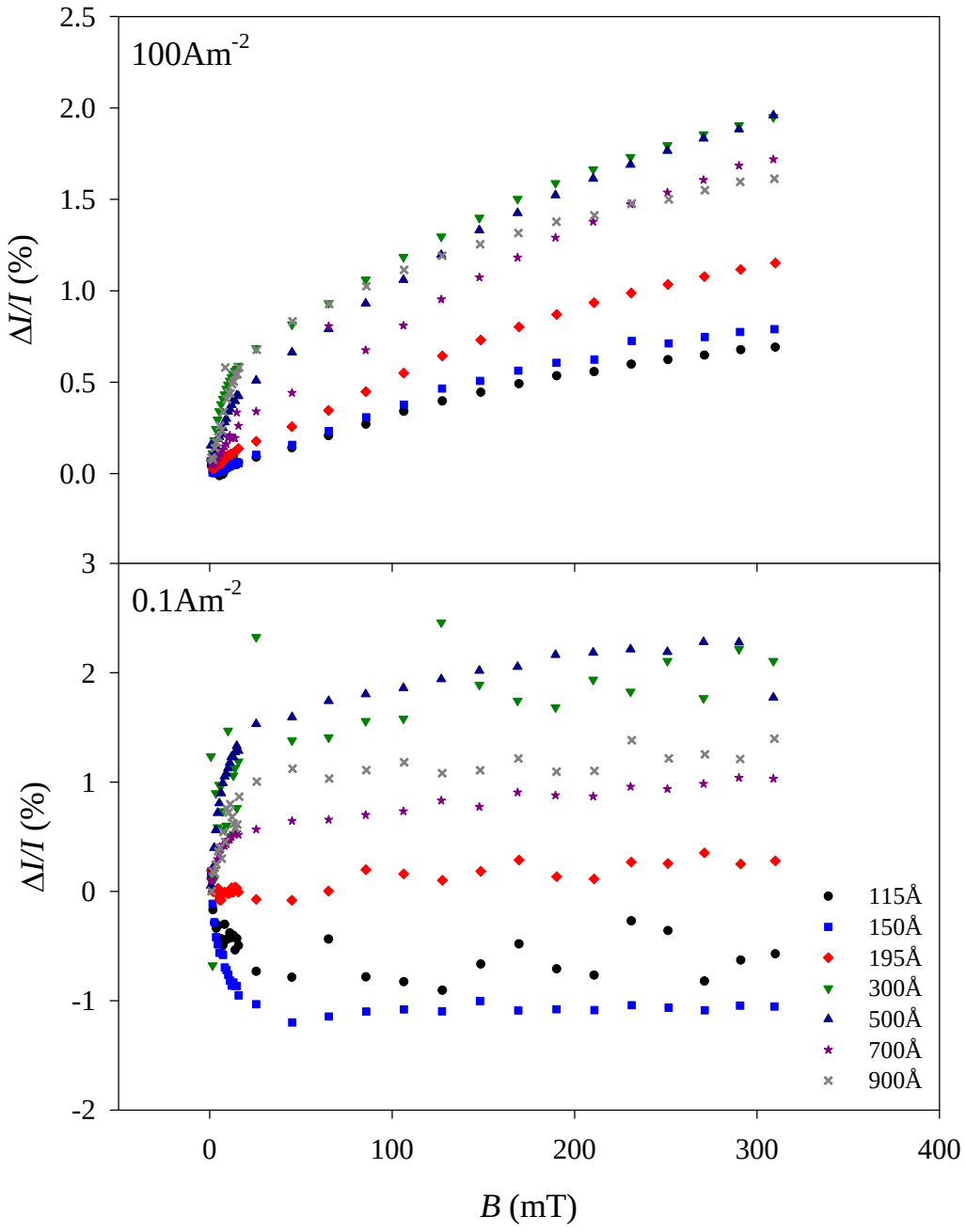

Figure 3.2-2: OMR at low and high current density for various thicknesses of Alq_3 OLEDs

OMR curves for various thicknesses of Alq_3 taken at constant drive voltages corresponding to currents of ~100Am^{-2} are shown in the top pane. The bottom pane shows the corresponding data for devices with currents of ~0.1Am^{-2}.

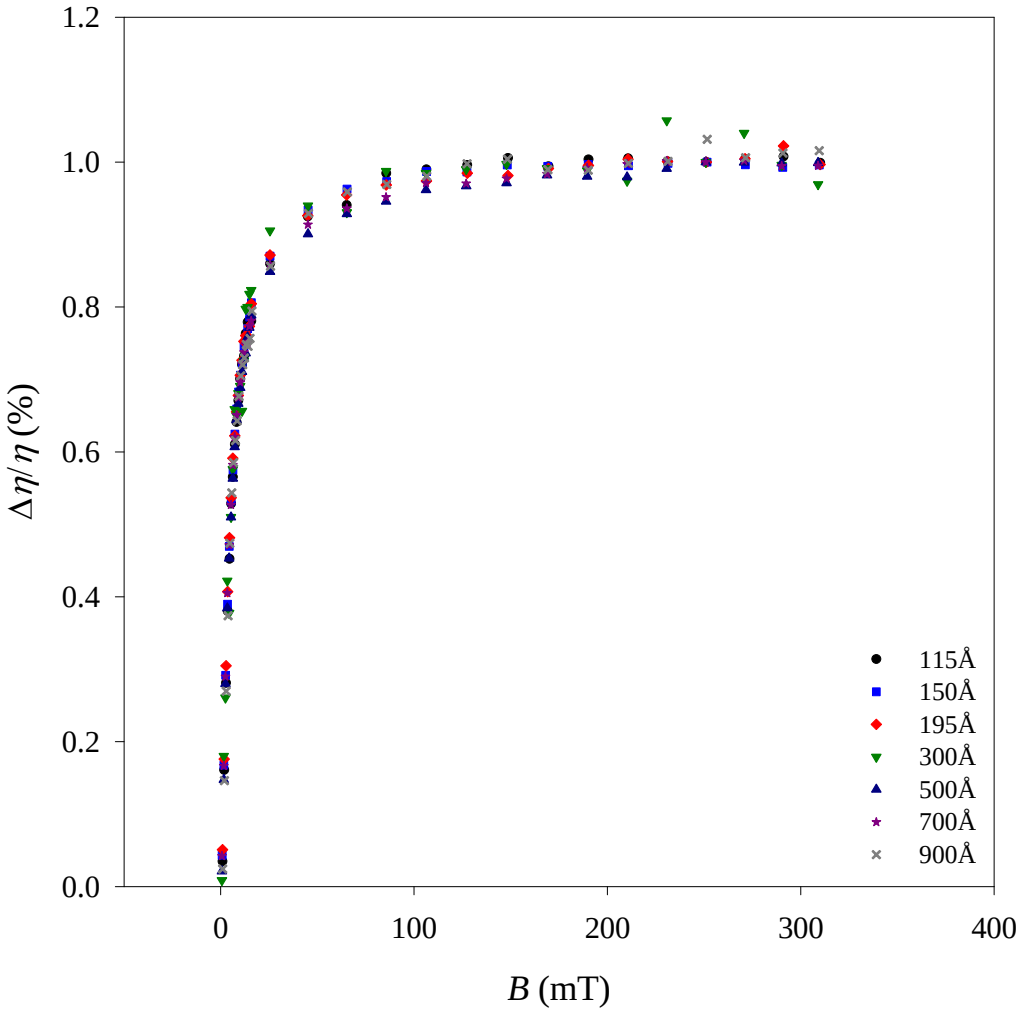

Figure 3.2-3: Normalised Δη/η taken at ~1Am^{-2}

This figure shows the normalised Δη/η results for various thicknesses of Alq_3. Results have been taken at constant voltages corresponding to ~1Am^{-2}.

It is not immediately clear why thin devices should give a negative OMR but the data in figure 3.2-2 shows the first observation of a true modulation of OMR as device thickness is varied. Also, since the onset of OMR in the 115Å and 150Å devices is negative and coincident with light output, this implies that whatever is causing the negative OMR is also linked to the presence of excitons.

3.2.4 Magnetic field trends and their components

The observation of negative OMR is not predicted by the triplet/free-carrier mechanism. According to the mechanism, the magnetic field would have to increase the triplet population in order to observe a drop in current. The magnetic field effect on efficiency data for all thicknesses at all operating voltages shows that even when negative OMR is observed there is still a positive change to efficiency, hence triplet to singlet conversion. So at first it would seem that the observation of negative OMR is inconsistent with the triplet/free-carrier model. In order to verify this premature idea some effort has to be made to understand the nature of the various components in the magnetic field effect data.

If we look at the OMR for Alq_3 devices thicker than 195Å, in figure 3.2-4, then there is no indication of negative OMR regardless of operating voltage. Even though the OMR for devices thicker than 195Å is always positive there are still differences between the various OMR traces. These differences are found in the proportions of the low and high field effects, which is easy to see in the 500Å data. At low voltages the 500Å data shows a large low-field rise and a relatively shallow rise at high-fields; at high operating voltages the low-field rise has dropped in magnitude while the high-field component appears steeper.

Even though there is a change in the shape of OMR trace with voltage the sharp low-field rise and the shallow high-field OMR is still observed. This overall shape is consistent with the $\Delta\eta/\eta$ data. So the triplet/free-carrier mechanism is consistent with the OMR observed for devices thicker than 195Å. Although other effects could well be playing some role in affecting the shape of the OMR curves.

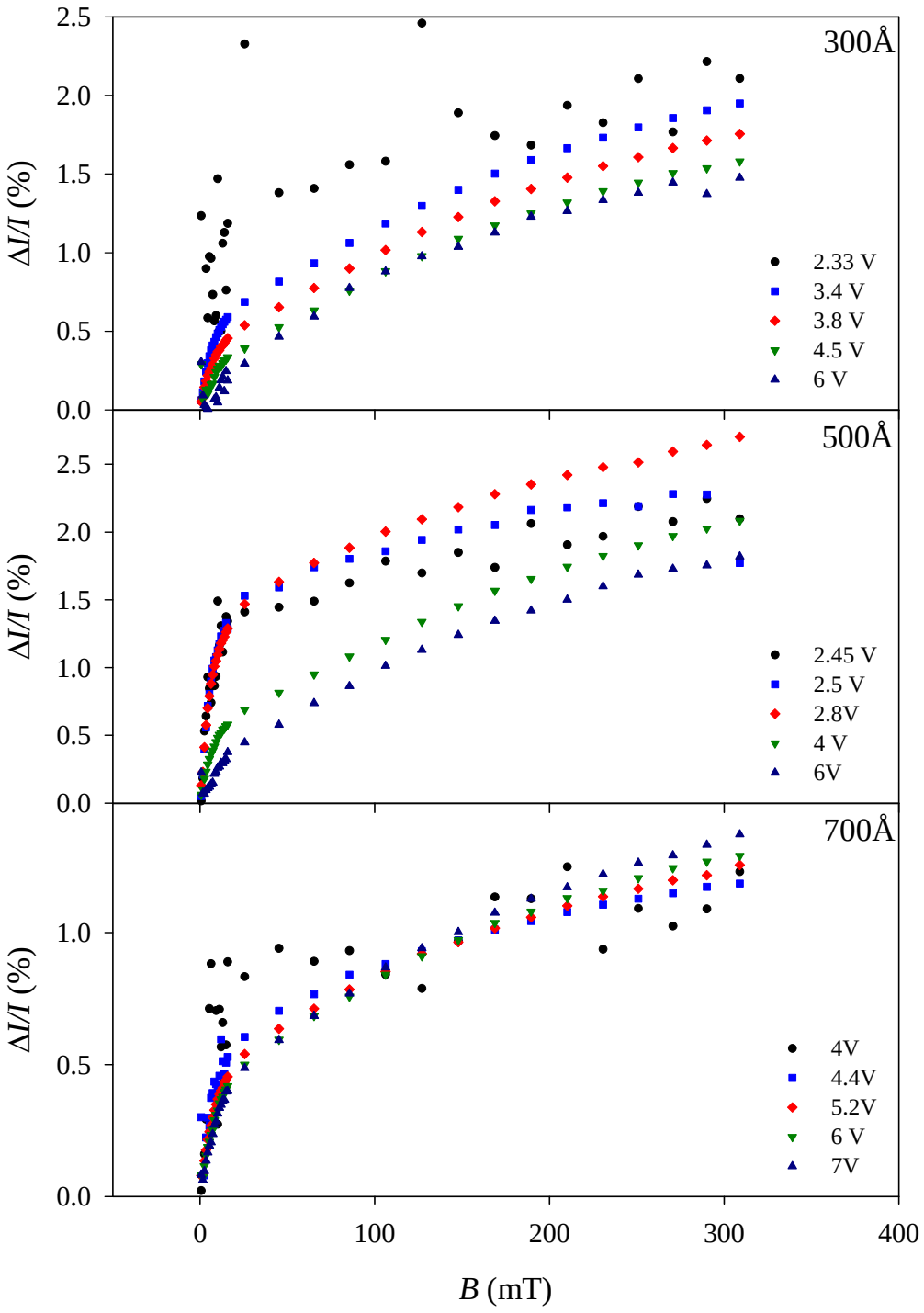

Figure 3.2-4: OMR of thick Alq_3 OLEDs

OMR for devices with Alq_3 layers thicker than 195Å are presented in this figure. Each pane shows a wide range of applied voltages to show how OMR varies with current density.

Figure 3.2-5 shows the OMR taken at various voltages for both the 115Å and 150Å devices. The transition from negative OMR at low current density to positive OMR at high current density can now been seen more clearly. The low current density OMR traces show a rapid fall in OMR at low fields followed by a plateau for fields above ~45mT. As the applied voltage is increased the rapid fall in OMR becomes smaller with the height of plateau region following suit. For both thicknesses of 115Å and 150Å, as the applied voltage is increased, there comes a point when the plateau ceases to be flat and starts to show some positive gradient. For higher voltages the low field component of OMR eventually disappears with only a positive high field OMR observed. This data implies that there are two distinct processes that operate at low and high field. One "positive" process gives rise to positive OMR at high current density, while the other "negative" process acts to give negative OMR at low current densities. The data also implies that these processes evolve differently depending upon current density. Another implication of this data is that the high current, positive OMR effect could be acting to counteract the negative low current density effect. For high current densities the positive hyperfine scale rise could be cancelled by the hyperfine scale drop seen for the "negative" process. This cancelling could explain why very little rise is seen at low magnetic fields in thin devices.

In order to see how low and high magnetic field effects evolve with drive voltage the OMR data for various applied magnetic fields was plotted against drive voltage. Figure 3.2-6 (page 126) shows this data for several device thicknesses. For the 300Å data it can be seen that for fields lower than ~45mT the OMR peaks at ~2.4V and then decays to almost zero from a peak of ~1%. For fields above ~45mT the OMR also peaks at 2.4V but the decay is much lower, with OMR dropping from ~2.6% to ~1.5%. So the higher field effects are seen for a wider range of applied voltages than the lower field effects. The 500Å data shows these effects more clearly, with the OMR for fields above ~45mT showing a much slower decay than the fields below ~45mT. For the 700Å device this effect becomes clearer still, with the OMR above ~45mT clearly increasing as voltage is increased, while the OMR below ~45mT falls. This data is consistent with the results for the 115Å and 150Å devices which also displays an increase in the OMR above 45mT as current density is increased.

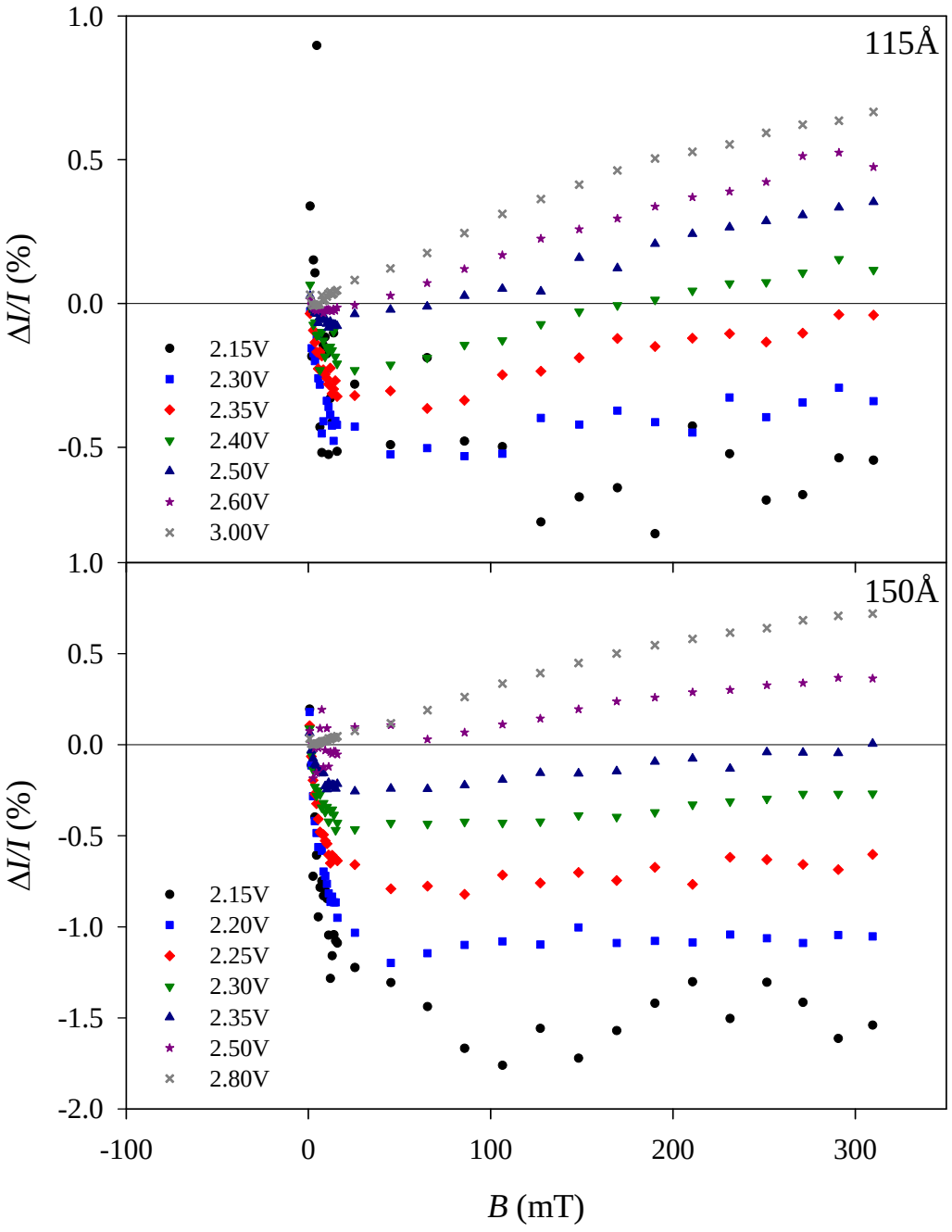

Figure 3.2-5: OMR of thin Alq_3 OLEDs

OMR for devices with Alq_3 layers thinner than 195Å are presented in this figure. Each pane shows a wide range of applied voltages to show how OMR varies with current density.

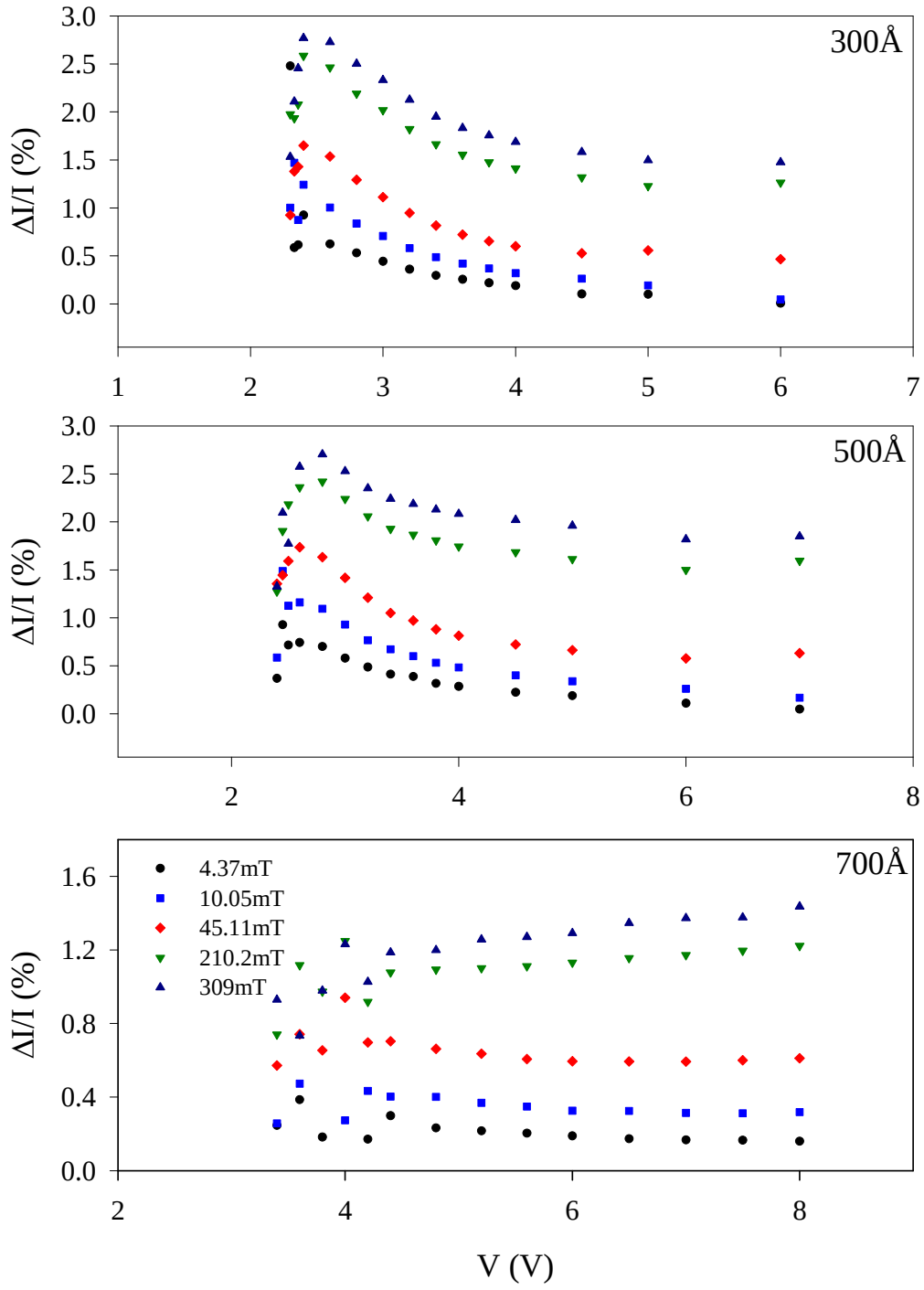

Figure 3.2-6: OMR versus applied voltage for thick Alq_3 OLEDs

The figure above shows how the high field and low field components for OMR vary with applied voltage.

Previous work from the Iowa group [32] showed that once normalised, OMR for different molecular systems was similar in shape as magnetic field was varied. From this, the notion of "universality of OMR" was described. This idea stated that since remarkably variant molecular systems could show identical OMR the cause behind OMR must be simple and universal. Further work from this group has taken this concept so far as to imply that OMR must have a single mechanism. The data shown here is not contradictory to the idea that OMR has some universality, but it does show that the weight given to this concept of universality is too great. Collectively the data from this thickness study shows that the cause behind any given OMR trace is multi-faceted, with OMR varying distinctly with current density and thickness.

Given that there is evidence to show that observed OMR effects are from a combination of effects, it is not necessarily the case that our first model of charge/triplet interactions is incorrect. Another process at low current densities and low Alq_3 thickness could explain the observed phenomena.

3.2.5 Exciton dissociation – Possible cause for negative OMR

As mentioned previously, the role of exciton dissociation on OMR or the percentage change in efficiency is not clear. Kalinowski and Prigodin propose mechanisms for OMR that involve the dissociation of singlets. However, the short decay lifetime of the singlet state limits the possible impact of singlet dissociation. More pertinently, the role of triplets in OLEDs was largely neglected by Kalinowski and Prigodin. If singlet dissociation is significant then it would be expected that triplet dissociation should also be significant, especially given the larger steady state population of triplets. Excitons have a relatively large binding energy of ~0.3-0.5eV, which means that dissociation from causes such as thermal excitation is unlikely. Instead dissociation requires a site where either the electron or hole in the exciton can lower its energy when compared with its energy in the exciton pair state. In an OLED these sites are usually the interfaces found in the device. Both the cathode and anode act as good sites for exciton dissociation as they have readily available sites for accepting charge carriers and are energetically favourable.

The probability of an exciton finding its way to a dissociation site is dependent upon the local environment and the movement of the exciton through it. In regards to charge transport, local environment is defined by factors such as available sites and overlap of the molecular orbitals, which in part determine the mobility of charge. An exciton with a longer lifetime will naturally have greater time to diffuse. So the combined factors of the local environment and the radiative lifetime of the exciton will determine the diffusion length of the exciton. Since the local environment and the radiative lifetime are material properties of the system, controlling dissociation is limited to methods which increase the likelihood of an exciton finding a dissociation site. Changing the thickness of the luminescent layer is one method for increasing the probability of dissociation.

In a device where Alq_3 is used as an electron transport/luminescent layer, with TPD used as a hole transport layer, exciton formation occurs close to the Alq_3/TPD interface. This is because this interface provides a large energetic barrier for the electrons to overcome while the holes are able to tunnel into the Alq_3, thus allowing for exciton formation close to the interface. The location of exciton generation means that we should consider the possibility of dissociation at the TPD/Alq_3 interface. If we also consider the OMR for thick devices in figure 3.2-2 then it is clear that there is no negative OMR that can be attributed to dissociation. Since excitons are generated at the TPD/Alq_3 interface any dissociation at this interface would be insensitive to changes in device thickness, hence one would expect to see negative OMR in thick devices if there was significant dissociation at the TPD/Alq_3 interface. Since there is no negative OMR for thick devices we can consider any dissociation that might be occurring at this interface to be negligible.

With the exciton generation being close to the TPD/Alq_3 interface it is important to consider the possible effects of an exciton migration into the TPD. It is well documented that in the described device structure the luminescence is from Alq_3 and not from TPD [52,53], despite the luminescent properties of TPD in an EL device [54]. So exciton diffusion into the TPD layer can be considered negligible. This means that the only diffusion we need consider is through the Alq_3 layer.

By altering the thickness of the Alq_3 layer we can alter the distance that an exciton needs to diffuse before meeting the cathode and dissociating. Thus, we have a method of controlling the dissociation current. If dissociation can affect OMR

then it would be expected that any subsequent effects should be clearer for decreasing Alq_3 thicknesses. From the low current data in figure 3.2-2 we can clearly see that OMR changes dramatically for thinner devices which matches well with the idea that dissociation could be responsible.

As previously mentioned the likelihood of an exciton finding a dissociation site is increased as the device thickness is decreased. For a device that is thin enough for dissociation to occur, a contribution to the overall device current will come from carrier recycling. This is to say that an exciton dissociating at the cathode will loose a hole to the cathode and leave a free electron which will be free to move under the applied potential gradient. So some percentage of the total device current will be from these recycled carriers.

Given their larger lifetime triplets are more likely to reach a dissociation site, hence we can assume that the contribution to current from dissociation is from the dissociation of triplets rather than the dissociation of singlets. We have already established that the application of a magnetic field increases the conversion of triplets to singlets. So if a device has a significant dissociation current applying a magnetic field will lower the triplet population and hence lower the dissociation current. This gives us mechanism in which a magnetic field lowers current, hence a negative magnetoresistance. Since this mechanism relies on the lowering of the triplet population it is in agreement with the existing model and does not contradict the observed OMR for thicker devices or any of the observed change in efficiency data.

Data published by our group on the effect of exciton blocking layers on OMR tests the theory that dissociation mechanisms are significant in thin devices [54]. Nominally identical devices to the ones used here were fabricated both with and without the exciton blocking material 2,9-dimethyl-4,7-diphenyl-1,10-phenanthroline (BCP). In figure 3.2-7 (page 105) the data for devices with BCP is taken from reference [55] and shows that for a given device structure the effect of an added exciton blocking layer is to completely eliminate negative OMR. In fact the 2.6V data also shows that the low field effect that is absent in devices in thin devices, reappears for devices with BCP, this shows that excitons interacting with the cathode is crucial to the new phenomena seen in thin devices. This data also confirms that dissociation at the TPD/Alq_3 interface is negligible; introduction of BCP between the Alq_3 and cathode eliminates negative OMR, if dissociation were

significant at the TPD/Alq_3 interface then you would expect to see negative OMR regardless of the introduction of BCP.
The fact that an exciton blocking layer can eliminate negative OMR is a good test of the idea that exciton dissociation occurs at the cathode and is in agreement with the idea that dissociation is significant in thin devices.

3.2.6 Two mechanisms – Combined effects on OMR

With the dissociation mechanism there are now two possible mechanisms that can affect OMR. These are, triplet/free-carrier interactions that act to hinder electron mobility and yield a positive OMR when a magnetic field is applied, and the dissociation of triplet excitons at the cathode which contributes to total device current, which yields a negative OMR when a magnetic field is applied. If we combine the two effects of exciton dissociation and triplet/free carrier interactions it is possible to explain the observed shapes of the OMR and percentage efficiency changes of the thinner devices.
As already established the magnetic field effect on efficiency indicates a hyperfine scale increase in singlet population and a corresponding drop in the triplet population, which is due to increased intersystem crossing. A change in triplet population has two effects; one is to reduce the magnitude of the dissociation current, the other is to reduce the scattering events from the triplet/free-carrier interaction. So in thin devices there simultaneously exist effects that will both reduce and increase the current.

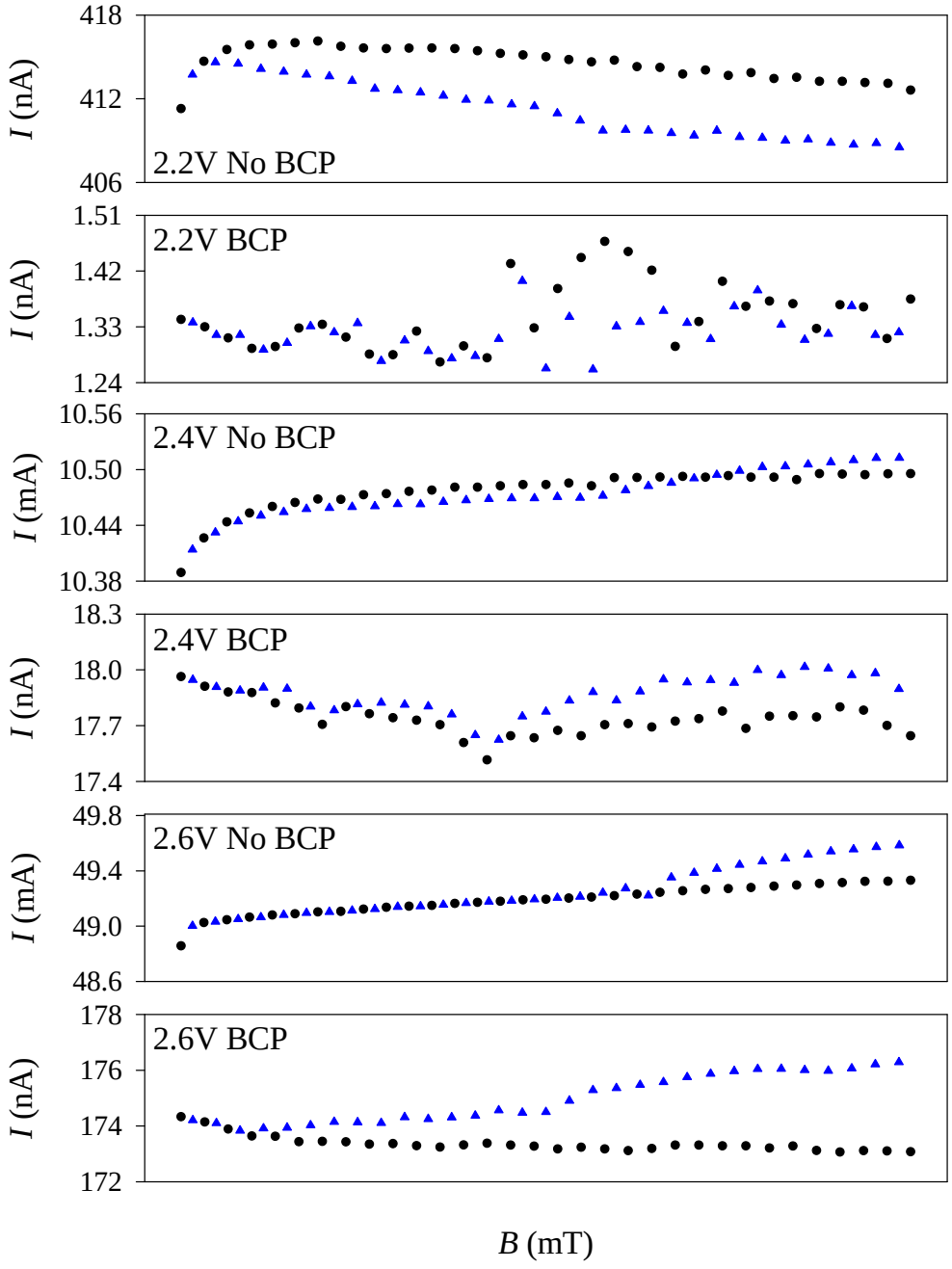

Figure 3.2-7: OLED current under magnetic field for devices with and without BCP

The data above shows the raw current through OLEDs with a 150Å of Alq_3 both with and without BCP. The abscissa is arbitrary, but the field is increasing from left to right. Black circles denote null field measurement, while blue triangles are the device current under a magnetic field

Whether an overall positive or negative change in current is seen is dependent upon the relative significance of dissociation and triplet/free-carrier interaction. For thick devices, regardless of current density, there is negligible dissociation current, so we only see a positive hyperfine scale rise in current caused by the triplet/free-carrier interaction. For thin devices where dissociation is significant, there is a negative OMR which is in balance with the positive OMR caused by the triplet/free-carrier interaction. At low current densities we see evidence for the dissociation effect being dominant. As the current density is increased we see a gradual change to a positive effect implying that the balance between the two effects has changed.

Both the dissociation and triplet/free-carrier mechanisms are dependent upon the intersystem crossing from triplets to singlet, so it is not immediately obvious why the balance between the two effects should change. The obvious implication is that both effects scale differently with current density. At low current densities there is a dominance of the dissociation effect while at high current densities the triplet/free-carrier effect becomes more significant.

At low voltages there will be a lower population of free carriers and subsequently there will be a lower population of singlets and triplets. Logically a lower population of free carriers and triplets in a system of fixed size will mean a lower probability of both a free carrier and exciton occupying the same site. This will mean that at lower current densities there is a lower probability of interaction between the triplet and free carrier. A lower probability of interaction will naturally mean that the significance of the triplet/free-carrier interaction will be diminished.

At this point it is also worth noting that the triplet/free-carrier interaction is likely to hinder the triplet exciton mobility as well as the free carrier mobility. Increased triplet mobility will lead to an increase in the triplets that reach the cathode, thus the dissociation current will increase. So at low current densities where the triplet/free-carrier interaction is inherently lower there is an added effect of an increase in dissociation current. As the drive voltage increases the population of excitons and free carriers increases which will increase the probability of interaction between the two. An increase in the triplet/free-carrier interaction and the subsequent positive OMR balances with the negative OMR from the dissociation effect. The high current density data in figure 3.2-2 shows that at high

current densities the two effects balance to give a relatively small rise below ~45mT. Also explained by this combination effect is the lack of a clear OMR onset for a 195Å device in table 3.2-1. At low voltages, for thicknesses below 195Å the OMR is dominated by the dissociation effect; above 195Å the OMR is dominated by the triplet/free-carrier interaction. So 195Å clearly signifies the transition in dominance from one effect to the other, hence it is not surprising that for 195Å the two effects largely cancel giving very little OMR, as indicated in the low current density data of figure 3.2-2. It is only when high current densities are achieved that we can see a clear OMR.

3.2.7 Triplet to singlet conversion

We now have a model in which we can qualitatively explain the occurrence of a wide range of OMR and magnetic field effects. As mentioned before, the triplet/free-carrier interaction and the dissociation mechanism can have an affect on device current. However it is the intersystem crossing between singlet and triplet states that ultimately affects these two mechanisms. What has not been addressed so far is the way in which intersystem crossing is being affected by the application of a magnetic field.

There are two key factors in determining the intersystem crossing between states, energy and spin. Figure 3.2-8 (109) shows a schematic of the energy level in Alq_3 structure with the rates between the various states indicated. The energetic barrier between the singlet and triplet state has been shown to be easily overcome at room temperature in various studies [30,56]. So in the context of the presented room temperature measurements on OLEDs the conversion of spin needs to be addressed. There are two well known mechanisms that can alter the spin state of a charge; namely hyperfine interactions and spin-orbit coupling. Hyperfine interactions are able to flip spin and thus can cause intersystem crossing between the singlet state and the entire triplet manifold. Spin-orbit coupling leads to splitting in energy levels between different spin orientations, this splitting can lead to a greater overlap between the singlet and triplet states, hence making it more likely for intersystem crossing to occur. Another way in which spin can be affected is through perturbations due to a magnetic field. Indeed this was mentioned in the introduction where Merrifield argued that different local fields

would cause the hole and electron within an exciton to have different precession, hence causing mixing between the singlet and triplet state; this argument is also mentioned in references [28,57]. In references [20,28] it was argued that an applied external field could provide a homogenising effect to the total field experienced by the charge carriers in an exciton, hence altering any inherent mixing that is caused by differing precession rates. This mechanism for altering the mixing between singlet and triplet states is not capable of spin flipping hence is limited to the mixing of the singlet and T_0 triplet state.

It is not clear in what way the mixing between the singlet and triplet state is being modulated. But regardless of the precise mechanism the outcome is that the intersystem crossing frequency is modulated by the applied field.

3.2.8 High field rise – Evidence for further magnetic effects

While the balance between the triplet/free-carrier and dissociation mechanisms explains the shift from negative to positive OMR it does not necessarily explain the observation of a slow rise in OMR above 45mT. This slow rise has been highlighted previously and can be seen in all devices so far presented, in particular figure 3.2-2 and figure 3.2-6. The slow rise above ~45mT appears to increase its influence for increasing drive voltages and therefore has a coincidence with the increasing influence of the triplet/free-carrier interaction. The slow rise above ~45mT is not unique to the data obtained for thin devices; it can be seen for all thicknesses. As the drive voltage is increased this slow rise appears to increase relative to the low field rise; this has already been highlighted in figure 3.2-6.

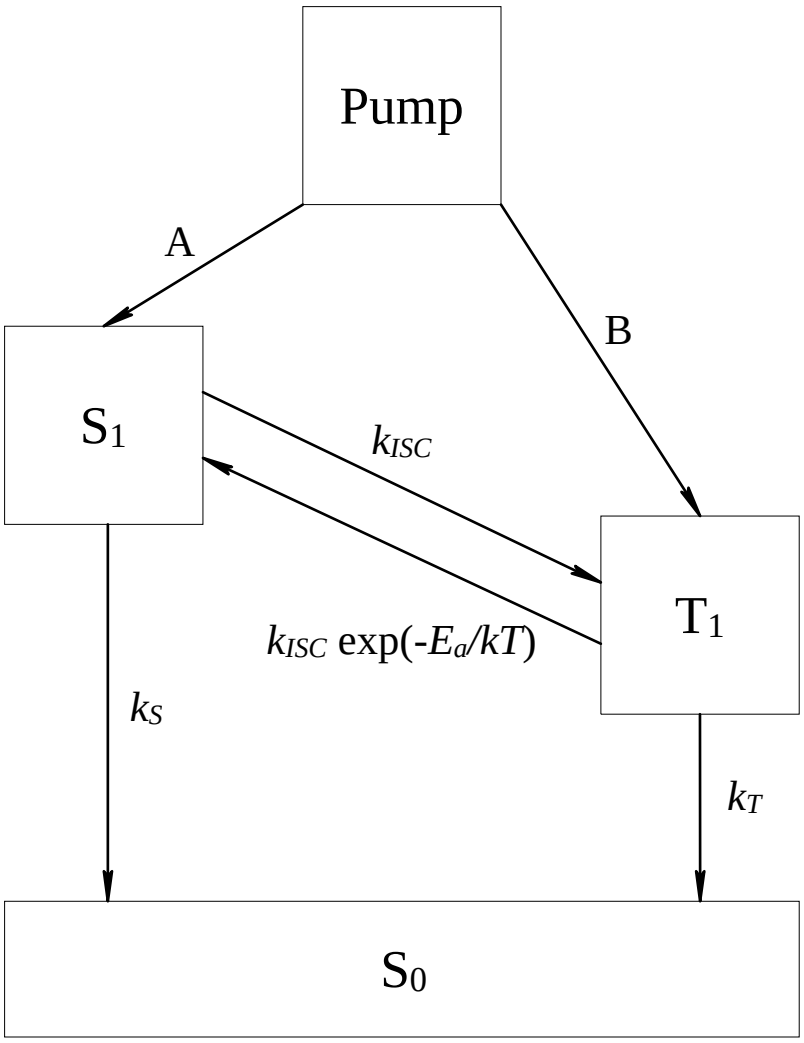

Figure 3.2-8: Rate schematic between exciton states in Alq_3

Above S_0 is the ground state, S_1 is the first excited singlet state, T_1 is the first excited triplet state and k is Boltzman's constant. The rates k_s and k_t are the decay rates from the singlet and triplet state respectively. The rate k_{ISC} is the intersystem crossing rate between the singlet and triplet, while E_a is the activation energy for the process. A and B denote the percentage of the total pump that is divided into the two excited states. For PL A=100% and B=0, while for EL A=25% and B=75%.

If we look at the magnetic field efficiency data in figure 3.2-1 then we can see that the efficiency reaches a plateau at ~45mT; so for all thicknesses at low current density the conversion between singlet and triplets has also saturated by ~45mT. So the effect of increased intersystem crossing has been shown to saturate at low fields and does not explain why the OMR continues to rise at high fields. Obviously if our current model is to hold true, any rise in OMR above 45mT cannot be due to an effect on ISC, else we would expect to see it in the efficiency data also. If we compare the magnetic field effect on efficiency data to the OMR at high current densities, figure 3.2-1 and figure 3.2-2 then a more complicated picture is observed. At high current densities the efficiency data and the OMR data both show a slow rise for fields greater than ~45mT.

At high current densities the appearance of the high field efficiency effect would imply a link to triplet-triplet annihilation effects. If TTA is in some way responsible for the slow high field rise then it means that the TTA interaction of equation 1.4-1 must have some magnetic field dependence. However, TTA is unlikely to explain the high field rise for low current densities. So regardless of whether or not TTA is a significant factor in the high field effect there must also be some other cause for the high field rise in OMR.

Looking again at equation 1.4-2 there are two rate constants, k_1 and k_2, which the original authors Ern and Merrifield stated as being B-field independent and B-field dependent, respectively. This conclusion was made upon the basis that the process described by k_2 involved ISC; hence there is a spin dependent component that would govern the final state. The process described using k_1 however does not involve any changes in spin and was described as an associated state. This weak association means that there is nothing for a B-field to act upon. If however the interaction between the free carrier and the triplet state is more direct than a mere association would imply, it would then be reasonable to believe that there would be spin selection rules that would affect this interaction. If the interaction is strong enough for spin to become a significant factor then some B-field dependence would also be logical. A B-field dependence upon k_1 would explain how the interaction time of a triplet and free carrier could be modified. This could explain how the mobility of free carriers and the subsequent OMR could be changed as a function of applied field and hence explain the rise in OMR seen in addition to any hyperfine scale effects.

In studying OMR as a function of device thickness a more complicated picture of OMR is unearthed. As with the cathode study, the data from different device thicknesses shows that triplet/free-carrier interactions are significant. However a second effect resulting in negative OMR, caused by triplet dissociation is significant for thin devices. This negative OMR in thin devices is unique when compared to negative OMR data already published [34,39]. The two effects of dissociation and triplet/free-carrier interactions show that OMR is multifaceted and not necessarily due to a single cause. Another important point highlighted by the thickness study data is that the rise of OMR at large fields implies that the triplet/free-carrier interaction is actually magnetic field dependent.

3.2.9 Synopsis – Thickness study

From the various devices thicknesses presented here it is clear that more than one mechanism can alter the current through an OLED. The basic effect of the magnetic field is still to change intersystem crossing rate between the singlet and triplet states. With the larger proportion of triplets in the system this change in the intersystem crossing rate acts to transfer excitons from the triplet to the singlet state. This intersystem crossing from triplet to singlet state is confirmed for all thicknesses by the positive trend in the magnetic field effect on device efficiency. What is clear from the OMR data is that a change in triplet population can be seen in multiple effects. In chapter 3.1 the triplet/free-carrier was suggested as a mechanism by which triplets can influence charge mobility and current. The second way in which triplets can affect device current is through dissociation current; this is highlighted in thin devices.

These two effects are seen to act in an opposite manner to one another. Triplet/free-carrier interactions give positive OMR while significant triplet dissociation yields a negative OMR. While the triplet/free-carrier affect is dominant for most cases, the dissociation of triplets can be a significant factor in OMR for thin devices at low voltages. Obviously this variation in OMR response shows that OMR is multi-faceted with a wide variety of possible OMR shapes.

In chapter 3.1 it was seen how the simple change of cathode to the device structure could alter the OMR and other magnetic field effects. The data gathered

for varying Alq_3 thickness furthers this idea showing that device structure can be crucial to the OMR observed.

In furtherance of the cathode study the data for various Alq_3 thicknesses emphasises the importance of intersystem crossing between the singlet and triplet state. However the data presented thus far is not able to discriminate between the various possible ways in which intersystem crossing could be affected by the application of a magnetic field.

Another important outcome of these results is in the analysis of the slow rise seen at high fields in the OMR data. It is clear that the increase in intersystem crossing brought about by the magnetic field is not enough to explain the rise at high fields. To explain this rise at high fields a magnetic dependence of the triplet/free-carrier interaction is proposed.

3.3 Illumination effects on OMR

From the study of devices with different thicknesses the potential significance of exciton dissociation was established. The great variety in OMR shapes observed can be explained by considering this dissociation mechanism in conjunction with the triplet/free-carrier interaction. Obviously these two mechanisms are excitonic in nature. OMR is not observed without the presence of excitons in the system; no OMR is seen for devices operated below turn-on, in the dark. Naturally this leads to the question of whether or not OMR can be seen with excitons introduced through photo-excitation rather than electrical pumping.

In order to further probe the excitonic effects on OMR, studies were performed with an OLED under illumination. Under illumination the OLED should essentially behave like a photodiode, with exciton dissociation giving a photocurrent. Since this thesis is using the term Organic Magnetoresistance to describe a magnetic modulation of current, for simplicity this term shall also be used to describe a modulation in the photocurrent in an organic device.

Operating an OLED as a photodiode will allow for the observation of magnetic field effects on photocurrent and photocurrent/exciton interactions. Past the turn-on voltage of the diode, electrically pumped carriers become significant. For any given device thickness this could give a situation similar to that of thin devices, where both dissociation and triplet/free-carrier interactions could be significant. At voltages below turn-on the device current will only be due to dissociation hence it would be expected that the balance between dissociation and triplet/free-carrier effects would shift towards dissociation, which should be reflected in the OMR data. Above turn-on the electrically pumped charge will become more significant as the applied voltage is increased. If the triplet/free-carrier interaction and dissociation effects give opposite OMR, as in thin Alq_3 devices, then it would be expected that the observed OMR for an illuminated device should undergo some transition as the applied voltage is increased past turn-on.

3.3.1 Basic measurements

In order to maximise absorption into the Alq_3 layer of the OLEDs, the devices were grown with slightly thicker layers of Alq_3. The devices tested have the

structure ITO/TPD (500Å)/Alq_3 (900Å)/LiF (10Å)/Al (1000Å). Aside from the change of Alq_3 thickness, the devices made for illumination studies were prepared and fabricated in the same manner as previous devices. Illumination data was taken using a 395nm LED (~10mW optical power at 20mA) to illuminate the OLED samples, which gives good excitation into the peak of the Alq_3 absorption. Figure 3.3-1a shows the absorption spectra of Alq_3.

Illuminated OMR data was taken for a range of voltages both above and below device turn-on. In the context of an illuminated device the definitions of turn-on used here are still the same as a non-illuminated device and are determined from the IVL curves. From table 3.2-1 in chapter 3.2 we see that the electrical turn-on for a 900Å device is 2.2V; the data obtained for the devices used in the illumination experiments is consistent with this value. The IV curve of a device under illumination and without illumination is shown in figure 3.3-1b; the data is shown on a semi-log plot with the negative photocurrent made positive for the purposes of comparison. From the IV plot under illumination the open-circuit voltage (V_{oc}) is determined to be between 1.99V and 2V.

3.3.2 OMR vs. voltage – New effects

Electrically driving the system gives us a 1:3 ratio of singlet to triplet generation, whereas illuminating the device at voltages below turn-on gives almost 100% singlet generation. From the previous results we know that an applied magnet field increases the intersystem crossing between the singlet and triplet states. More specifically there is an increase in the rate constant k_{ISC} as indicated in figure 3.2-8. Looking back at the rate schematic in figure 3.2-8 the transfer between states is governed by the rate constant and the population of those states.

When the device is operating at voltages greater than turn-on there is a large excess of triplets in the system, so increasing the intersystem crossing rate, k_{ISC}, has the effect of increasing the singlet population at the expense of the triplet population. Similarly, when the system is dominated by a photocurrent there is an excess of singlets due to the sole generation of singlets by photons. In a system where singlets are in excess, an applied magnetic field and the subsequent increase in intersystem crossing will have the effect of increasing the triplet population.

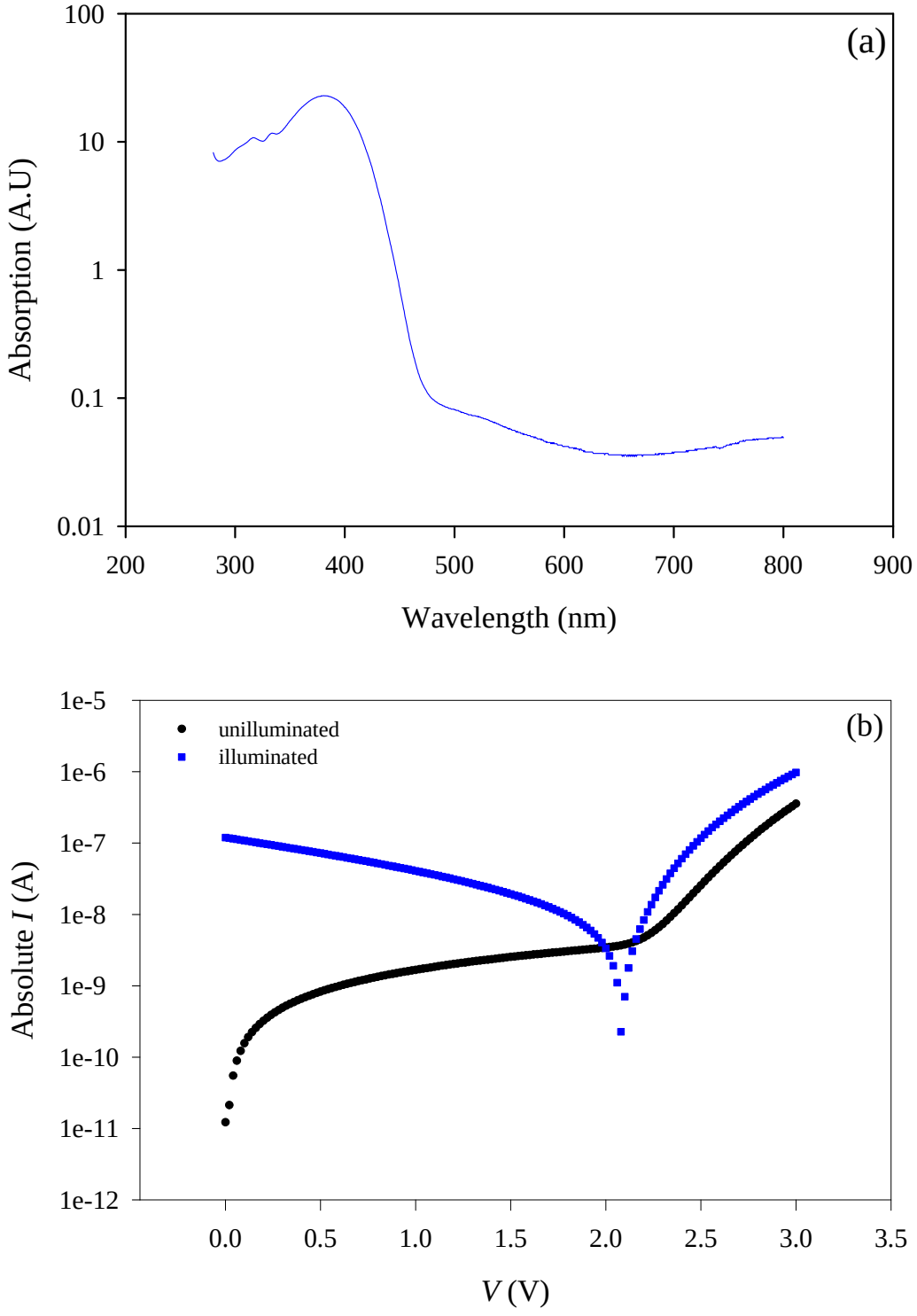

Figure 3.3-1: Absorption spectra of Alq_3 and IV curves for an OLED with and without illumination

Pane (a) shows the absorption spectra of Alq_3 measured using a Hitachi U-3000 spectrophotometer. The bottom pane, (b), shows the IV curves of a ITO/TPD(500Å)/Alq_3(900Å)/LiF(10Å)/Al OLED. Illumination was from a 395nm LED.

For a 900Å Alq_3 device, as described above, figure 3.3-2 shows the OMR of an illuminated device as a function of drive voltage in a magnetic field of 288mT. Also shown are various sections of this curve with the scale altered in order to give a more detailed view. From these plots three distinct regions are clearly visible and are indicated on the plot. These regions are defined by the open circuit voltage of the device and a point at which the device is close to turn-on at ~2.14V. When we drive the device such that the applied voltage is less than the open circuit voltage ($V_{app}<V_{oc}$) we see a large positive OMR which rises asymptotically as $V_{app}\rightarrow V_{oc}$; this defines region 1, which is indicated in figure 3.3-2a. For $V_{app}>V_{oc}$ the OMR displays a sudden switch to negative values. As the applied voltage is increased away from the asymptote the magnitude of the OMR is seen to decrease sharply, quickly falling back to magnitudes that are more comparable to those seen in the previous chapters. This negative region of OMR between the open circuit voltage and turn-on voltage is defined as region 2 in figure 3.3-2a. For applied voltages approaching the turn-on voltage of the device, the OMR reduces towards zero; it then rises positively as V_{app} becomes greater than 2.14V. This transition from negative OMR to positive OMR at 2.14V defines the third region and is shown more clearly in the lower pane in figure 3.3-2b.

While the results shown in figure 3.3-2 are for an applied magnetic field of 288mT the same features and effects were seen at all the fields available with the available equipment. The only difference between the 288mT data and that taken at lower fields is that the magnitude of OMR is lower, which is to be expected. The remarkable feature of the results in regions 1 and 2 is magnitudes of the OMR at applied voltages close to V_{oc} and the switch to negative OMR. While there superficially seems to be many new effects to address, a more detailed look at the data shows that these new variations are consequences of some simple considerations of effects that have been previously established.

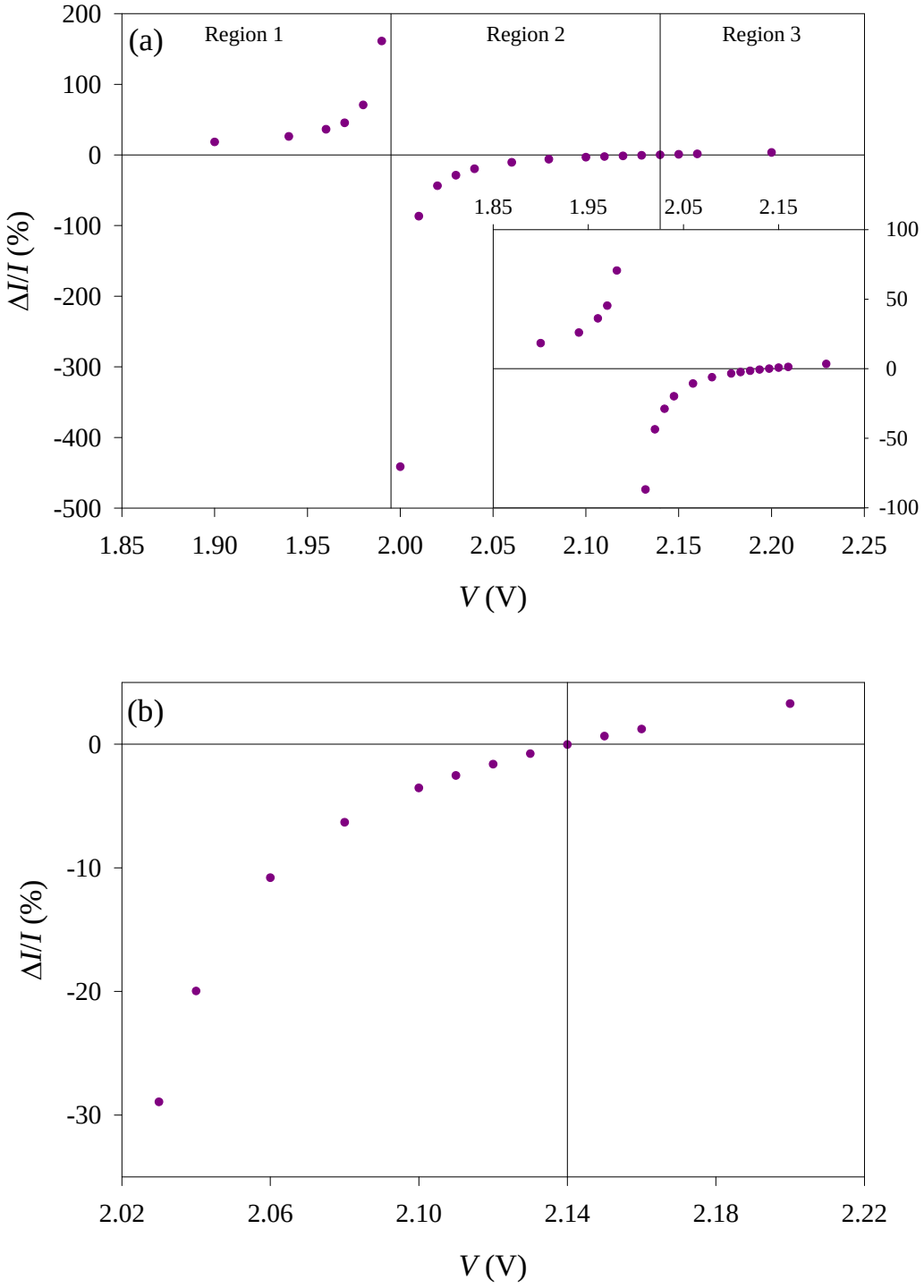

Figure 3.3-2: OMR of an illuminated Alq_3 OLED under illumination

OMR recorded at various voltages for an illuminated OLED in a magnetic field of 288mT. Top pane gives an overview of all measured data, while the inset provides a closer view around the asymptote and the region approaching turn-on. The bottom pane shows the region approaching turn-on in greater detail.

3.3.3 Raw current measurements – Isolating new effects

With the OMR in figure 3.3-2 showing such remarkable variation a close look at the raw current data is required in order to fully appreciate the OMR effects observed. The raw current data taken at several key voltages is shown in figure 3.3-3; circles denote null field measurements, while triangles denote current measured under an applied magnetic field. While the abscissa of these plots has arbitrary units, the applied field is increasing looking from left to right.

Previously we observed the device current increasing under the application of a magnetic field. The 1.9V data from figure 3.3-3 shows a decrease in the current under an applied field. At 1.9V the device is firmly below the turn-on voltage, so the current measured is purely due to exciton dissociation. So it is more pertinent to view this decrease in current as an increase in the dissociation current. For the two voltages either side of V_{oc}, 1.99V and 2V, it is clear that the current also decreases when a field is applied. This is the first piece of evidence that the large positive OMR and large negative OMR are not due to different mechanisms. At 2.14V the applied voltage is close to the turn-on voltage. The OMR corresponding to 2.14V shows a drop in current at low fields which then rises to give approximately zero OMR at high fields, which is similar to the OMR of thin devices in figure 3.2-5. Obviously this data matches well with the idea that we could have a negative to positive transition in OMR even in thick devices, simply through the use of illumination. At 2.16V we can see that the current is now increasing with magnetic field, with the increase scaling with field.

3.3.4 OMR around the open-circuit voltage

We have already established that the current around V_{oc} drops as a magnetic field is applied. As the illumination is creating singlet excitons we have the situation described above where an applied magnetic field goes to increasing the triplet population. As mentioned previously triplet excitons have longer diffusion lengths and are hence more likely to reach the cathode and dissociate. So by increasing the triplet population it is logical that we should observe an increase in the dissociation current.

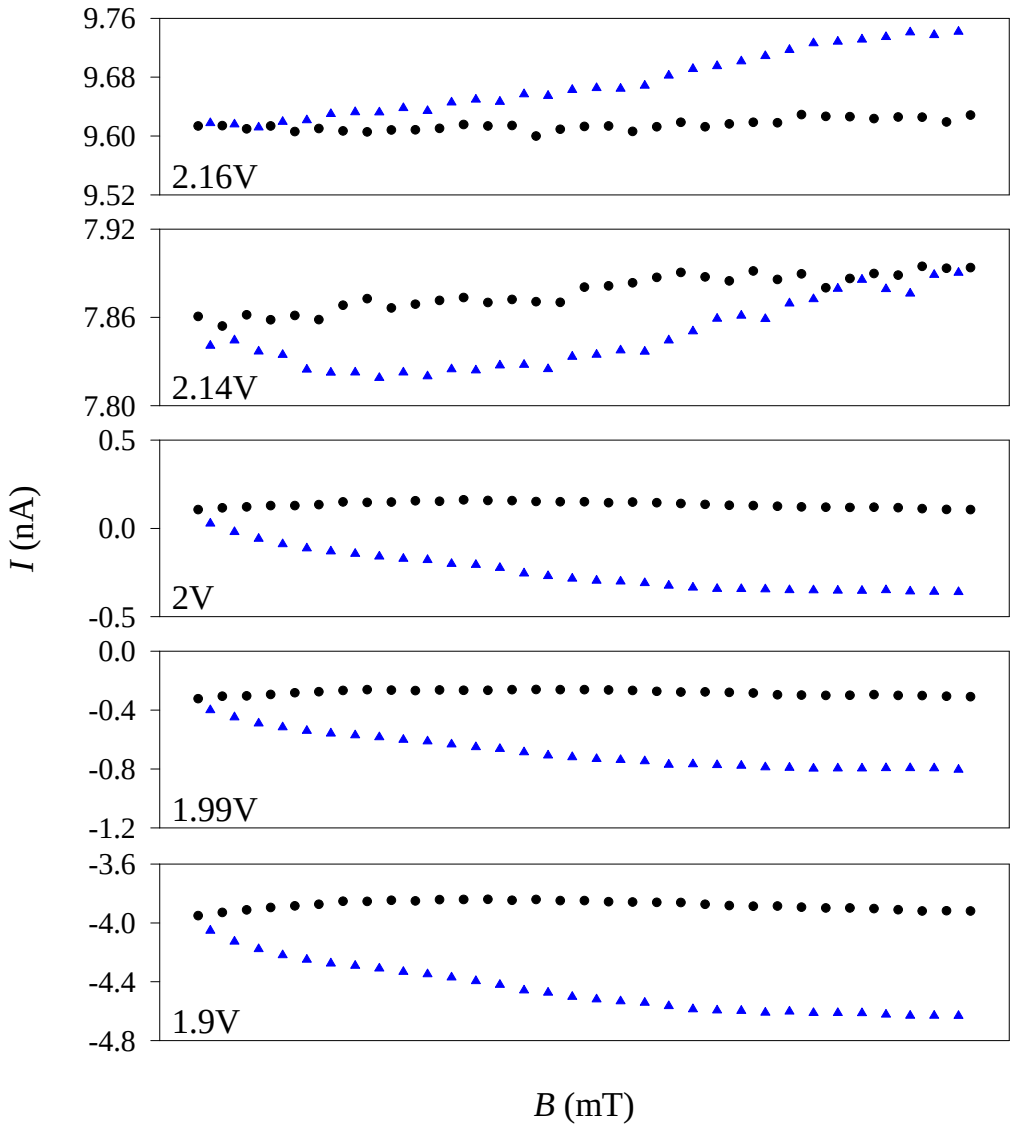

Figure 3.3-3: OLED current for an illuminated device in a magnetic field

The plots above show the raw current measurements recorded at several key voltages that define the three regions indicated in figure 3.3-2. While the abscissa is arbitrary the magnetic field is increasing from left to right. Black circles represent null field device current, while blue triangles represent the device current with an applied magnetic field.

Taking a closer look at the voltage region close to the open-circuit voltage gives remarkably large OMR traces, which reach >100%. For the device data presented in figure 3.3-2 we can see that the point where the large OMR begins to appear to the point where it disappears spans an approximate region of ~1.94V - ~2.04V. Figure 3.3-4 shows the *IV* curve at 288mT and 0mT, as reconstructed from the OMR scans at various drive voltages. From this figure we can see that in the region where large OMR is observed the change in current with applied magnetic field is relatively constant. A closer look at ΔI shows that it is in fact decreasing as V_{oc} is approached and continues to decrease past V_{oc}. This means that the magnitude of the high magnitude OMR traces cannot be due to ΔI and must therefore be due to the absolute current.

The change in current over the large OMR region is ~4-8x10^{-10}A, while the current goes from -10^{-9}A to +10^{-9}A. Since the current is changing polarity the device current, at null field, becomes very small ~10^{-10}A. Therefore the relative invariance of ΔI and the small values of absolute current explain the asymptotic behaviour of OMR at voltages close to V_{oc}.

Another consequence of the transition between negative and positive photocurrents is the observation of negative OMR. When the current is negative the effect of magnetic field is to make the current more negative, which yields a positive OMR. Just above V_{oc} when the current is positive the effect of the magnetic field is to make the current less positive, hence giving a negative OMR.

So, despite the shift from positive to negative OMR around V_{oc} the *IV* data of figure 3.3-4 and the raw current data of figure 3.3-3 shows that the first two regions of OMR that are indicated in figure 3.3-2 are not distinct in the observable effect on current. They are in fact exhibiting the same effect on current and must therefore be due to the same mechanisms.

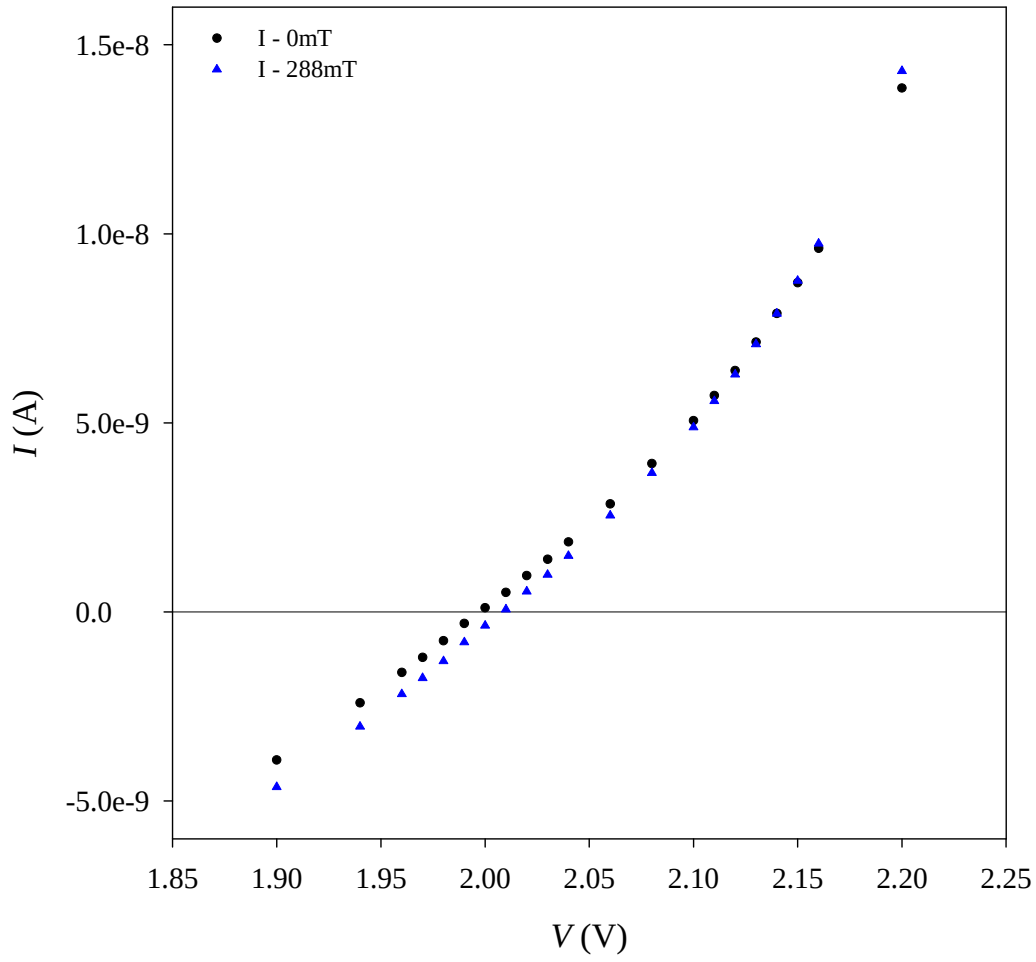

Figure 3.3-4: Inferred IV of an OLED in a magnetic field

The two curves above show the *IV* characteristics of an illuminated OLED under null field and 288mT. Data was taken from the raw current data for individual OMR scans.

3.3.5 OMR effects on IV characteristics

Realising that the first and second regions, indicated in figure 3.3-2, are due to the same processes, gives rise to a possible contradiction to the existing model where the intersystem crossing rate is a function of magnetic field. Below V_{oc} there is an increase in dissociation current which is consistent with the idea of an increase in the triplet population. When the applied voltage is between V_{oc} and the turn-on voltage the change in current is now negative, which corresponds to a drop in dissociation current. Since the device is below the limit of charge injection and the system is dominated with singlets a drop in dissociation current would correspond to a drop in intersystem crossing and subsequent lowering of triplet dissociation. Obviously this is contradictory to the idea that the applied magnetic field is acting to increase the triplet population in both regions one and two.

Another observation that may help to elucidate the apparent contradiction in the OMR either side of V_{oc} is the difference in the position of V_{oc} when a magnetic field is applied. Figure 3.3-4 clearly shows that there is a shift in the position of V_{oc} when a magnetic field is applied. So far we have been considering the magnetic field change on current at a constant applied voltage. The shift in V_{oc} leads to the question of whether or not the magnetic field affects the potentials within the device, with the change in current being a consequence of a change in potential. The idea that a magnetic effect on device potentials might be the more significant effect is not new and has been proposed by the Iowa group [34].

One way in which the position of V_{oc} can be affected is by varying the illumination level that is experienced by the diode. By lowering the illumination level the number of incident photons on the device is lowered. If there are a smaller number of incident photons, then the maximum number of photons that can possibly be absorbed is also lower. If the absorption into the device is lower then this naturally means that there are less excitons and subsequently a lower dissociation current. If the dissociation current is lower then a lower applied potential is required to negate any current flow, hence a lower V_{oc}.

Figure 3.3-5a shows the *IV* curves of a 900Å device that is illuminated with various power levels of illumination from a 460nm diode. The shift in V_{oc} towards higher values is clear as the illumination level increased. Taking a closer look at

the figure 3.3-5b it can be seen that the difference between the various illumination levels is very similar to the difference between *IV* curves seen in figure 3.3-4. This similarity leads to the interpretation that the effect of an applied field on an illuminated device is to alter the shape of the *IV* characteristics as if there was a higher level of illumination. Since a higher level of illumination corresponds to a higher level of dissociation the translation of the *IV* curve in figure 3.3-4 does not contradict the idea that the magnetic field is increasing the intersystem crossing and subsequent triplet dissociation. So rather than seeing the effect of the magnetic field as modulating current, it is more pertinent to view the effect of the magnetic field as shifting/modifying the *IV* curve.

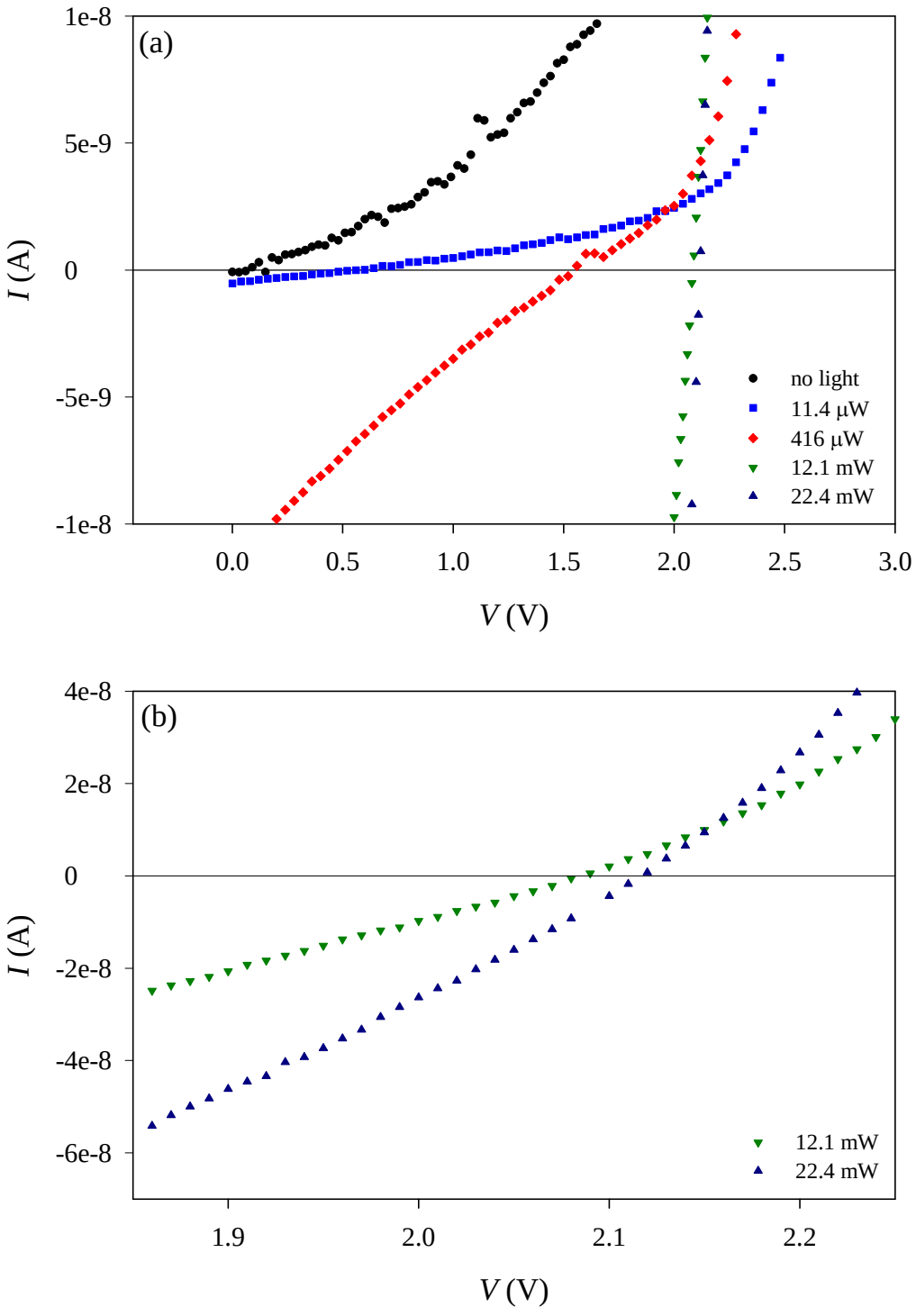

Figure 3.3-5: *IV* of Alq_3 OLED with various levels of illumination

Top pane shows a range of *IV* curves for a wide range of illuminations with a 460nm LED. The bottom pane shows two illuminations to highlight how a change in luminescence has an analogous effect to a magnetic field as indicated in figure 3.3-4.

3.3.6 OMR around the turn voltage

As the applied voltage is increased from V_{oc} the device currents become comparable to the magnetically induced change in current, hence OMR returns to smaller values. As the drive voltage approaches the turn-on voltage for the device we see that the OMR reduces towards zero before becoming positive. In this region around the turn-on voltage there is no change in the direction of current to account for the change from negative to positive OMR. Figure 3.3-6 shows that at high magnetic fields the OMR changes from negative to positive for voltages greater than ~2.14V. Figure 3.3-7 shows raw current data for applied voltages from 2.1V to the turn-on voltage of 2.2V. This data shows the transition from negative to positive OMR in greater detail. For 2.1V the decrease in current is evident. By 2.14V this decrease has diminished for high fields. At an applied voltage of 2.15V this diminished negative OMR continues at low fields before switching to a clear positive OMR at high fields. At the next voltage above turn-on we see a similar OMR to the data obtained for thin devices; small response at low fields, followed by a linear like rise at fields above ~45mT. The 2.2V data shows that the OMR falls back to the previously observed normal shape, showing a sharp rise at low fields followed by slower rise above ~45mT. Figure 3.3-6 shows how the OMR between 2.08V and ~2.15V is analogous to OMR in thin devices (figure 3.2-5) while the OMR at the turn-on voltage of 2.2V is like that seen in thick devices where no significant dissociation effects are observable.

While the non-illuminated thin device data shows strong similarities to a thick illuminated device, there is a clear difference at high drive voltages. At high drive voltages the thin non-illuminated device shows a negligible hyperfine scale rise, while the thick illuminated device shows normal OMR with a significant hyperfine scale component. This disparity between the two devices can be explained from the fact the dominance of dissociation effects in the thin device is due to geometric factors, whereas the dissociation effects in the thick device is due to photo absorption.

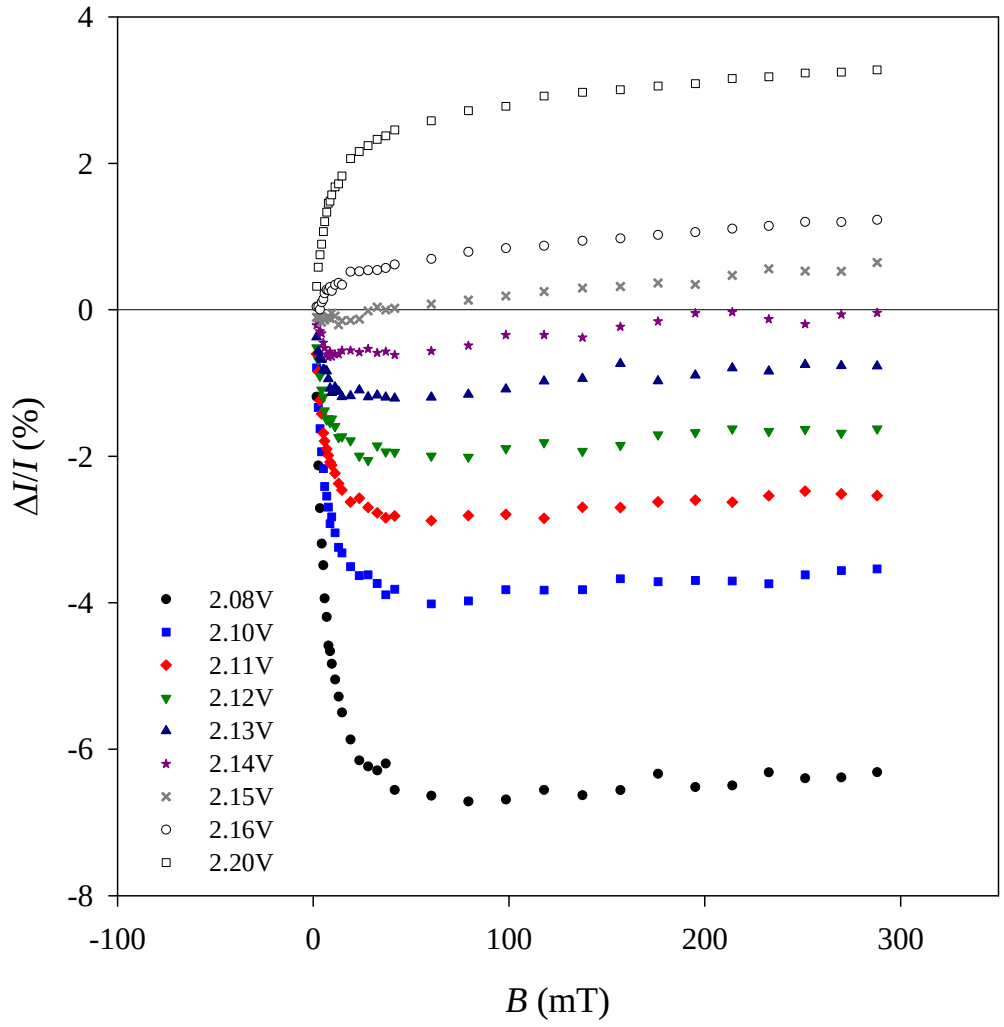

Figure 3.3-6: OMR of an illuminated OLED close to the turn-on voltage

The above figure shows the OMR of an Alq_3 OLED recorded for applied voltages close to the electrical turn-on of the device

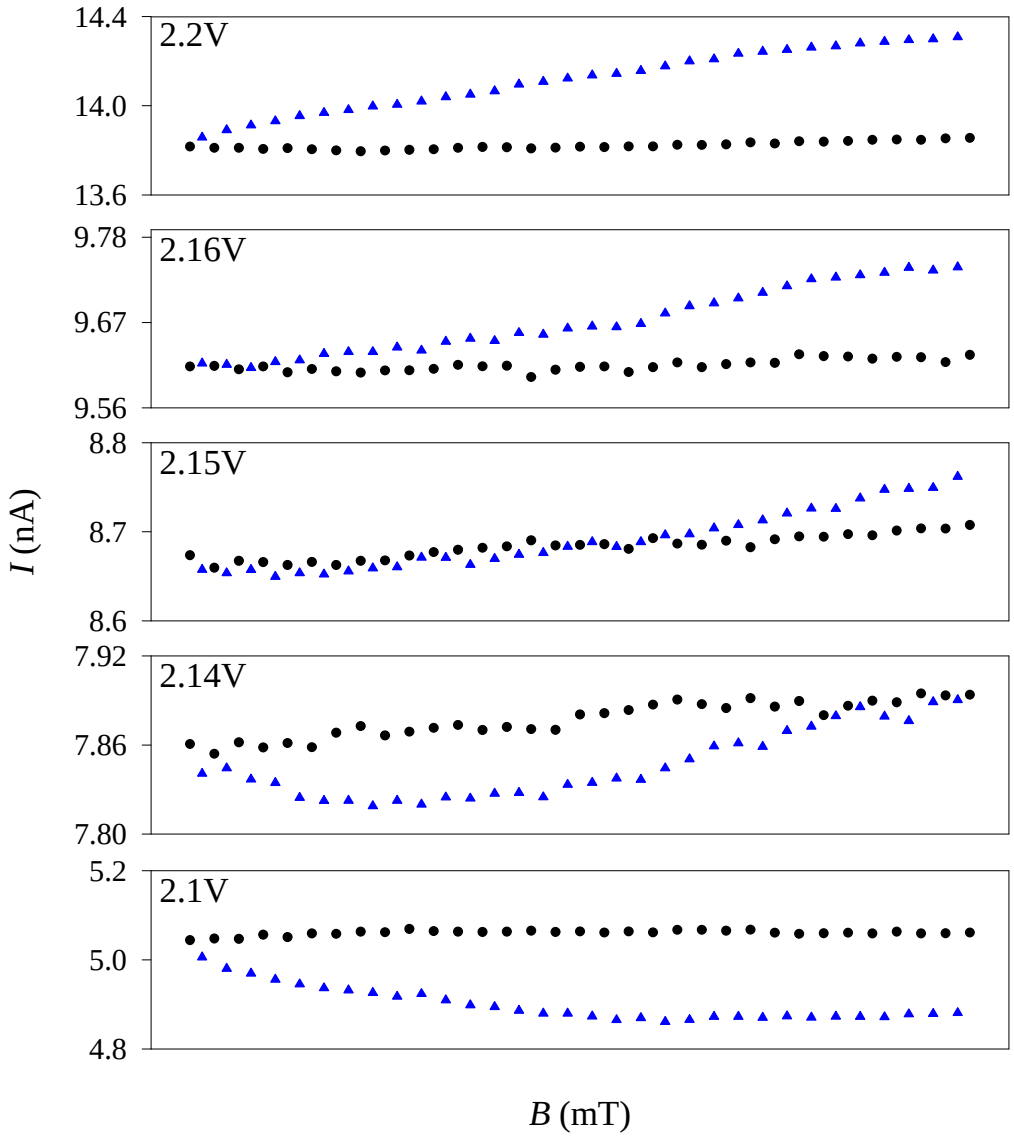

Figure 3.3-7: Illuminated OMR currents for a device close to turn-on

The plots above show the raw current measurements recorded for small voltage steps up to the device turn-on limit. While the abscissa is arbitrary the magnetic field is increasing from left to right. Black circles represent null field device current, while blue triangles represent the device current with an applied magnetic field.

With the thin device the geometry is obviously constant, so if the observation of dissociation effects is due to the geometry, one would expect these effects to scale with current density and maintain significance with respect to the total device current. As explained previously this is not to say that the nature of the dissociation effects cannot change, especially since the ratio of both exciton types and free carriers would be expected to change with current density. So it is reasonable that even for large current densities the hyperfine scale process remains negligible.

For the thick device we know that any latent dissociation effects are not significant hence only the dissociation caused from illumination need be considered. Since the level of illumination is constant we know that the dissociation from photo-excited excitons will not scale with current density. So it is also reasonable to believe that we should observe normal OMR for high applied voltages where the injected current is greater than any contribution from dissociation.

The implication of the considerable similarity between the thin non-illuminated device and the thick illuminated device is that the underlying mechanisms of the effects seen in both devices are indeed shared. Both devices are consistent with the idea that magnetic field modulation of the intersystem crossing rate is a major factor in OMR. Thus, this data reinforces the conclusion that excitons are pre-requisite for the observation of OMR.

As explained before, when the applied voltage is below the turn-on voltage of 2.2V, we have the situation where the system is dominated by a pump into the singlet level, giving an increased dissociation current upon the application of a magnetic field. As the applied voltage approaches turn-on, figure 3.3-6 shows that there is a positive slope at high magnetic fields above ~45mT. What is also seen is the drop in the hyperfine scale portion of the OMR. This situation mirrors the effects seen in thin devices; for a device thickness that previously showed no sign of dissociation effects.

In chapter 3.2 it was argued that the rise in OMR seen for fields above ~45mT could be due to the possible magnetic field dependence of the triplet/free-carrier interaction. Below turn-on the population of triplets is low, so while a magnetic field will not act to give a positive OMR as it does above turn-on, it will have the effect of increasing the triplet population and subsequent interactions with free-

carriers. These triplet/free-carrier interactions would also be expected to show a magnetic field dependence similar to the data seen in section 3.2.4 and figure 3.2-5. The data from section 3.2.4 showed an increase in OMR at high fields, which implies that the triplet/free-carrier interaction actually decreases for an increasing field.

Figure 3.3-7 shows that the OMR in figure 3.3-6 is for positive currents. So if the triplet/free-carrier interaction is to decrease at high fields then it would be expected that the current should increase. For a negative OMR an increase in current would act against the existing negative trend. For a positive OMR an increase in current at high fields would act in addition to the existing trend. Both figure 3.3-6 and figure 3.3-7 demonstrate this high magnetic field effect on the triplet/free-carrier interaction clearly.

3.3.7 OMR shapes – Possible isolation of carrier interactions

The shape of the OMR traces shown in figure 3.3-6 and figure 3.3-8 gives further insights into the behaviour of carriers around the limits of open-circuit and turn-on voltage. Looking at figure 3.3-8, excluding the two traces either side of V_{oc}, the shape of the traces appear, at first glance, to be similar to the change in efficiency data presented earlier in figure 3.2-1. Regardless of being positive or negative the traces show a sharp hyperfine scale rise followed by a plateau from ~45mT. The apparent similarity with the percentage change in efficiency from figure 3.2-1 seems to add further evidence to the notion of the observed magnetic field effects on photocurrent being due to the intersystem crossing between singlet and triplet states. However, from figure 3.3-6 we know that there is also a measurable effect at fields above ~45mT that adds a slope to the OMR. This effect is attributed to the magnetic field effect on the interaction defined in equation 1.4-2. This is not to say that intersystem crossing between singlet and triplet is not the cause of the OMR, but it does highlight the need for further consideration of other effects in determining the overall shape of the OMR.

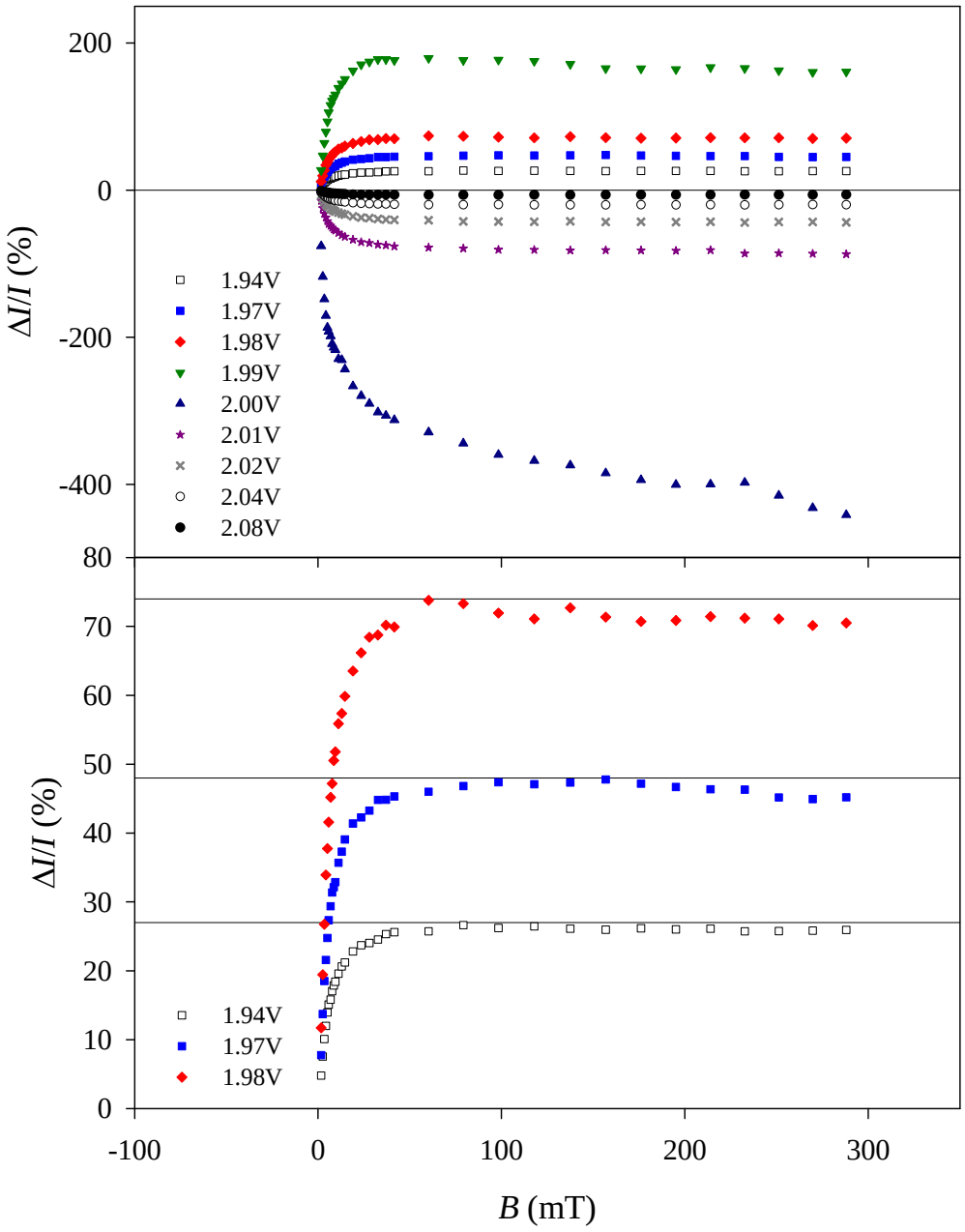

Figure 3.3-8: OMR of an illuminated OLED around V_{oc}

The above figure shows the OMR of an Alq_3OLED recorded for applied voltages around the open-circuit voltage. The top pane shows the effects for a wide range of voltages. The bottom pane shows the large positive with guidelines indicating a possible negative trend in the high field data.

One important difference between the negative OMR of figure 3.3-6 and the negative OMR of thin devices in figure 3.2-2 is that for thin devices the data was obtained with the applied voltage above turn-on, while the negative OMR for the data in figure 3.3-8 was obtained with the operating voltage below device turn-on. Below turn-on there are no injected charge carriers so the current is purely due to dissociation. From section 3.2.5 we know that the dissociation of excitons within a TPD/Alq_3 device is limited to the cathode. Figure 3.3-9 shows a representation of the band structure in the device either side of open-circuit voltage. Above V_{oc} the current is positive hence the potential gradients are aligned such that dissociation at the cathode will give an electron that is free to move under the influence of the potential gradient, while the hole can only move into the cathode. This is an important realisation since it shows that below the device turn-on any triplet/free-carrier interactions that occur can only be due to triplet interactions with electrons.

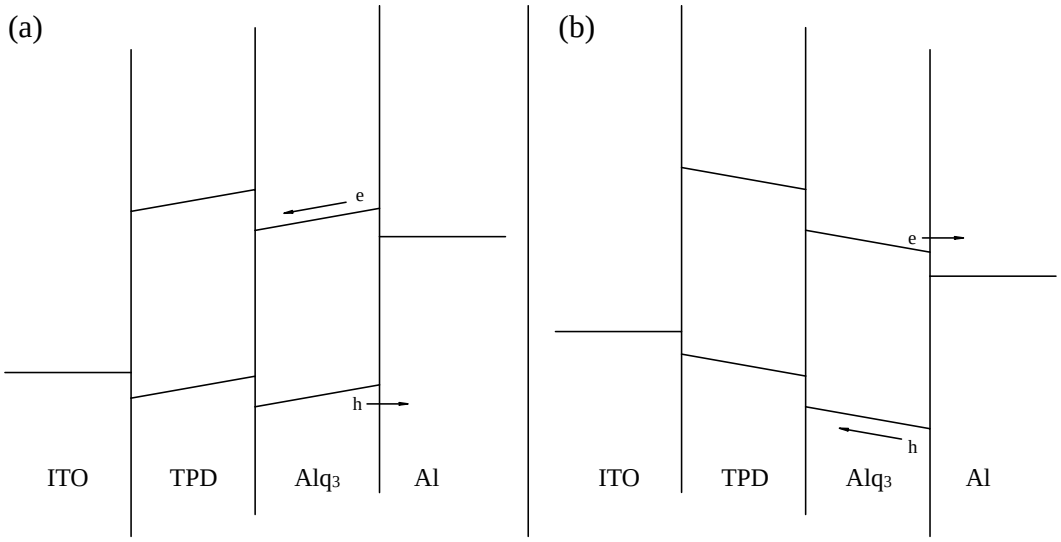

Figure 3.3-9: Schematic of band structure around V_{oc} for an Alq_3 OLED

(a) Represents the potentials within the device when operated above V_{oc}. In this case a dissociated electron will travel through the device towards the anode, while the hole will enter the cathode. (b) Shows the case where the applied voltage is below V_{oc}. In this case the hole will transit the device while the electron enters the Aluminium layer.

Looking more closely at the OMR of figure 3.3-8, the lower pane shows that there is in fact a negative going slope on all the OMR traces before V_{oc}. In figure 3.3-6 the high-field effects were in addition to positive OMR, whereas the high-field effect in figure 3.3-8 is acting against the positive rise. This would imply that the causes for the high-field effect below V_{oc} are different. Figure 3.3-9 also shows the schematic for the band structure when the device is operated below turn-on. In this case a dissociated exciton at the cathode will release a hole that is free to move through the device while the electron is trapped at the interface. So, below the open-circuit voltage, any interactions between free-carriers and triplets must be due to holes only.

The high magnetic field effect seen in figure 3.3-8 acts against the predominant positive OMR; the implication of this is that the magnetic field effect on triplet/hole interactions is actually opposite to the effect on triplet/electron interactions. This is not intuitive and it is not clear why the magnetic field should act oppositely for triplet/hole and triplet/electrons interactions.

There is one anomaly in these observations, which is the 2V OMR that can be seen in figure 3.3-8. The high field effect is clearly very prominent but it appears to be acting in the opposite direction to the high field trends seen for the other negative OMR in figure 3.3-6. It is not obvious why this should be the case, however it is worth noting that a look at the raw current data for this voltage in figure 3.3-5 shows that the effect of the magnetic field is to push the current from positive to negative. So possibly the inconsistency of the 2V OMR is due to the crossing from positive to negative current and the very low currents seen here.

Another important consideration in making these observations is that the operating voltages discussed here are over a very small range of 0.3V. In order to substantiate any possible triplet/hole or triplet/electron interactions it would be necessary to see these effects of a wider range of voltages.

3.3.8 Synoposis – Illumination study

The data from illuminated devices gives very interesting results. OMR is seen below device turn-on, as both dissociated charge carriers and photo-induced excitons are present in the system, this correlates well with normal OMR. The difference in normal OMR is that the charge carriers are introduced through

injection from the electrodes and excitons are created through coulombic attraction of charge pairs.

The illumination gives rise to a dissociation current that shows a similar OMR to the negative OMR seen for non-illuminated thin devices. Since the OMR in illuminated devices is purely an effect of dissociation current we can confidently confirm that the assignment of dissociation effects to negative OMR in non-illuminated thin devices is correct. Above turn-on, the positive OMR seen for an illuminated device matches up well with the OMR seen for a non-illuminated device. The transition between the negative and positive OMR effects also correlates well with the data obtained for a thin non-illuminated device, which further confirms and highlights how significant dissociation effects can be in determining the observed OMR response.

Another outcome of the illuminated OMR results relates to the experimental techniques used. The illuminated OMR shows how crucial it is to isolate samples from light when performing OMR measurements. While appropriate precautions have been taken in gathering the data in this document it is not clear if other data presented in the literature has been compromised by high levels of background light.

From looking at the raw current data it is seen that the effect of the applied field is best viewed as affecting the shape of the IV. This change in IV is as if a higher level of illumination was incident on the sample. Higher illumination corresponds with increase dissociation and as such the OMR of an illuminated device is still consistent with the idea that the magnetic field acts to increase intersystem crossing between excited states.

The effect of magnetic field on the IV curve of an illuminated device is of particular importance as it shows that modifying the populations of excited states has a big effect on the shape of the curve. This implies that the shape of the IV curve is actually dependent upon excited states. If this is the case for an illuminated device, there is no reason that this principle cannot be applied to an electrically pumped device. The implication of this data is that the IV characteristics of any given OLED are actually determined by excited states and charge interactions with those excited states.

4 Conclusions and future work

This thesis has presented the results of three studies on OMR effects in Alq_3 based OLEDs. The first two studies follow an approach of varying the structural properties of an Alq_3 OLED in order to probe OMR. Various cathode materials were studied in order to observe the effect of varying charge injection into the OLED. OLEDs with various Alq_3 thicknesses were studied to probe bulk/interface effects on OMR. Both of these studies point to a crucial role for excitons in the observation of OMR. In order to confirm the importance of excitons, photoconduction experiments were conducted on OLED structures.

In varying the cathode material it is found that OMR is coincident with the turn-on limit of a device. This shows that bipolar charge injection and the presence of excitons are coincident with the observation of OMR. The results obtained for devices with an aluminium cathode are a good example of this principle. For a device with an aluminium cathode the electrical turn-on voltage and the voltage at which light is measurable have a clear separation. It is found that OMR was coincidental with the point at which light was observable which is a strong link between OMR and excitons. Analogous results are observed when the Alq_3 thickness is altered. OMR is only observable when light output is measured from the device.

These observations are corroborated in reference [54] which shows that for a device structure that is heavily optimised for hole transport (ITO/TPD/Au), OMR is only seen when the electron injection limit is reached and light can be observed. The strong evidence linking OMR to excitons and the evidence showing that OMR is not observable in unipolar transport regimes is contradictory to the proposed mechanism of OMR that is based on bipolaron formation. OMR is not observed simply through injecting charge into an organic semiconductor. Since OMR data in unipolar devices in the literature is stated as having “weak luminescence” it would be worthwhile performing more rigorous studies of OMR in various unipolar devices, with particular attention paid to luminescent properties. Magnetic effects on organic field effect transistors could also be a good way of probing magnetic effects in unipolar devices.

From the literature, modulation of hyperfine transitions between the singlet and triplet state are proposed in various mechanisms for OMR. The importance of hyperfine effects could be probed through the use of organic compound that have had hydrogen eliminated through deuteration or fluorination. In an OLED spin-statistics determine that triplets will dominate the total exciton population in the system. Due to the excess of triplets compared to singlets, any increase in the intersystem crossing rate will increase the singlet population at the expense of the triplet population. This corresponds nicely with all data presented here and in the literature; only increases in luminescent output, and the related singlet population, is seen with the application of a magnetic field. As such any explanation of OMR should be linked to either the increase in singlet population, or the decrease in triplet population. As highlighted in the introduction the short lifetime of the singlet state makes it unlikely that the singlet state plays any significant role in OMR. This is especially true for proposals that involve singlet dissociation; the long lifetime of the triplet state makes it more likely to dominate any dissociation effects.

From the literature it is found that triplet interactions with free carriers are a known phenomenon in organic semiconductors. This leads to the proposal that triplet/free-carrier interactions are the cause of OMR in modern OLEDs. Triplets and free-carriers are able to form a pair state, from this pair state the triplet can be quenched or can dissociate back to an unpaired state. The formation and subsequent dissociation of a triplet/free-carrier pair state essentially acts as a scattering mechanism. Decreasing the triplet population with the application of a magnetic field will decrease this form of scattering. Decreasing the scattering will increase the mobility, thus the current will be seen to increase, hence positive OMR. So the triplet/free-carrier interaction qualitatively explains all the observed data. Charge injection experiments to measure the mobility of charge carries in the presence of excited states would be a direct way of measuring the importance of triplet/free-carrier interactions in organic semiconductors.

Studies on various device thicknesses showed that negative OMR can be observed in thin devices. The magnetic field effect on device efficiency showed the same positive trend regardless of the shape of the OMR. So the observation of negative OMR must also be linked to the decrease in triplet population. Since negative OMR is observed in thin devices this raises the question of the importance of the

distance of the cathode from the exciton generation region. It is proposed that for thin devices dissociation of triplets at the cathode provide a significant contribution to the total device current. So decreasing the triplet population in the OLED would decrease this contribution and hence lower the device current.

This leads to the conclusion that there are two ways in which triplets can affect device current. Triplet/free-carrier interactions give a positive OMR while triplet dissociation gives a negative OMR. Whether a positive or negative OMR is seen depends on the relative significance and subsequent balance between the two effects.

As a way of verifying the effects seen in the cathode and thickness studies devices were measured under illumination. OMR was seen below the device turn-on giving a modulation to the photocurrent. The measured OMR curves match very well to the OMR curves of thin devices. Both show a similar transition from negative to positive OMR. This confirms the significance of dissociation effects in OMR.

Due to the generation of singlet excitons through photo-excitation, the effect of increasing the intersystem crossing by the magnetic field is to increase the triplet population and decrease the singlet population. Increasing the triplet population increases the dissociation due to the longer diffusion length of the triplet. Increasing the dissociation current affects the IV characteristics by increasing the open circuit voltage and increasing the power generation curve. The effect on the IV curve from the application of a magnetic field compares well to the effect of increased illumination on the IV curve. Increasing the illumination increases the dissociation hence this corroborates the idea that the magnetic field is acting to increase the triplet population and subsequent dissociation. Time-resolved OMR studies or the magnetic dependence of photoluminescence are two ways in which the effect of magnetic field on exciton populations and intersystem crossing could be studied further.

Collectively the data presented here highlights the importance of excitons to the current through an OLED. In particular, the effect on the IV curve of an illuminated device shows that triplets could have a significant role in determining the overall shape of the IV characteristics of an OLED.

References

[1] C. W. Tang and S. A. Van Slyke, Appl. Phys. Lett. **51** (12), 913 (1987).

[2] M. Pope, H. P. Kallman and P. Magnante, J. Chem. Phys. **38**, 2042 (1963).

[3] W. Helfrich and W. G. Schneider, Phys. Rev. Lett. **14** (7), 229 (1965).

[4] J. Dresner, RCA Rev. **30**, 322 (1969).

[5] G. T. Pott and D. F. Williams, J. Chem. Phys. **51**, 203 (1969).

[6] J. H. Burroughes, D. D. C. Bradley, A. R. Brown, R. N. Marks, K. Mackay, R. H. Friend, P. L. Burns and A. B. Holmes, Nature **347**, 539 (1990).

[7] R. H. Friend, R. W. Gymer, A. B. Holmes, J. H. Burroughes, R. N. Marks, C. Taliani, D. D. C. Bradley, D. A. Dos Santos, J. L. Bredas, M. Logdlund and W. R. Salaneck, Nature **397**, 121 (1999).

[8] R. G. Kepler, P. M. Beeson, S. J. Jacobs, R. A. Anderson, M. B. Sinclair, V. S. Valencia and P. A. Cahill, Appl. Phys. Lett. **66** (26), 3618 (1995).

[9] G. G. Malliaras, Y. Shen, D. H. Dunlap, H. Murata and Z. H. Kafafi, Appl. Phys. Lett. **79** (16), 2582 (2001).

[10] M. A. Baldo, S. Lamansky, P. E. Burrows, M. E. Thompson and S. R. Forrest, Appl. Phys. Lett. **75** (1), 4 (1999).

[11] C. W. Tang, S. A. Vanslyke and C. H. Chen, J. Appl. Phys. **65**, 3610 (1989).

[12] M. A. Baldo, D. F. O'Brien, Y. You, A. Shoustikov, S. Sibley, M. E. Thompson and S. R. Forrest, Nature **395**, 151 (1998).

[13] A.D. Walser, R. Priestley and R. Dorsinville, Synth. Met. **102**, 1552 (1999).

[14] M. A. Baldo, D. F. O'Brien, M. E. Thompson and S. R. Forrest, Phys. Rev. B **60** (20), 14422 (1999).

[15] M. Cölle and C. Gärditz, Appl. Phys. Lett. **84** (16), 3160 (2004).

[16] R. C. Johnson, R. E. Merrifield, P. Avakian and R. B. Flippen, Phys. Rev. Lett. **19** (6), 285 (1967).

[17] V. Ern and R. E. Merrifield, Phys. Rev. Lett. **21** (9), 609 (1968).

[18] S. Z. Weisz, P. Richardson, A. Cobas and R. C. Jarnagin, Mol. Crystals **3**, 168 (1967).

[19] R. P. Groff, R. E. Merrifield, A. Suna and P. Avakian, Phys. Rev. Lett. **29** (7), 429 (1972).

[20] R. P. Groff, A. Suna, P. Avakian and R. E. Merrifield, Phys. Rev. B **9** (6), 2655 (1974).

[21] M. Wittmer and I. Zschokke-Gränacher, J. Chem. Phys. **63** (10), 4187 (1975).

[22] E. L. Frankevich, A. A. Lymarev, I. Sokolik, F. E. Karasz, S. Blumstengel, R. H. Baughman and H. H. Hörhold, Phys. Rev. B **46** (15), 9320 (1992).

[23] E. Frankevich, A. Zakhidov, K. Yoshino, Y. Maruyama and K. Yakushi, Phys. Rev. B **53** (8), 4498 (1996).

[24] J. Kalinowski, J. Szmytkowski and W. Stampor, Chem. Phys. Lett. **378**, 380 (2003).

[25] M. Wohlgenannt and Z.V. Vardeny, J. Phys.: Condens. Matter **15**, R83 (2003).

[26] J. Kalinowski, M. Cocchi, D. Virgili, P. Di Marco and V. Fattori, Chem. Phys. Lett. **380**, 710 (2003).

[27] G. Giro, M. Cocchi, P. Di Marco, E. Di Nicolò, V. Fattori, J. Kalinowski and M. Ghedini. Synth. Met. **102**, 1018 (1999).

[28] A. H. Davis, K. Bussman, J. Vac. Sci. Technol. A **22** (4), 1885 (2004).

[29] M. A. Baldo, S. R. Forrest, Phys. Rev. B **62** (16), 10958 (2000).

[30] M. Cölle, C. Gärditz and M. Braun, J. Appl. Phys. **96** (11), 6133 (2004).

[31] T. L. Francis, O. Mermer, G. Veeraraghavan and M. Wohlgenannt, New J. Phys. **6**, 185 (2004).

[32] Ö. Mermer, G. Veeraraghavan, T. L. Francis and M. Wohlgenannt, Solid State Commun. **134**, 631 (2005).

[33] M. Redecker, D. D. C. Bradley, M. Inbasekaran and E. P. Woo, Appl. Phys. Lett. **73**, 1565 (1998).

[34] Ö. Mermer, G. Veeraraghavan, T. L. Francis, Y. Sheng, D. T. Nguyen, M. Wohlgenannt, A. Köhler, M. K. Al-Suti and M. S. Khan, Phys. Rev. B **72**, 205202 (2005).

[35] V. N. Prigodin, J. D. Bergeson, D. M. Lincln and A. J. Epstein, Synth. Met. **156**, 757 (2006).

[36] Y. Sheng, D. T. Nguyen, G. Veeraraghavan, Ö. Mermer, M. Wohlgenannt, S. Qiu and U. Scherf, Phys. Rev. B **74**, 045213 (2006).

[37] G. Veeraraghavan, T. D. Nguyen, Y. Sheng, O. Mermer and M. Wohlgenannt, J. Phys.: Condens. Matter **19**, 036209 (2007).

[38] Y. Sheng, T. D. Nguyen, G. Veeraraghavan, Ö. Mermer and M. Wohlgenannt, Phys. Rev. B **75**, 035202 (2007).

[39] T. D. Nguyen, Y. Sheng, J. Rybicki, G. Veeraraghavan and M. Wohlgenannt, J. Mater. Chem. **17**, 1995 (2007)

[40] P. A. Bobbert, T. D. Nguyen, F. W. van Oost, B. Koopmans and M. Wohlgenannt, Phys. Rev. Lett. **99**, 216801 (2007).

[41] Y. Wu, Z. Xu, B. Hu and J. Howe, Phys. Rev. B **75**, 035214 (2007).

[42] F. L. Bloom, W. Wagemans, M. Kemerink and B. Koopmans, Phys. Rev. Lett. **99**, 257201 (2007).

[43] A. J. Campbell, D. D. C. Bradley, H. Antoniadis, M. Inbasekaran, W. S. W. Wu and E. P. Woo, Appl. Phys. Lett. **76** (13), 1734 (2000).

[44] D. Troadec, G. Veriot, R. Antony and A. Moliton, Synth. Met. **124**, 49 (2001).

[45] J. D. Bergeson, V. N. Prigodin, D. M. Lincoln and A. J. Epstein, Phys. Rev. Lett. **100**, 067201 (2008).

[46] R. H. Parmenter and W. Ruppel, J. Appl. Phys. **30**, 1548 (1959).

[47] C. C. Wu, C. I. Wu, J. C. Sturm and A. Kahn, Appl. Phys. Lett. **70**, 1348 (1997).

[48] K. Furukawa, Y. Terasaka, H. Ueda and M. Mtsumura, Synth. Met. **91**, 99 (1997)

[49] L. S. Hung, C. W. Tang and M. G. Mason, Appl. Phys. Lett. **70**, 152 (1997).

[50] G. E. Jabbour, Y. Kawabe, S. E. Shaheen, J. F. Wang, M. M. Morrell, B. Kippelen and N. Peyghambarian, Appl. Phys. Lett. **71**, 1762 (1997).

[51] M. A. Baldo and S. R. Forrest, Phys. Rev. B **64**, 085201 (2001).

[52] Y. Ohomori, A. Fujii, M. Uchida, C. Morishima and K. Yoshino, Appl. Phys. Lett. **63** (14), 1871 (1994).

[53] K. Itano, H. Ogawa and Y. Shirota, Appl. Phys. Lett. **72** (6), 636 (1998).

[54] P. Shakya, P. Desai, T. Kreouzis and W. P. Gillin, J. Appl. Phys. **103**, 043706 (2008).

[55] P. Shakya, Ph.D Thesis, University of London, to be submitted (2008).

[56] M. Cölle, C. Gärditz and A.G. Mückl, Synth, Met. **147**, 97 (2004).

[57] M. Pope and C. E. Swenberg, Electronic Processes in Organic Crystals and Polymers, 152 (Oxford Science, 1999).